

การย่อยสลายไดยูรอนด้วยปฏิกิริยาที่เร่งด้วยแสงโดยใช้ไทเทเนียมไดออกไซด์
ในเครื่องปฏิกรณ์ขนาดไมโคร



นางสาวรุ่งทิพย์ น้อยสำราญ

จุฬาลงกรณ์มหาวิทยาลัย

CHULALONGKORN UNIVERSITY

วิทยานิพนธ์นี้เป็นส่วนหนึ่งของการศึกษาตามหลักสูตรปริญญาวิศวกรรมศาสตรมหาบัณฑิต

สาขาวิชาวิศวกรรมเคมี ภาควิชาวิศวกรรมเคมี

คณะวิศวกรรมศาสตร์ จุฬาลงกรณ์มหาวิทยาลัย

ปีการศึกษา 2556

ลิขสิทธิ์ของจุฬาลงกรณ์มหาวิทยาลัย

บทคัดย่อและแฟ้มข้อมูลฉบับเต็มของวิทยานิพนธ์ตั้งแต่ปีการศึกษา 2554 ที่ให้บริการในคลังปัญญาจุฬาฯ (CUIR)

เป็นแฟ้มข้อมูลของนิสิตเจ้าของวิทยานิพนธ์ ที่ส่งผ่านทางบัณฑิตวิทยาลัย

The abstract and full text of theses from the academic year 2011 in Chulalongkorn University Intellectual Repository (CUIR) are the thesis authors' files submitted through the University Graduate School.

PHOTOCATALYTIC DEGRADATION OF DIURON ON TITANIUM DIOXIDE
IN MICROREACTOR

Miss Rungthip Noisomran



จุฬาลงกรณ์มหาวิทยาลัย

CHULALONGKORN UNIVERSITY

A Thesis Submitted in Partial Fulfillment of the Requirements
for the Degree of Master of Engineering Program in Chemical Engineering

Department of Chemical Engineering

Faculty of Engineering

Chulalongkorn University

Academic Year 2013

Copyright of Chulalongkorn University

Thesis Title	PHOTOCATALYTIC DEGRADATION OF DIURON ON TITANIUM DIOXIDE IN MICROREACTOR
By	Miss Rungthip Noisomran
Field of Study	Chemical Engineering
Thesis Advisor	Assistant Professor Varong Pavarajarn, Ph.D.

Accepted by the Faculty of Engineering, Chulalongkorn University in Partial Fulfillment of the Requirements for the Master's Degree

.....Dean of the Faculty of Engineering
(Professor Bundhit Eua-arporn, Ph.D.)

THESIS COMMITTEE

.....Chairman
(Associate Professor Prasert Pavasant, Ph.D.)

.....Thesis Advisor
(Assistant Professor Varong Pavarajarn, Ph.D.)

.....Examiner
(Assistant Professor Apinan Sootitawat, D.Eng.)

.....External Examiner
(Chanchana Thanachayanont, Ph.D.)

รุ่งทิพย์ น้อยสำราญ: การย่อยสลายไดยูรอนด้วยปฏิกิริยาที่เร่งด้วยแสงโดยใช้ไทเทเนียมไดออกไซด์ในเครื่องปฏิกรณ์ขนาดไมโคร. (PHOTOCATALYTIC DEGRADATION OF DIURON ON TITANIUM DIOXIDE IN MICROREACTOR) อ.ที่ปรึกษาวิทยานิพนธ์
 หลัก: ผศ. ดร.วรงค์ ปวราจารย์, 110 หน้า.

การย่อยสลายไดยูรอนด้วยปฏิกิริยาที่เร่งด้วยแสงในเครื่องปฏิกรณ์ไมโครได้ถูกศึกษาโดยใช้ไทเทเนียมไดออกไซด์เกรดการค้าเป็นตัวเร่งปฏิกิริยา โดยตัวเร่งปฏิกิริยาได้ถูกสังเคราะห์ด้วยวิธีการเคลือบแบบหมุนเหวี่ยง ในงานวิจัยนี้ทำการศึกษาการย่อยสลายไดยูรอนที่ความเข้มข้น 10 ppm ในเครื่องปฏิกรณ์ที่ทำการเคลือบไทเทเนียมไดออกไซด์ไว้ โดยความหนาของช่องทางไหลของเครื่องปฏิกรณ์มีขนาดเท่ากับ 250 ไมโครเมตร เนื่องจากระยะทางในการถ่ายโอนมวลสั้นและมีการสูญเสียความเข้มแสงจากการดูดซับน้อย จึงทำให้การย่อยสลายในเครื่องปฏิกรณ์ขนาดไมโครมีประสิทธิภาพมากขึ้น ตัวอย่างสารละลายถูกเก็บไปวัดความเข้มข้นของไดยูรอนที่เปลี่ยนไปด้วยเครื่องโครมาโทกราฟีชนิดของเหลวเป็นระยะๆ ในขณะที่การระบุถึงสารตัวกลางที่เกิดขึ้นจะใช้เครื่องโครมาโทกราฟีชนิดของเหลวกับแมสสเปกโตรมิเตอร์ การเพิ่มขึ้นของเวลาที่สารอยู่ในเครื่องปฏิกรณ์ ส่งผลให้ประสิทธิภาพของการย่อยสลายเพิ่มมากขึ้น หลังจากไดยูรอนไหลผ่านเครื่องปฏิกรณ์ไป 15 นาที สามารถย่อยสลายไดยูรอนได้ 63% นอกจากนี้ยังศึกษาผลกระทบของการเปลี่ยนแปลงความหนาของช่องทางไหลที่มีต่อการย่อยสลาย การย่อยสลายไดยูรอนจะเกิดสารตัวกลางมากมาย สารตัวกลางที่เกิดจากปฏิกิริยานั้นเกิดจากการเข้าทำปฏิกิริยาของอนุมูลไฮดรอกซีที่ตำแหน่งต่างๆ ของไดยูรอน โดยมีปฏิกิริยาที่เกี่ยวข้อง 3 ปฏิกิริยา คือ ดีไฮโดรจีเนชันของวงเบนซีน ไฮดรอกซิเลชันของวงเบนซีน และการกำจัดหมู่เมทิล



จุฬาลงกรณ์มหาวิทยาลัย
 CHULALONGKORN UNIVERSITY

ภาควิชา วิศวกรรมเคมี

ลายมือชื่อนิสิต

สาขาวิชา วิศวกรรมเคมี

ลายมือชื่อ อ.ที่ปรึกษาวิทยานิพนธ์หลัก

ปีการศึกษา 2556

5570351621: MAJOR CHEMICAL ENGINEERING

KEYWORDS: DIURON / MICROREACTOR / TITANIUM DIOXIDE / PHOTOCATALYTIC
DEGRADATION / INTERMEDIATE

RUNGTHIP NOISOMRAN: PHOTOCATALYTIC DEGRADATION OF DIURON ON
TITANIUM DIOXIDE IN MICROREACTOR. ADVISOR: ASST. PROF. VARONG
PAVARAJARN, PH.D., 110 pp.

Photocatalytic degradation of diuron in a microreactor was investigated by using Degussa P25 titanium dioxide as photocatalyst. In this work, photocatalytic degradation of 10-ppm diuron aqueous solution was conducted in a 250 μm -thick micro-channel coated with titanium dioxide thin film. Due to a short mass transfer distance and negligible loss in light intensity by absorption, the photodegradation is significantly enhanced by using the microreactor. The solution was periodically sampled to monitor the concentration of diuron by using high performance liquid chromatography (HPLC) while the intermediates products were identified by using chromatography with mass spectroscopy (LC-MS/MS). The increase in residence time resulted in the increased. The degradation of diuron by 63% was achieved after passing through the reactor for 15 minutes. The effect of thickness of the micro-channel was also investigated. The degradation generates several intermediate products. Several degradation intermediates are generated by reactions of hydroxyl radical attacking at different sites of diuron structure during the photocatalytic degradation. There are 3 main reaction pathways, including dehalogenation of aromatic ring, hydroxylation of the aromatic ring and demethylation. In addition, the intermediate products that are formed under exposure of light and those are formed without light were investigated.

Department: Chemical Engineering Student's Signature

Field of Study: Chemical Engineering Advisor's Signature

Academic Year: 2013

ACKNOWLEDGEMENTS

The author would like to express her gratitude to her advisor, Assistant Professor Dr.Varong Pavarajarn, for his extensive guidance, patience, support, and encouragement throughout the research.

I would also grateful to thank to Associate professor Prasert Pavasant as the chairman, Assistant Professor Apinan Sootitantawat, and Dr. Chanchana Thanachayanont, members of the thesis committee for their kind cooperation, comment, and discussions.

I would like to thank the Scientific and Technological Research Equipment Centre for analysis of LC-MS/MS.

I would also like to thank all my friends and all members of the Center of Excellent in Particle Technology who always provide the encouragement and cooperate along the research study.

This work was also partially by Centennial Fund of Chulalongkorn University for the partial financial support to this work.

Finally, I would like to dedicate this thesis to my parents and my families, who have always been the source of her support and encouragement.

CONTENTS

	Page
THAI ABSTRACT.....	v
ENGLISH ABSTRACT.....	vi
ACKNOWLEDGEMENTS	vi
CONTENTS.....	vii
CONTENT OF TABLES	x
CONTENT OF FIGURES.....	xi
CHAPTER I	1
INTRODUCTION	1
CHAPTER II.....	4
THEORY AND LITERATURE REVIEW.....	4
2.1 Diuron.....	4
2.2 Physical and Chemical Properties of Titanium dioxide	6
2.3 Photocatalytic reaction.....	10
2.3 Photocatalytic degradation of diuron	14
2.3.1 The kinetic of photocatalytic degradation	16
2.3.2 Intermediate products from the degradation of diuron.....	17
2.4 Photocatalytic reaction in Microreactor	23
CHAPTER III.....	27
EXPERIMENTAL.....	27
3.1 Materials	27
3.2 Preparation of catalyst film	27
3.3 Fabrication of a microreactor.....	28
3.4 Characterization of catalyst film.....	29
3.4.1 Field Emission Scanning Electron Microscope (FESEM).....	29
3.4.2 Inductive Coupled Plasma Optical Emission Spectrometer (ICP-OES).....	29
3.5 Photocatalytic Activity Testing.....	29
3.5.1 Photocatalytic degradation of diuron in a microreactor.....	29

	Page
3.5.2 Study of effect of light light on intermediate formation.....	30
3.5.3 Photocatalytic degradation of three standard intermediates	31
CHAPTER IV.....	32
RESULTS AND DISCUSSION.....	32
4.1 Synthesis of TiO ₂ film via Spin-coating method	32
4.1.1 Characterization of TiO ₂ thin films.....	33
4.1.2 Quantity of TiO ₂ in runoff samples.....	34
4.2 Photocatalytic degradation of diuron in microreactor.....	35
4.2.1 Effect of residence time.....	35
4.2.2 Effect of thickness of micro-channel.....	39
4.2.3 Kinetics of diuron in microreactor	45
4.2.4 Degradation kinetic of some intermediate standard	48
4.3 Intermediate product of the photocatalytic degradation of diuron	49
4.4 Effect of light on intermediates formation	68
CHAPTER V.....	78
CONCLUSIONS AND RECOMMENDATIONS	78
5.1 Summary of Results	78
5.2 Conclusions	78
5.3 Recommendations.....	79
REFERENCES.....	80
APPENDIX A.....	87
DIURON CARIBRATION CURVE.....	87
APPENDIX B.....	88
CALCULATION OF TITANIUM DIOXIDE IN SOLUTION.....	88
APPENDIX C.....	89
CALCULATION OF REYNOLDS NUMBER.....	89
APPENDIX D	91

	Page
LC-MS/MS MASS SPECTRUM.....	91
APPENDIX E.....	109
LIST OF PUBLICATION	109
VITA	110



จุฬาลงกรณ์มหาวิทยาลัย
CHULALONGKORN UNIVERSITY

CONTENT OF TABLES

	PAGE
Table 2.1 Physicochemical properties of Diuron	5
Table 2.2 The physical properties of TiO ₂ : Rutile phase.....	7
Table 2.3 The physical properties of TiO ₂ : Anatase phase.....	7
Table 2.4 The physical properties of TiO ₂ : Brookite	8
Table 2.5 Comparative oxidising power of common oxidants	14
Table 2.6 Possible intermediates generated from photodegradation of diuron on and titanium dioxide	21
Table 4.1 The apparent rate constant (k_{app}) and R^2 value for the photocatalytic degradation of three intermediate standards using TiO ₂ coated films	49
Table 4.2 The informations of three standard samples.....	54
Table 4.3 Main fragments obtained from MS/MS spectra and proposed structures of intermediates generated from photodegradation of diuron.	58

CONTENT OF FIGURES

	PAGE
Figure 2.1 Crystal structure of TiO ₂ ; (a) Anatase, (b) Brookite, (c) Rutile	9
Figure 2.2 Key steps of spin coating process	10
Figure 2.3 Schematic diagram of photocatalytic reaction	12
Figure 2.4 The active sites of electrophilic attack on the aromatic ring of diuron.....	18
Figure 2.5 The main pathway of photocatalytic degradation of diuron.	19
Figure 2.6 Proposed degradation mechanism of diuron by the photocatalytic system.....	20
Figure 3.1 Microreactor set up.....	28
Figure 3.2 Equipments set-up for photocatalytic degradation process.....	30
Figure 3.3 Equipment set-up for controlling the time of exposing with the black tape.....	30
Figure 4.1 SEM images of TiO ₂ film from spin-coating method.....	34
Figure 4.2 Concentration of diuron in the outlet stream from the reactor with consider to the initial concentration at residence time 1 minute. The thickness of microchannel is 250 μm	36
Figure 4.3 Concentration of diuron in the outlet stream from the reactor with consider to the initial concentration at residence time 5 minutes. The thickness of microchannel is 250 μm	36
Figure 4.4 Concentration of diuron in the outlet stream from the reactor with consider to the initial concentration at residence time 10 minutes. The thickness of microchannel is 250 μm	37
Figure 4.5 Concentration of diuron in the outlet stream from the reactor with consider to the initial concentration at residence time 15 minutes. The thickness of microchannel is 250 μm	37
Figure 4.6 Concentration of diuron in the outlet stream from the reactor with consider to the initial concentration for all four residence time	38
Figure 4.7 Photocatalytic degradation of diuron in microreactor for all four residence time and degradation efficiency	39
Figure 4.8 Concentration of diuron in the outlet stream from the reactor with consider to the initial concentration: (Δ) 750 μm, (□) 500 μm and (◇) 250 μm. The residence time is 1 minute.....	40

Figure 4.9 Concentration of diuron in the outlet stream from the reactor with consider to the initial concentration: (Δ) 750 μm , (\square) 500 μm and (\diamond) 250 μm . The residence time is 5 minutes	40
Figure 4.10 Concentration of diuron in the outlet stream from the reactor with consider to the initial concentration: (Δ) 750 μm , (\square) 500 μm and (\diamond) 250 μm . The residence time is 10 minutes.....	41
Figure 4.11 Concentration of diuron in the outlet stream from the reactor with consider to the initial concentration: (Δ) 750 μm , (\square) 500 μm and (\diamond) 250 μm . The residence time is 15 minutes.....	41
Figure 4.12 Efficiency of the degradation as a function of mean residence time: (Δ) 750 μm , (\square) 500 μm and (\diamond) 250 μm	42
Figure 4.13 Reynolds number (Re) under various the thickness of micro-channel (250 μm , 500 μm and 750 μm).....	45
Figure 4.14 First-order linear transforms plot of the photocatalytic degradation of diuron on TiO_2 coated film	47
Figure 4.15 First-order linear transforms plot of the photocatalytic degradation of three intermediate standards on TiO_2 coated film: (\diamond)1-(3,4-dichlorophenyl)-3-methylurea, (\square) 3-(3,4-dichlorophenyl)-1-formyl-1-methylurea and (Δ)3,4-dichloroaniline.....	48
Figure 4.16 Chemical structure of diuron	50
Figure 4.17 HPLC peak height of intermediates generated during photocatalytic degradation of diuron on TiO_2 coated film. The residence time is 1 minute	51
Figure 4.18 HPLC peak height of intermediates generated during photocatalytic degradation of diuron on TiO_2 coated film. The residence time is 5 minutes.....	51
Figure4.19 HPLC peak height of intermediates generated during photocatalytic degradation of diuron on TiO_2 coated film. The residence time is 10 minutes	52
Figure 4.20 HPLC peak height of intermediates generated during photocatalytic degradation of diuron on TiO_2 coated film. The residence time is 15 minutes	52
Figure 4.21 The concentrations of diuron and its intermediates under various mean residence times.....	55
Figure 4.22 Hydroxylation reaction.....	57
Figure 4.23 Decarboxylation reaction.....	57

Figure 4.24 Hydroxylation of the aromatic ring during photocatalytic degradation of Diuron.....	61
Figure 4.25 Dechlorination during photocatalytic degradation of Diuron.....	61
Figure 4.26 Chlorine substituted on the aromatic ring during photocatalytic degradation of diuron	62
Figure 4.27 Oxidation of the alkyl side chain by $\bullet\text{OH}$	63
Figure 4.28 Proposed degradation mechanism of diuron.....	64
Figure 4.29 Proposed degradation mechanism of diuron that may less toxic	67
Figure 4.30 The intermediate compounds formed under exposure of light. The residence time is 1 minute	68
Figure 4.31 The intermediate compounds formed when the middle 1/3 section of the reactor was shaded. The residence time is 1 minute	69
Figure 4.32 The intermediate compounds formed when the last 1/3 section of reaction was shaded. The residence time is 1 minute.....	70
Figure 4.33 The intermediate compounds formed when the second and the forth 1/5 section of the reactor was shaded. The residence time is 1 minute.....	71
Figure 4.34 The intermediate compounds formed when the middle 1/3 section of the reactor was shaded. The residence time is 3 minute	72
Figure 4.35 The intermediate compounds formed when the last 1/3 section of reaction was shaded. The residence time is 3 minute.....	73
Figure 4.36 Proposed degradation mechanism of diuron.....	76

CHAPTER I

INTRODUCTION

Thailand is regarded as an agricultural country. Chemicals used in agricultural activities in the past have contaminated the environment such as soil and groundwater. At present, it becomes a very serious environmental problem for the human health and the environment [1]. The common chemicals used in agriculture are pesticides and herbicides. One of these chemicals is diuron [N'-(3, 4-dichlorophenyl)-N, N-dimethylurea], which is one of the most widely used herbicides in Thailand. It belongs to the family of halogenophenylureas that represent an important class of contact herbicides applied in pre- and post-emergence to control broadleaf weeds. Diuron is also considered as highly toxic and persistent since it is bio-recalcitrant and has a great chemical stability. It has a long half-life over 300 days when used in high dosages to the soil. As the result, it can slowly penetrate through soil and contaminates water [2, 3].

Many methods to remove pesticide from water including adsorption, filtrations, biological treatment, photochemical and electrochemical treatments have been reported. The photocatalytic method is especially promising. Diuron can be degraded by the photocatalytic reaction on TiO_2 [3]. TiO_2 is one of the most commonly used semiconductor photocatalysts because it has wide band-gap energy (3.0 eV for rutile and 3.2 eV for anatase and high photoactivity). It is also relatively inexpensive, easy to handle and environmental friendly [3, 4]. Normally, large-scale reactors or batch reactors are widely used for photocatalytic degradation of diuron [3, 5-7]. However, limitation of the photocatalytic reaction in a batch reactor includes

high mass transfer resistance for the diffusion of diuron to the surface of the catalyst and low light penetration throughout the reactor. Moreover, the catalyst in form of nanoparticles that suspend in the solution is difficult to be separated from the aqueous solution.

Microreactor is one alternative that can be used to solve those problems. The unique features of the microreactor include laminar flow, short molecular diffusion distance, large surface-to-volume ratio and excellent heat transfer characteristics [8]. For photochemical reaction in the microreactor, high spatial illumination homogeneity and excellent light penetration throughout the reactor are also easily achieved [9]. Furthermore, it is relatively easy to deposit catalyst onto the surface of the micro-channel, so that it is more active for photocatalysis [10].

When the photocatalytic degradation of diuron is initiated, several intermediate products are generated which may have higher toxicity than diuron [7, 11, 12]. Many researchers reported about the intermediate products and the pathway of the degradation process by using TiO_2 in large-scale reactor [3, 5, 11]. However, it has never been reported about the intermediate products and the pathway of photodegradation of diuron by using TiO_2 in micro-system. It could be identify the intermediate formation that was formed before or after product. Using the continuous flow system, identification of intermediate products which are formed under exposure of light and those formed without light could be investigated. Therefore, it is an interest of this research to identify the in-depth formation of intermediates during the photocatalytic degradation of diuron.

The prime objective of this research is to investigate the kinetics of the photocatalytic degradation of diuron in a microreactor using TiO_2 as the photocatalyst whereas the effect of mass transfer resistance is excluded from the reaction system. It is also the objective of this work to identify intermediates from the reaction as well as the reaction pathway.

This thesis is consisted of five chapters as following:

Chapter I gives introduction of this research.

Chapter II describes theory and surveys of previous works relating to photocatalytic reaction such as photocatalyst synthesis, chemical and physical properties of titanium dioxide, chemical and properties of diuron, microreactor, the photocatalytic degradation of diuron, kinetics of photocatalytic degradation and intermediate products from the reaction.

Chapter III indicates materials, preparation of the catalyst, fabrication of a microreactor, characterizations of the catalyst and photocatalytic degradation of diuron in the microreactor.

Chapter IV describes the results and discussion of this research.

Chapter V concludes the overall results of this research.

CHAPTER II

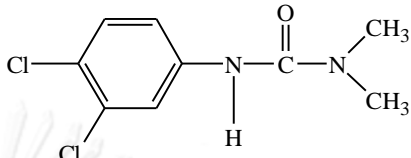
THEORY AND LITERATURE REVIEW

Theory and literature review relating to properties of diuron, physical and chemical properties of titanium dioxide, photocatalytic reaction, photocatalytic degradation of diuron and microreactor will be described in this chapter.

2.1 Diuron

Diuron [3-(3,4-dichlorophenyl)-1,1-dimethylurea] is an herbicide belonging to the family of halogenophenylureas [3]. It is one of the most frequently used herbicides on agriculture for elimination or control grass and broadleaf weed in a wide variety agricultural area. Diuron is considered highly toxic, bio-recalcitrant and chemically stable with a half-life of over 300 days [3, 5, 13, 14]. In addition, diuron is classified in the category of harmful chemical which a carcinogenic and genotoxic compound [15]. Since, diuron is slightly soluble (solubility in water is 36.4 mg/l, at 25°C) it can slowly penetrate through soil and contaminate underground water. In Europe-wide survey, diuron was detected in 70% of European river samples so it is considered a Priority Substance of the European Parliament on environmental quality standards (EQS) in the field of water policy and the EQS of Diuron is set to 0.2 µg/l [14]. The widespread use and environmental release of diuron have resulted in the contaminated in the surrounding. The properties of Diuron are shown in Table 2.1.

Table 2.1 Physicochemical properties of Diuron

Properties	Data
Chemical structure	
Molecular formula	$C_6H_{10}Cl_2N_2O$
Molecular weight	233.10
Melting point	158 – 159°C
Vapor pressure	0.0041 Pa at 30°C
Appearance	White crystalline solid
Synonyms	Cekiuron, Crisuron, Dailon, Diater Di-on, Derex4L, Diurex etc.
Solubility	42 mg/l in water at 20°C
Toxicity	The concentrated material may cause irritation to the eyes and mucous membrane, but a 50% water paste was not irritating to the intact skin of mammal.
Half-life	Over 300 days in soil [3]

2.2 Physical and Chemical Properties of Titanium dioxide

Titanium dioxide (TiO_2), also known as titanium (IV) oxide or titania is widely applied in many fields such as catalyst, catalyst support, electronics, cosmetic pigment especially in the field of environmental purification. Normally, titanium dioxide which found in nature has three crystalline structures, i.e. rutile, anatase and brookite as shown in Figure 2.1. The structure of titanium dioxide in each phase has different applications. Rutile phase is a thermodynamically stable phase. Anatase phase is a metastable phase which can transform to rutile by heating. For brookite phase, it is formed under hydrothermal condition and usually found in mineral. Among three crystalline structures, anatase crystal structure has the most photoactive phase. Anatase phase has a wide band gap of 3.2 eV.

For the photocatalysis application, anatase crystal structure is better than rutile for the following reasons: (a) the conduction band location for anatase is more favorable for driving conjugate reactions involving electrons, and (b) very stable surface peroxide groups can be formed on the anatase phase during photo-oxidation reaction but not on the rutile surface [16-19]. TiO_2 generates electrons and holes by irradiation with light. Most of the organic pollutants are decomposed into carbon dioxide and water by the effect of the holes with highly oxidation. Among the different sources of TiO_2 , Degussa P25 TiO_2 (Germany) has selected for this research. The physical properties of TiO_2 are shown in Table 2.2-2.4.

Table 2.2 The physical properties of TiO₂: Rutile phase [18].

Material name			Rutile			
Composition			TiO ₂			
System			Tetragonal			
Temperature (°C)			25			
$a(\text{Å}), b(\text{Å}), c(\text{Å})$			4.593(2)	4.593(2)	2.959(2)	
α (deg), β (deg), γ (deg)			90	90	90	
Unit cell volume (Å ³)			62.42			
D_x (g/cm ³)			4.25			
Space group			$P4_2/mnm$ (No. 136)			
Atom	Site	G	x/a	y/b	z/c	B (Å ²)
Ti	$2a$	1	0	0	0	0.42(6)
O	$4f$	1	0.3051(7)	0.3051(7)	0	0.6(6)

Table 2.3 The physical properties of TiO₂: Anatase phase [18].

Material name			Anatase			
Composition			TiO ₂			
System			Tetragonal			
Temperature (°C)			25			
$a(\text{Å}), b(\text{Å}), c(\text{Å})$			3.7842(13)	3.7842(13)	9.5146(15)	
α (deg), β (deg), γ (deg)			90	90	90	

Material name			Anatase			
Unit cell volume (\AA^3)			136.3			
D_x (g/cm^3)			3.89			
Space group			$I4_2/amd$ (No. 141)			
Atom	Site	G	x/a	y/b	z/c	B (\AA^2)
Ti	4a	1	0	0	0	0.390(63)
O	8e	1	0	0	0.2081(2)	0.613(90)

Table 2.4 The physical properties of TiO_2 : Brookite [18].

Material name			Brookite			
Composition			TiO_2			
System			Orthorhombic			
Temperature ($^\circ\text{C}$)			25			
a (\AA), b (\AA), c (\AA)			9.174(2)	5.449(2)	5.138(2)	
α (deg), β (deg), γ (deg)			90	90	90	
Unit cell volume (\AA^3)			257			
D_x (g/cm^3)			4.13			
Space group			$Pbca$ (No. 61)			
Atom	Site	G	x/a	y/b	z/c	B (\AA^2)
Ti	8c	1	0.1289(1)	0.0972(1)	0.8628(1)	0.37(3)
O	8c	1	0.0095(4)	0.1491(5)	0.1835(5)	0.46(6)
O	8c	1	0.2314(4)	0.1110(4)	0.5366(6)	0.53(7)

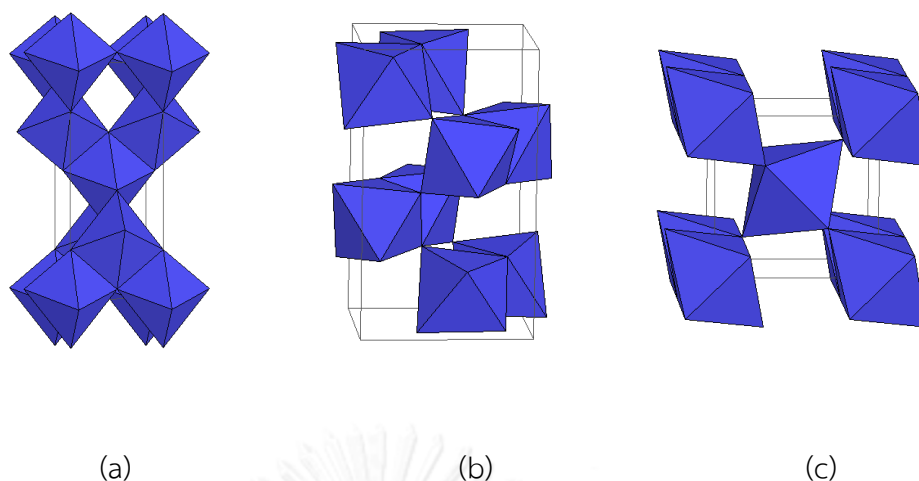


Figure 2.1 Crystal structure of TiO_2 ; (a) Anatase, (b) Brookite, (c) Rutile

Generally titanium dioxide is usually a powdery substance which requires special manage in handling. The used catalyst is recovered by filtration for its recycle; this is quite a difficult process because of the very fine nature of the powder. Thin film would be an attractive alternative to overcome the catalysts separation problems. In order to promote the practical application of material, it is necessary to immobilize TiO_2 photocatalyst through coating on the substrate.

Titanium dioxide thin film has been widely reported due to its potential applications as photocatalyst, gas sensor, solar cell, waste water treatment and so on. There are many techniques for fabrication TiO_2 film; vacuum evaporation, sputtering, laser-assisted vacuum evaporation, etc. These techniques are energy-intensive, high temperature and rather complicate. Also, these techniques have advantages in controlling over film growth and the feasibility to obtain a pure material. However, researchers studied wet chemical process from the economic investigations and some other advantages as simplicity and low temperature processing etc. Spin-coating method is widely applied amongst many wet chemical

processes as chemical bath deposition, electrodeposition, spray pyrolysis and sol-gel process etc. The sol-gel technique via spin-coating is one of the versatile techniques to prepare thin films even at low temperature. This technique has been properly used to make TiO_2 film because of appropriate homogeneity, easy to control composition, time-saving and low-cost. The procedure of spin-coating process is shown in Figure 2.2.

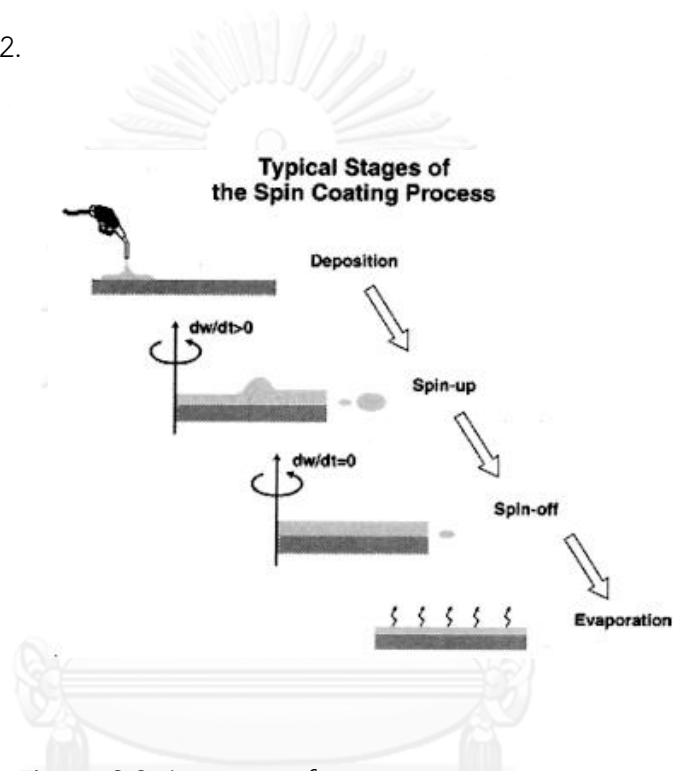


Figure 2.2 Key steps of spin coating process

2.3 Photocatalytic reaction

Recently, photocatalytic process has been widely used as an alternative physical-chemical process for the elimination of toxic and hazardous organic substances in wastewater, drinking water and air. Photocatalytic process has shown a great potential as inexpensive, environmental friendly and sustainable treatment technology. It can use sunlight or UV light which is available in abundance as the energy source to initiate the photo-decomposition of pollutants. The final products

of this treatment process are usually harmless compounds such as carbon dioxide, water and inorganic ions such as acids, chloride and nitrate. Photocatalytic reaction can also occur homogeneously or heterogeneously, but heterogeneous reaction is more intensively studied in recent year because of its potential use in variety of environmental. In heterogeneous reaction, the reaction implies that the formation at an interface between a solid catalyst (metal or semiconductor) and fluid as the reactants. Photocatalyst which particular used are semiconductor.

In this process, when a semiconductor activated by ultra-violet (UV) radiation or by photons of appropriate energy (equal to or more than its band gap width), an electron from the valence band promotes to the conduction band leads to the formation of a positive hole (h^+) in the valence band and an electron (e^-) in the conduction band (CB). The positive hole (h^+) in the valence band oxidizes either the pollutant directly or water to produce hydroxyl radical $\cdot OH$, whereas the electron in the conduction band reduces the oxygen adsorbed on the photocatalyst (TiO_2). Organic pollutants adsorb onto the surface of the catalyst are subsequently oxidized by $OH\cdot$ radicals as shown in Figure 2.3.

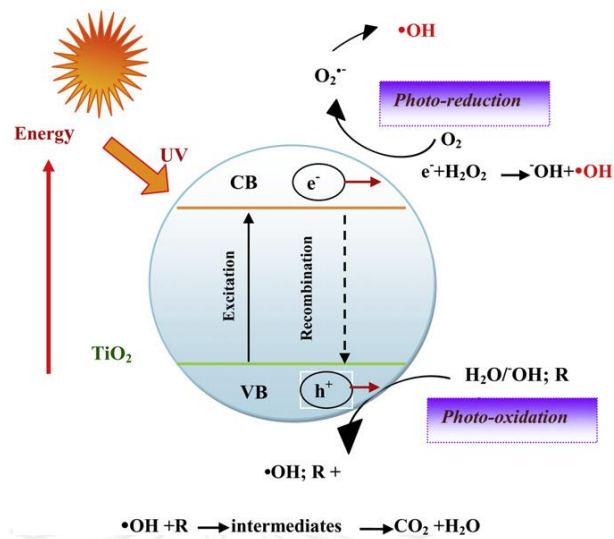


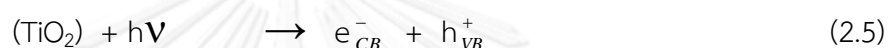
Figure 2.3 Schematic diagram of photocatalytic reaction

The generations of electron-hole pairs are represented in Eq. (2.1). The photo-generated holes and electrons give rise to oxidation and reduction processes, respectively. In an aqueous solution, water molecules adsorb onto surface of the catalyst. They are oxidized giving rise to OH[•] radicals. As the process is usually carried out in aerobic conditions, the species to be reduced is oxygen, generating the superoxide radical as following Eq. (2.2) to (2.4).



The required energy that has to be supplied by the photons for the promotion of the electrons depends on the band gap for the specific material. The band gap energy, E_g of TiO_2 (anatase) is 3.2 eV, which corresponds to photons with a wavelength of 388 nm. The mechanism of the photocatalytic degradation of aqueous organic compound on anatase titania can be expressed by a series of advanced oxidation process as following [20].

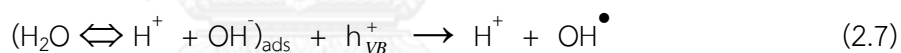
- 1) Absorption of efficient photons ($h\nu \geq E_g = 3.2$ eV) by titania



- 2) Oxygen ionosorption (first step of oxygen reduction)



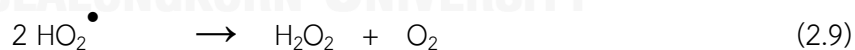
- 3) Neutralization of OH^- groups by photoexcited holes



- 4) Neutralization of $\text{O}_2^{\bullet-}$ by protons



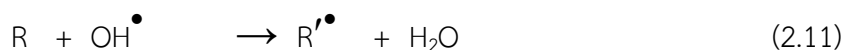
- 5) Transient hydrogen peroxide formation



- 6) Decomposition of H_2O_2 and second reduction of oxygen



- 7) Oxidation of the organic reactant via successive attack by OH^{\bullet} radical



8) Direct oxidation by reaction with holes



Eventually, an organic compound or degradation products can be completely degraded to carbon dioxide and water because the hydroxyl radical is a powerful oxidising agent. Table 2.5 below compares the oxidising power of common oxidising agent with the hydroxyl radical produced in photocatalysis.

Table 2.5 Comparative oxidising power of common oxidants. [17]

Oxidant	Oxidation Potential (V)
OH radical	2.80
O ₃	2.07
H ₂ O ₂	1.77
ClO ₂	1.49
Cl ₂	1.35

2.3 Photocatalytic degradation of diuron

Nowadays there are many treatment technologies for eliminating an herbicide including filtration [21-23] or adsorption [24, 25]. However all of these techniques can only separate the herbicide from the solution. Therefore, advanced oxidation process (AOPs) which can mineralize diuron to non-toxic compounds are increasingly interested as an alternative for the treatment of herbicide in soils or groundwater. AOPs are based on the use of highly reactive oxidizing

radicals such as hydroxyl radical (OH^\bullet) to oxidize organic contaminants [26, 27]. Hydroxyl radical is much more reactive than other radicals and it is easily created by photocatalyst. The complete oxidation of diuron was proposed as the following stoichiometric equation [3]:



Several researchers have studied about photocatalytic degradation of Diuron by using titanium dioxide. Sayeh et al. (2007) [2] degraded diuron in aqueous solution using TiO_2 as photocatalyst in oxidation process. This experiment was performed in a batch reactor equipped with UV-lamp (254 nm). The results indicated that the degradation rate of diuron solution was also increased with increasing amount of catalyst, pH adjustment toward acidic condition and increased light intensity. The percentage of degradation obtained were about 70-90% within in the degradation time over 60-120 min.

Katsumata et al. (2009) investigated the photodegradation of diuron in aqueous solution by platinized TiO_2 catalyst. Platinization of TiO_2 was found to increase the photocatalytic activity. The optimum condition for doping Pt was 0.2 wt% and the degradation of diuron was achieved after 20 min. When diuron was irradiated by UV or sunlight, it generated many by-product compounds which have higher toxic effect than parent Diuron during degradation [7, 11, 12]. Hence it is interest not only to monitor the degradation of the parent compound but also to identify the intermediate compounds formed. Mestankova et al. [12] studied the toxicity of degradation products of diuron that was

formed during photo-oxidation process. *Pseudokirchneriella subcapitata* is algae used for evaluation the toxicity. From the result, they found that hdroxylated compounds presented toxicity lower or similar to diuron but other compounds are more toxic than parent compound. The pathways of the photocatalytic degradation of diuron were reported by many researchers. Lopez et al. [11] studied photolytic degradation of phenylurea herbicides including diuron, linuron and isoproturon etc. by UV light (250 nm) in batch reactor.

2.3.1 The kinetic of photocatalytic degradation

Since photocatalysis is a surface reaction, the important step in intervening for the effectiveness of photodegradation is the adsorption process of the pollutants on the surface photocatalyst. Many researchers found that the kinetics of photocatalytic degradation is well represented by the Langmuir-Hinshelwood (L-H) kinetics model. This model assumed that the reaction occurs on the surface and the rate of reaction (r) is proportional to the fraction of surface covered by the substrate (θ).

$$r = -\frac{dC}{dt} = k_r \theta = k_r \frac{KC}{1+KC} \quad (2.14)$$

Integrating the above equation:

$$\ln\left(\frac{C_0}{C}\right) + K(C_0 - C) = k_r Kt \quad (2.15)$$

where; k_r is the true reaction rate constant

K is the constant of adsorption equilibrium of L-H model

C is the substrate concentration

t is the irradiation time

When the solution is highly diluted, the term KC can be neglected. In this case the reaction is essentially an apparent first order reaction and after integration, Eq. 2.15 can be simplified in Eq. 2.16.

$$r = -\frac{dC}{dt} = k_r KC = k_{ap}C \quad (2.16)$$

Eq. 2.16 can be simplified to the first order reaction when C_0 is very small, integrating Eq. 2.16. into simplified Eq. (2.17)

$$\ln \frac{C_0}{C} = k_{ap}t \quad (2.17)$$

Where k_{ap} is the apparent rate constant of the pseudo first order reaction.

Bamba et al., (2008) and Bouquet et al., (2000) studied the photocatalytic degradation of diuron by two commercial titanium dioxide. The result has shown that the kinetic model followed the L-H model and the rate of degradation is proportional to the initial concentration.

2.3.2 Intermediate products from the degradation of diuron

The effect of the presence of TiO_2 on intermediate product in photolytic degradation was investigated. [3, 11, 28, 29] In the absence the TiO_2 the irradiation of diuron yielded mainly 2 products, hydroxychloro derivatives, probably through a photohydrolysis reaction. In the presence of TiO_2 (Degussa P-25), the photocatalytic degradation of diuron proceeds by several pathway;

- (1) The oxidation of the methyl group of the side chain.
- (2) Chlorine substitution on the aromatic ring.

(3) Hydroxylation of the aromatic ring.

(4) Dechlorination.

Carrier et al. [5] studied the mechanism detail of photocatalytic oxidation of diuron which has been performed in presence of TiO_2 suspensions by stirred batch reactor equipped with 365 nm UV light. The degradation of diuron was completed within 90 min and the mineralization was longer process that was only completed after a 540 min treatment. The main pathway of photocatalytic degradation of diuron was proposed as shown in Figure 2.5.

(1) Dehalogenation of the aromatic ring including [3-(3-chloro-4-hydroxy)-1,1-dimethyl-urea] and [3-(3-hydroxy-4-chlorophenyl)-1,1-dimethylurea].

(2) Hydroxylation of the aromatic ring that positions in ortho of C-N on the aromatic cycle will be preferentially hydroxylated and of the side chain (as shown in Figure 7 including [3-(3,4-dichloro)-1-hydroxymethyl-1-methylurea].

(3) Demethylation including [3-(3,4-dichlorophenyl)-1-formyl-1-methylurea] and [3-(3,4-dichlorophenyl)-1-hydroxymethyl-urea].

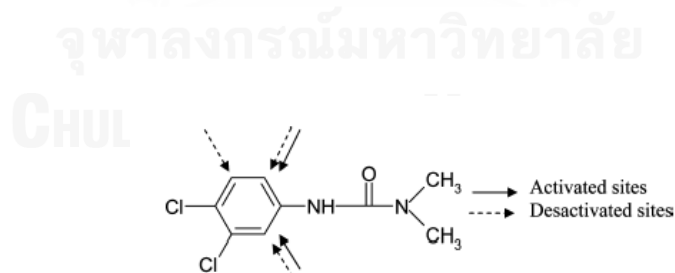


Figure 2.4 The active sites of electrophilic attack on the aromatic ring of diuron. [5]

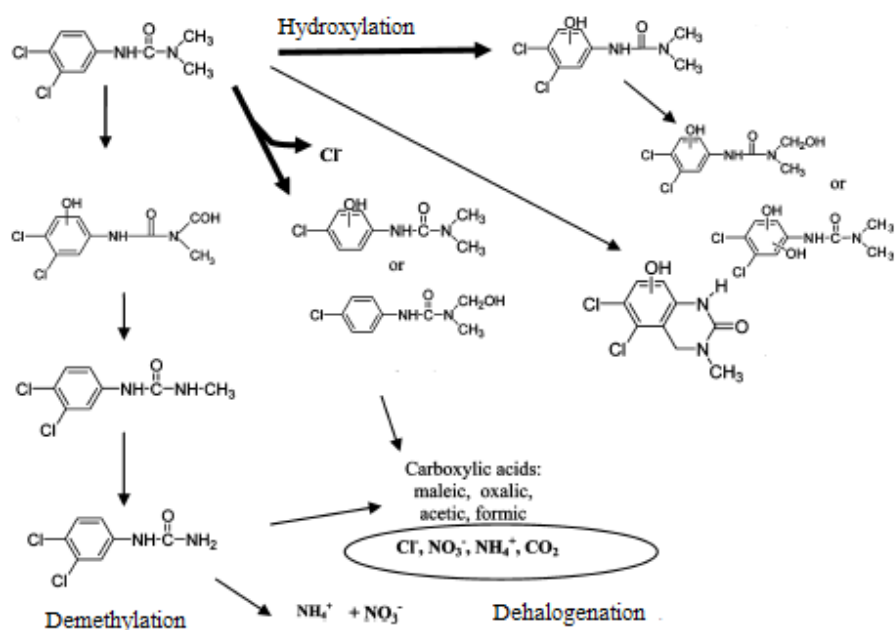


Figure 2.5 The main pathway of photocatalytic degradation of diuron.

Katsumata et al. [3] proposed the pathway of the photocatalytic degradation of diuron in aqueous solution by platinized TiO_2 as shown in Figure 2.6. Four products were identified by GC/MS. Other degradation products still possibly would exist in the reaction system but can not be detected because of their low concentration. For the pathway, the first step was initiated by the attack on the aromatic ring by OH^\bullet radicals without dechlorination or alkyl chains. The next step involved a series of oxidation processes that eliminated alkyl groups and chlorine atoms. The last step involved oxidative opening of the aromatic ring, lead to small organic ions and inorganic species.

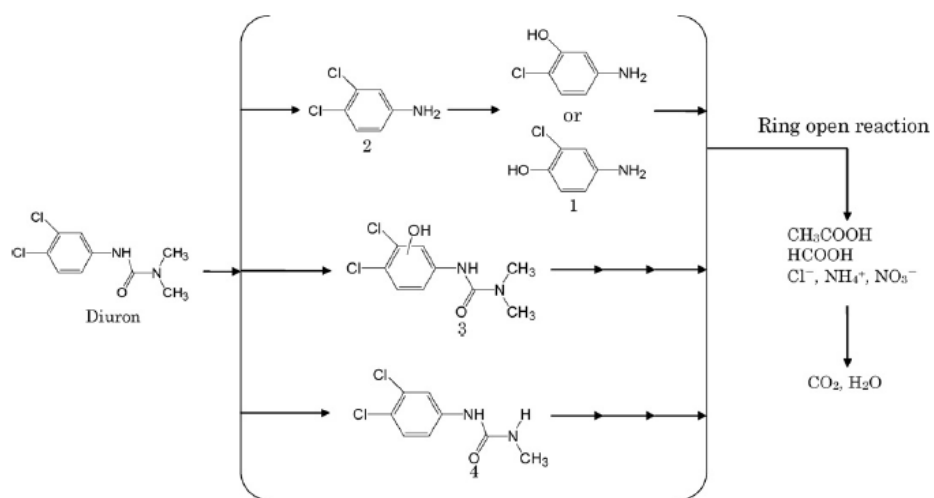


Figure 2.6 Proposed degradation mechanism of diuron by the photocatalytic system

The other structures of intermediates detected were proposed in Table 2.6.

Table 2.6 Possible intermediates generated from photodegradation of diuron on and titanium dioxide. [3, 5, 6, 26, 30, 31]

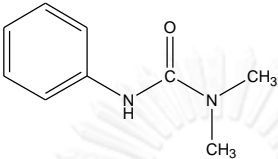
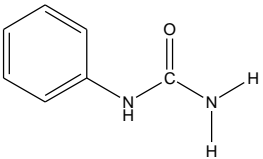
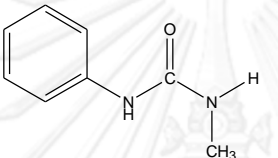
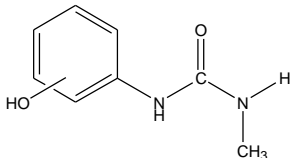
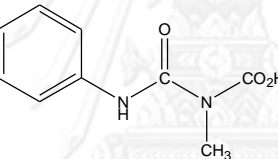
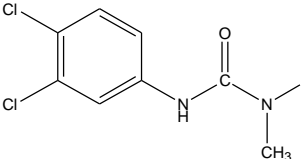
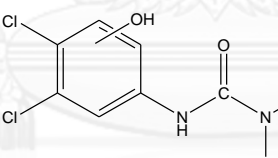
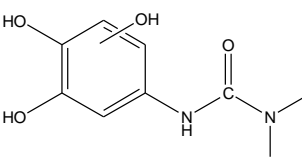
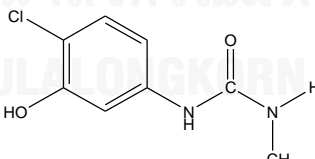
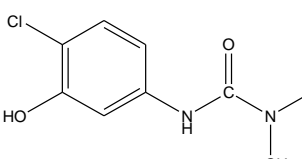
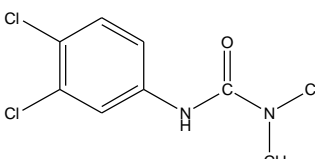
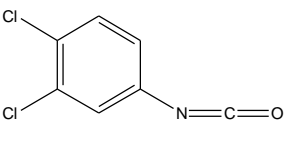
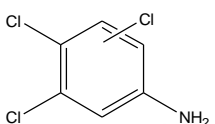
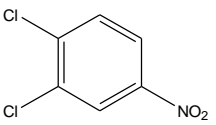
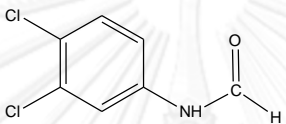
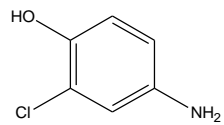
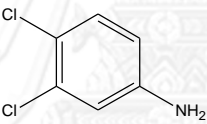
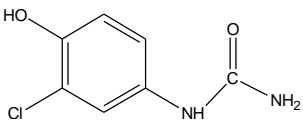
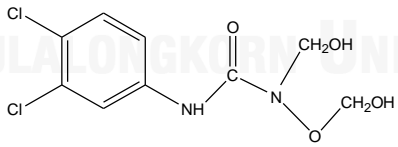
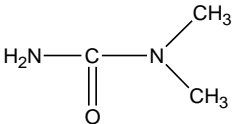
Compound	Structural formular	Compound	Structural formular
1		2	
3		4	
5		6	
7		8	
9		10	
11		12	

Table 2.6 (continue).

Compound	Structural formular	Compound	Structural formular
13		14	
15		16	
17		18	
19		20	

2.4 Photocatalytic reaction in Microreactor

During recent years, microreaction technology has developed into a valuable tool for the chemical industry and many other users who are looking for miniaturized and mobile applications of chemical systems [32]. A microreactor or microstructured reactor is a device in which chemical reactions take place in a confinement with typical lateral dimensions below 1 mm; the most typical form of such confinement are microchannels which is used for flow fluid through it. The microreactor is usually a continuous flow reactor. The unique properties of microreactor over conventional scale reactors include vast improvements in energy efficiency, reaction speed and yield, safety, reliability, scalability, on-site/on-demand production, a much finer degree of process control, laminar flow, short molecular diffusion distances, large surface-to-volume ratio and excellent heat transfer characteristics [8]. These properties can improve efficiency of reaction as well. So, microreaction systems have been examined for wide range of applications of organic chemistry. However, there are still few researches on photoreaction in microreactors nowadays.

For photochemical reactions, microreactors exhibit high spatial illumination homogeneity and excellent light penetration throughout the reactor [9]. Moreover, it is relatively easy to coat catalysts onto the surface of microchannel to increase surface-to-volume ratio and avoid a costly separation step necessary after reaction. So, it can improve efficiency of photocatalytic reactions very well. Gorges et al. [33] degraded 4-chlorophenol by using a microreactor in which immobilized TiO_2 used as photocatalyst. This microreactor was illuminated by UV-A light emitting

diode. The microreactor had 19 microchannel and cross-section of $200 \times 300 \mu\text{m}^2$. TiO_2 was deposited on the microreactor surface by CVD and anodic spark deposition. The results indicated that higher degradation was observed for lower initial concentration (for the initial concentration of 0.05 mmol/L , the degradation achieved $C/C_0=0.62$ within 10 min). Furthermore, the degradation activity was increased with decreasing flow rate because of decreasing in residence time of the reactant in the microchannel. The limitation of the overall degradation rate by mass transfer could be excluded by evaluating appropriate Damköhler number as following Eq. 2.18.

$$Da_{II} = \frac{k_a}{\beta a / K + \beta a c_b} \quad (2.18)$$

Where: k_a is the apparent rate constant

β is the mass transfer coefficient

a is the interfacial area per unit volume

K is the Langmuir adsorption coefficient

c_b is the bulk concentration of the solution

The mass transfer coefficient can be estimated from Sherwood numbers as following Eq.2.19.

$$Sh = \frac{\beta d_h}{D} \quad (2.19)$$

Where: Sh is Sherwood numbers
 d_h is the hydrodynamic diameter of microchannel
 D is the molecular diffusion coefficient

The asymptotic behavior of a system is given by

$Da \ll 1$ (Slow reaction, the reaction rate is limited by surface reaction)

$Da \gg 1$ (Rapid reaction, the reaction rate is limited by mass transfer)

The illuminated specific surface of the microreactor was larger than that of the conventional reactor about 4-400 times.

For typical fluid dynamic conditions in microchannels, such as low flow rates and laminar flow, Sh numbers reach the asymptotic value of 3.66 (M. Fichtner, et al, 1998). The mass-transfer coefficient can be estimated from Sherwood numbers with $Sh = \beta d_h / D$, where d_h is the hydrodynamic diameter of a microchannel and D the molecular diffusion coefficient. The value of D for diuron is $8 \times 10^{-10} \text{ m}^2 \text{ s}^{-1}$ (Polcaro, 2004). Therefore, mass-transfer coefficients can be calculated with $\beta = 3.66D/d_h$.

Matsushita et al. [9] examined the photo-oxidation process of high-concentration phenol in aqueous solution in both of a microreactor and a large-scale flow system. For the microreactor, microchannels were coated with a thin layer of TiO_2 by using sol-gel method and illuminated with a 365-nm UV-LED. For large-scale reactor, the cone-shaped photocatalytic fiber modules (TiO_2 -covered SiO_2 fiber) were stacked in a cylindrical reaction chamber and excited with Hg lamp. The results indicated that the

photodegradation yield reached 17% by 5 min of the irradiation of the microreactor while the yield was 15% by 360 min in the large-scale system. The reaction in large-scale system was formed intermediates from the photocatalytic degradation of phenol which are hydroquinone and catechol. They are observed in large-scale system, while these compounds were not detected in microreactor. These compounds prevented light penetration to inside large-scale system. In microreactor, the residence time is very short and does not retain the reaction products, so they prevented intermediates and increase efficiency of reaction. In real case, the microreactor will be used in water treatment processes for consume or drinking. The use of microreactor for developing scaleable process regimes is using an approach engineer call 'numbering up'.

CHAPTER III

EXPERIMENTAL

This chapter describes about the experimental procedures for catalyst preparation, characterization of catalyst film and photocatalytic degradation of diuron in a microreactor. It is divided into five parts: materials, preparation of P25 Degussa TiO₂ for coating, fabrication of a microreactor, characterization of catalyst, photocatalytic degradation in a microreactor.

3.1 Materials

Diuron (99.5% purity, N-(3,4-dichlorophenyl)-N,N-dimethylurea) was purchased from Aldrich Company. The photocatalyst which used in this research was Degussa P-25 titanium dioxide (80:20 anatase/rutile, average particle size 21 nm, specific surface area 35-62 m²/g (BET)) obtained from Sigma-Aldrich. Ethanol (99.9%) was used as solvent for preparation of P25-TiO₂ solution for coating. Acetonitrile (99.9%) was used for mobile phase for HPLC analysis. The soda-lime glasses were used as the substrates for the TiO₂ film. Before of coating, the soda-lime glasses were washed in deionized water, ethanol and acetone respectively for 1 hour in each solution with ultrasonic bath.

3.2 Preparation of catalyst film

Thin P25 TiO₂ films were deposited on glass substrate by a spin-coating technique. The catalyst (P25 TiO₂, 5 g) was suspended in 100 ml of ethanol. The suspension was stirred for 30 minutes to disperse the solution effectively. The solution about 1 dropper (1 ml) was spin coated for 1 minute. After coating, catalyst

film was dried at 80 °C for 24 hrs to displace solvent. The amount of TiO₂ coated on the substrate supports was estimated from the difference in the weight of the supports before and after coating. Each film coated in glass substrate contains about 2 mg of catalyst.

3.3 Fabrication of a microreactor

In this study, we fabricated a microreaction system in which TiO₂ was deposited as the photocatalyst. The microstructured device was manufactured from soda-lime glass. One piece of glass substrate was deposited with TiO₂ film by spin-coating method as mentioned above. The other blank soda-lime glass, which was drilled for inlet and outlet stream and then was placed together on the coated soda-lime glass. A layer of teflon and aluminium foil with 0.8 cm x 4.8 cm opening was placed between the glass substrates to create a micro-channel as shown in Figure 3.1. The microstructure was set in stainless steel housing. The microreactor was fabricated at various thickness by varied the number of the layer of teflon (1 layer was approximately equal 250 μm). The volume of reactor is 0.096 ml.

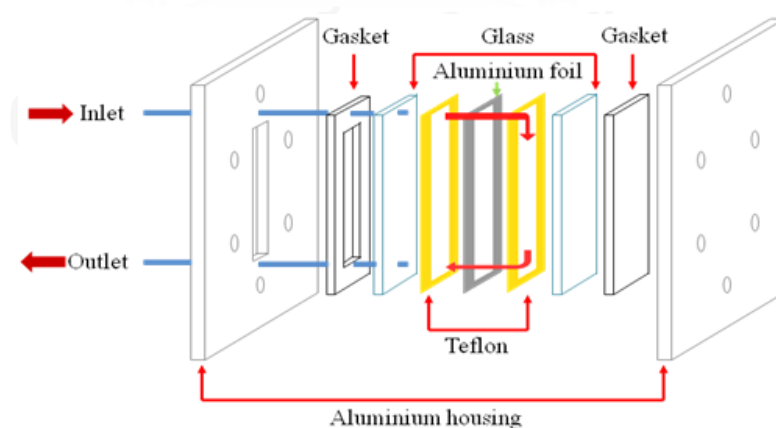


Figure 3.1 Microreactor set up.

3.4 Characterization of catalyst film

3.4.1 Field Emission Scanning Electron Microscope (FESEM)

The morphology and the thickness of TiO₂ thin film were observed by field emission scanning electron microscope (FESEM, JSM-7001F) at Thailand Center of Excellence in Physics (ThEP), Chulalongkorn University.

3.4.2 Inductive Coupled Plasma Optical Emission Spectrometer (ICP-OES)

The amount of TiO₂ that may come out into the sample was investigated by Inductive Coupled Plasma Optical Emission Spectrometer (ICP-OES, OES700) at Chulalongkorn University.

3.5 Photocatalytic Activity Testing

3.5.1 Photocatalytic degradation of diuron in a microreactor.

Photocatalytic degradation of diuron in aqueous solution was employed to investigate the photocatalytic activity of film TiO₂ that deposited in a microreactor under UV irradiation. The initial concentration of diuron solution was fixed at 10 ppm. The diuron solution was continuously pumped into micro-channel of the microreactor by a syringe pump. Flow rate of the diuron solution were varied from 0.4 – 5.8 ml/hr. At first, the diuron solution was supplied to the reactor in the dark at least 1 hr to ensure that the adsorption of diuron solution onto the catalyst was completed. The photocatalytic reaction was initiated by exposing microreactor to light from UV-A lamp (Sylvania F40W/350 BL). The schematic diagram of the

equipment set-up for photodegradation of diuron in a microreactor is shown in Figure 3.2.

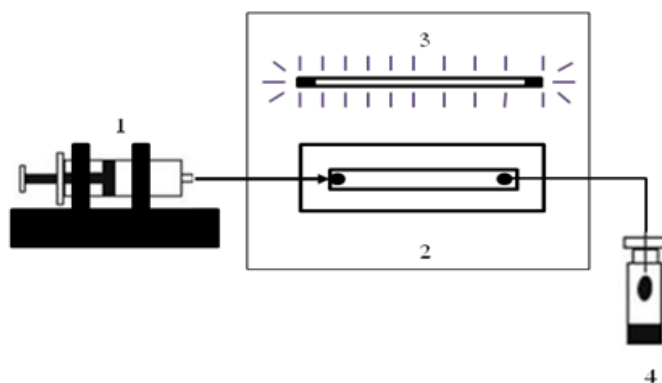


Figure 3.2 Equipments set-up for photocatalytic degradation process. The processes are consist: (1) Syringe pump, (2) Microreactor, (3) UV-A lamp and (4) Sample

3.5.2 Study of effect of light light on intermediate formation

An in-depth, studying formed of intermediate products during the reaction was investigated. The experiment was set as the same as in section 3.5.1. We have done by controlling the time of exposing with the black tape. We varied condition into three conditions: on-off-on, on-on-off and on-off-on-off-on as shown in Figure 3.3, respectively.

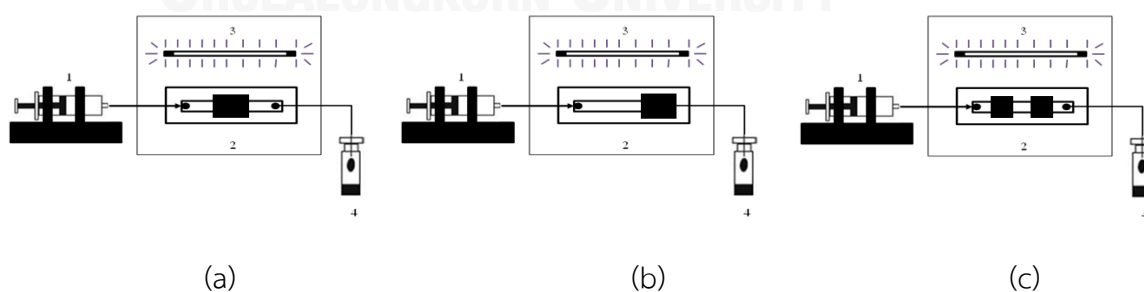


Figure 3.3 Equipment set-up for controlling the time of exposing with the black tape: (a) on-off-on, (b) on-on-off and (c) on-off-on-off-on

After the reaction was started, the sample was collected and periodically analyzed using a reverse phase high performance liquid chromatography (HPLC), model Class VP (Shimadzu) with C18 column (Phenomenex Luna 5 μ m particle size, 250x4.6 mm). The mobile phase was consisted of 70% (v/v) acetonitrile and 30% (v/v) deionized water with a flow rate of 1.5 ml/min and a UV detector at 254 nm. Intermediate products formed during the photocatalytic degradation of diuron were identified by liquid chromatography with mass spectrometer (LC-MS, Bruker Daltonics) with phenyl column (Vertisep UPS column, 2.1x100mm) and an ESI ion source operating both positive ion mode and negative ion mode in range 70-1,000 m/z. The mobile phase was consisted of 60% (v/v) acetonitrile and 40% (v/v) deionized water with flow rate of 0.2 ml/min.

3.5.3 Photocatalytic degradation of three standard intermediates

In this section, we also performed the experiments to correctly predict path way of diuron degradation. Photocatalytic degradation of three standard intermediates including 1-(3, 4-dichlorophenyl-3-methylurea), 3-(3, 4-dichlorophenyl)-1-formyl-1-methylurea and 3, 4-dichloroaniline were studied under the same condition in photocatalytic degradation of diuron in microreactor. The initial concentration of each solution was 10 ppm and the concentration in the outlet stream was analyzed by HPLC.

CHAPTER IV

RESULTS AND DISCUSSION

The photocatalytic degradation of diuron can be successfully applied in a microreactor to eliminate organic compounds from wastewater. In this chapter, titanium dioxide thin films were used as catalyst and effects of residence time, thickness of microchannel and the formation of intermediate products during the photocatalytic degradation were studied. Moreover, intermediate products formed under exposure of light and without light were investigated.

4.1 Synthesis of TiO₂ film via Spin-coating method

Titanium dioxide used in this work is the commercial Degussa P25 titanium dioxide (80:20 anatase/rutile, average particle size 21 nm, specific surface area 35-62 m²/g (BET)) obtained from Sigma-Aldrich. The catalyst films can also be prepared by many methods but spin-coating method was used in this work. Spin-coating method is easily handled, fast process time, using inexpensive equipment and high uniformity. The morphology and the thickness of thin films which prepared in this process were observed by the cross-sectional image using a field emission scanning electron microscopy instrument (FESEM, JSM-7001F). The amount of TiO₂ that may come out into the sample was investigated by Inductive Coupled Plasma Optical Emission Spectrometer (ICP-OES, OES700).

4.1.1 Characterization of TiO₂ thin films

After spin-coating process, the product was dried at 80 °C for 24 hours and then a sample of this product was investigated by SEM. The surface morphology of SEM images is shown in Figure 4.1 (a-d). Image 4.1a is a substrate without catalyst while Figure 4.1b is a surface morphology of TiO₂. This feature in Figure 4.1b shows that the powder of commercial TiO₂ is spreaded over the surface. Most of nano-TiO₂ particles remained to their original shapes. Another observable characteristic is the thickness of the films that was verified by the cross-sectional image with SEM. Figure 4.1c and 4.1d show the SEM image of TiO₂ coated films with rather rough surface and the thickness of films was about 5 μm, respectively.

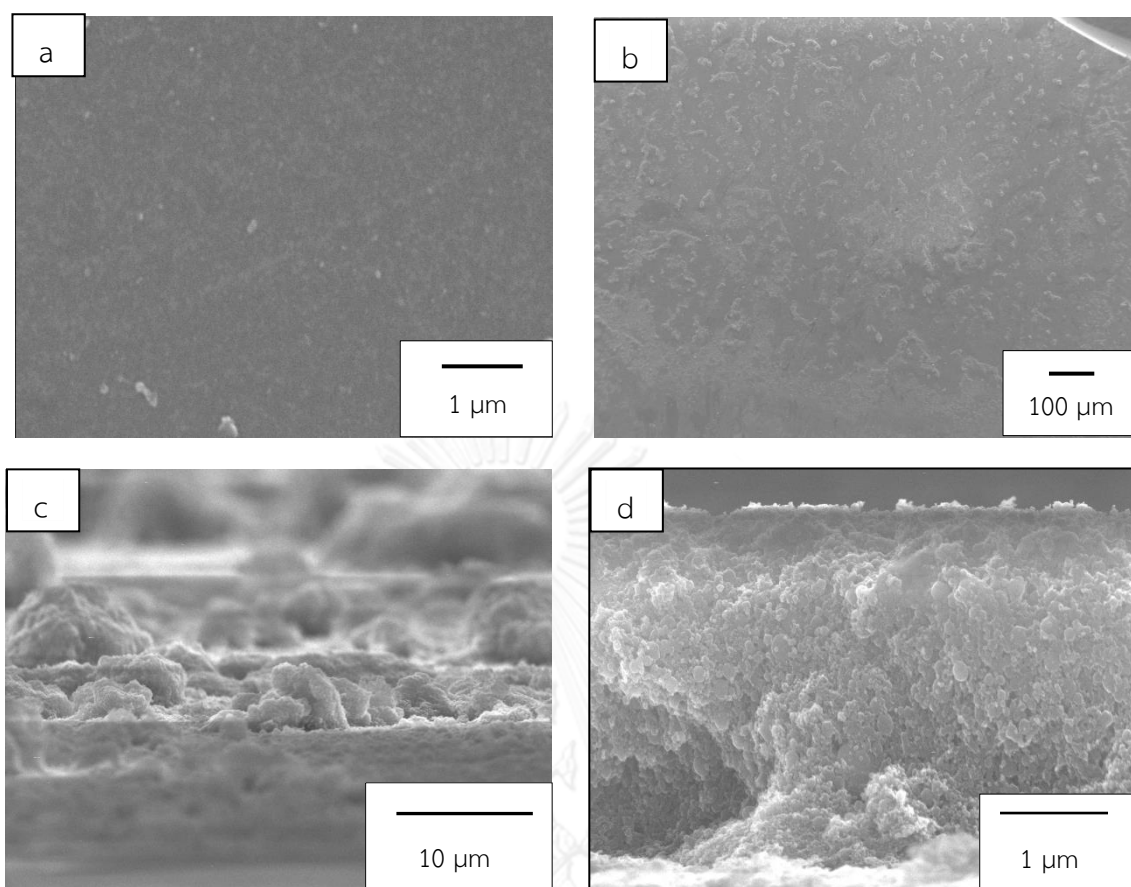


Figure 4.1 SEM images of TiO_2 film from spin-coating method: (a) substrate without catalyst, (b) surface morphology of product, (c-d) cross-sectional of product.

4.1.2 Quantity of TiO_2 in runoff samples

The quantitative information about the concentration of metals including titanium (Ti) in the form of titanium oxide nanoparticles was measured by inductive coupled plasma optical emission spectrometry (ICP-OES, OES700). The sample solution about 25 ml is prepared by adding nitric acid to dissolve titanium dioxide nanoparticles present in the diluted sample, the ICP-OES measurements was done at a wavelength of 336.122 nm for Ti.

The Ti concentration in the sample solution that analyzed by ICP was 0.0941 mg/l. It is directly related to the concentration of TiO₂ in the sample then amount of TiO₂ can be calculated. Based on weight of TiO₂ as coated on substrate, it was able to give a rough estimate the amount of TiO₂ in runoff samples. The result of ICP detection traces amount of TiO₂ respond to < 1%. This experiment verifies that the TiO₂ particles were not washed off by the flow of liquid.

4.2 Photocatalytic degradation of diuron in microreactor

In this work, the photocatalytic degradation of diuron in aqueous solution was employed to investigate the photocatalytic activity of the TiO₂ deposited as a thin film under UV-A irradiation. The amount of TiO₂ coated on the substrate supports contains about 2 mg. The initial concentration of diuron solution was fixed at 10 ppm. The diuron solution was continuously pumped into microchannel of the microreactor by syringe pump. Flow rate of the diuron solution were varied from 0.4 to 5.8 ml/hr (which corresponded to residence time of 1-15 minutes). Prior to the reaction, the diuron solution was supplied to the microreactor in the dark at least 1 hour to ensure that the adsorption of diuron solution onto the catalyst was completed. After the reaction started, the sampling was taken every 30 minutes and analyzed by HPLC.

4.2.1 Effect of residence time

The effect of residence time on the photocatalytic degradation of diuron was studied. Residence times varying from 1 to 15 minutes were conducted and the corresponding flow rates were decreased from 5.8 h to 0.4 ml/h. The

concentration of diuron in the outlet stream of the microreactor with respect to the inlet concentration (C_{out}/C_{in}) is shown in Figure 4.2-4.5.

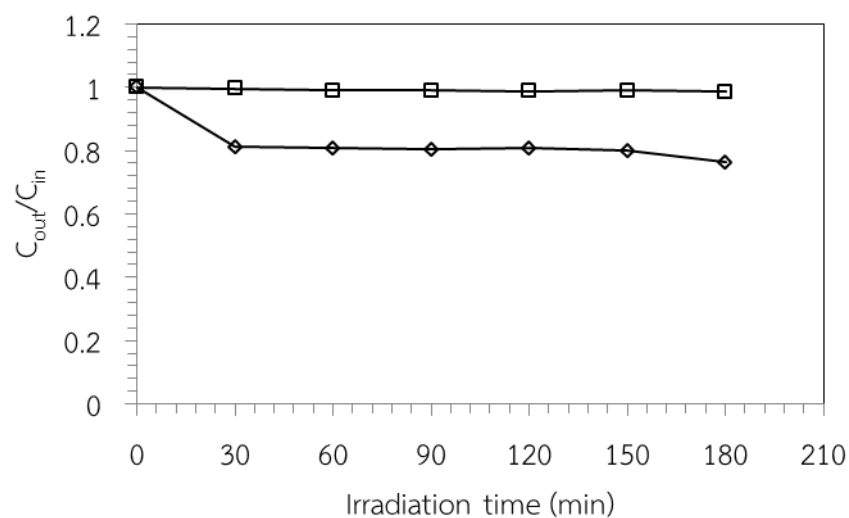


Figure 4.2 Concentration of diuron in the outlet stream from the reactor with consider to the initial concentration at residence time 1 minute: (\square) photolysis and (\diamond) photocatalytic reaction on TiO_2 . The thickness of microchannel is 250 μm .

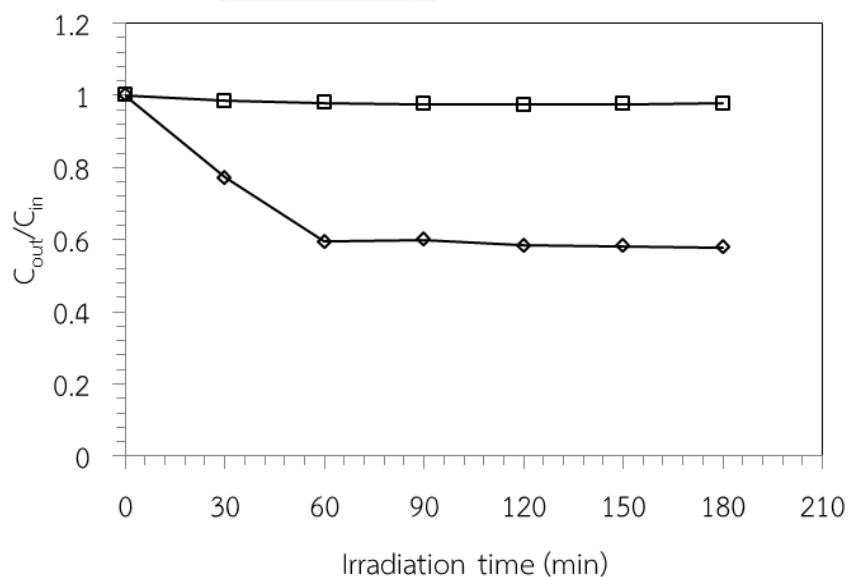


Figure 4.3 Concentration of diuron in the outlet stream from the reactor with consider to the initial concentration at residence time 5 minutes: (\square) photolysis and (\diamond) photocatalytic reaction on TiO_2 . The thickness of microchannel is 250 μm .

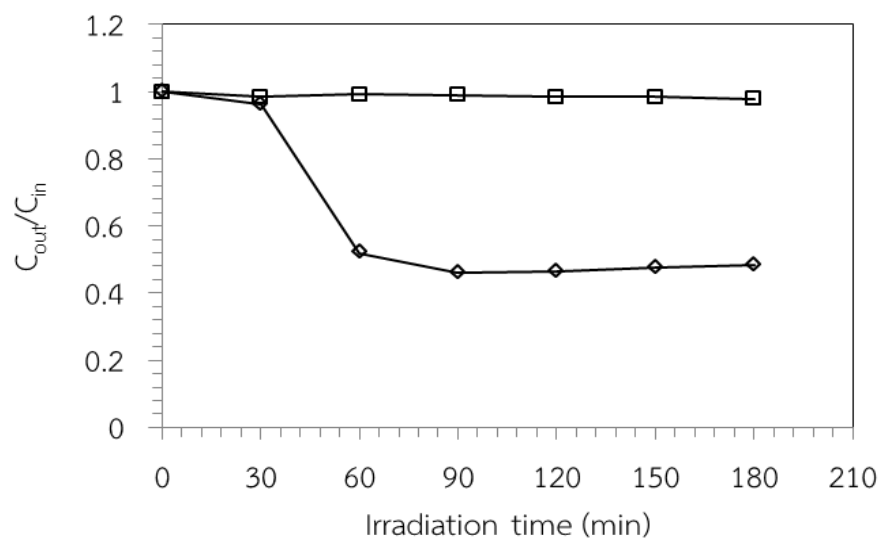


Figure 4.4 Concentration of diuron in the outlet stream from the reactor with consider to the initial concentration at residence time 10 minutes: (\square) photolysis and (\diamond) photocatalytic reaction on TiO_2 . The thickness of microchannel is 250 μm .

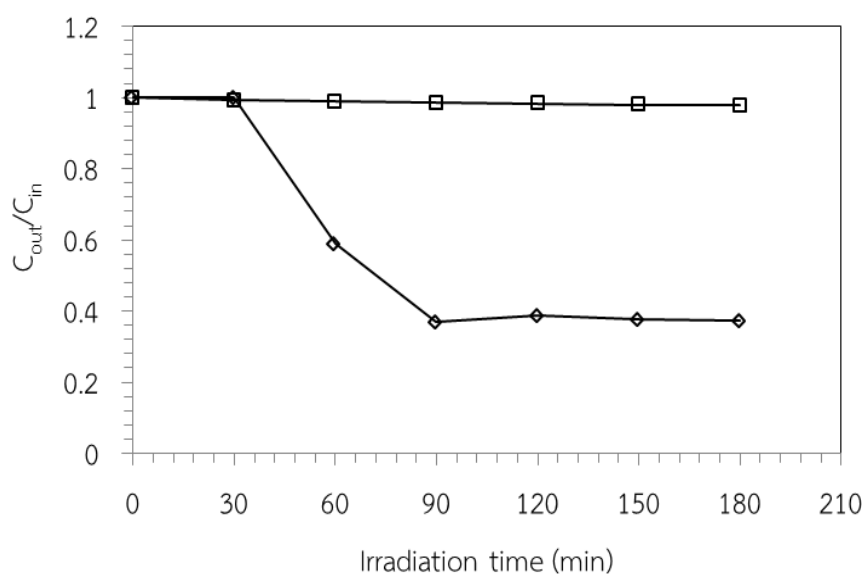


Figure 4.5 Concentration of diuron in the outlet stream from the reactor with consider to the initial concentration at residence time 15 minutes: (\square) photolysis and (\diamond) photocatalytic reaction on TiO_2 . The thickness of microchannel is 250 μm .

From Figure 4.2-4.5, the results are compared with the photolysis. The degradation via the photolysis can be neglected because diuron has high chemical stability. Thus it can be inferred that there is significant degradation occur on TiO_2 . As the residence time increased, interactions between diuron and TiO_2 increased which resulted in a higher yield of degradation. From the results, residence time of 1, 5, 10, 15 minutes yields the steady-state degradation of 24%, 42%, 52% and 63%, respectively. Figure 4.6 shows photocatalytic degradation of diuron in microreactor for different residence time. Figure 4.7 shows photocatalytic degradation of diuron in microreactor for different residence time and degradation efficiency.

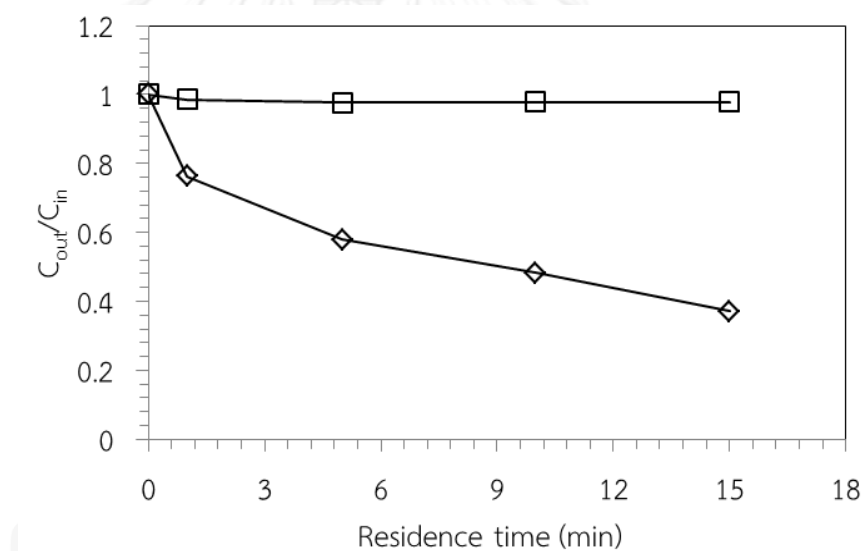


Figure 4.6 Concentration of diuron in the outlet stream from the reactor with consider to the initial concentration for all four residence time: (\square) photolysis and (\diamond) photocatalytic reaction on TiO_2 . The thickness of microchannel is $250 \mu\text{m}$.

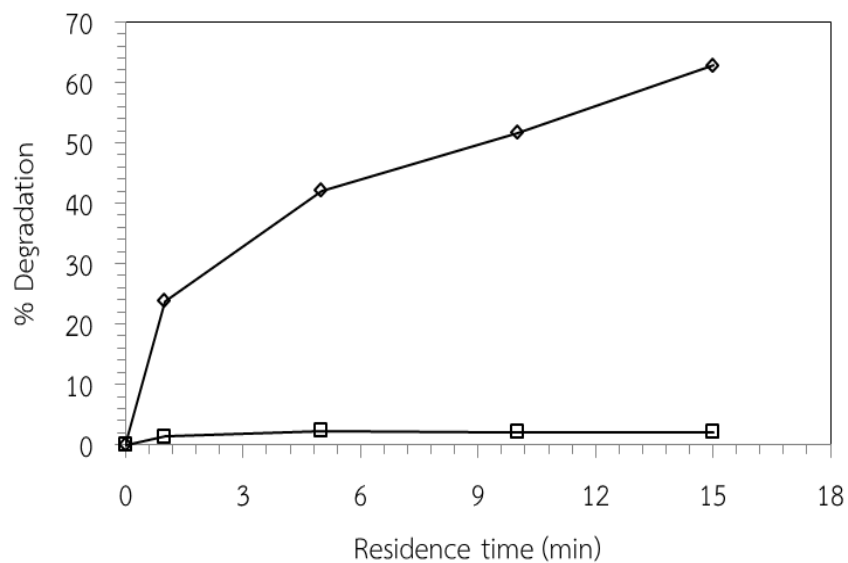


Figure 4.7 Photocatalytic degradation of diuron in microreactor for all four residence time and degradation efficiency: (□) photolysis and (◇) photocatalytic reaction on TiO₂. The thickness of microchannel is 250 μm.

4.2.2 Effect of thickness of micro-channel

The effect of thickness of micro-channel on the photocatalytic degradation of diuron was studied. In this effect, the residence times were fixed at 1, 5, 10 and 15 minutes, respectively. Three value of the thickness include 250, 500 and 750 μm were conducted in each the residence time. . The concentration of diuron in the outlet stream of the microreactor with respect to the inlet concentration (C_{out}/C_{in}) under various thickness are shown in Figure 4.8-4.11.

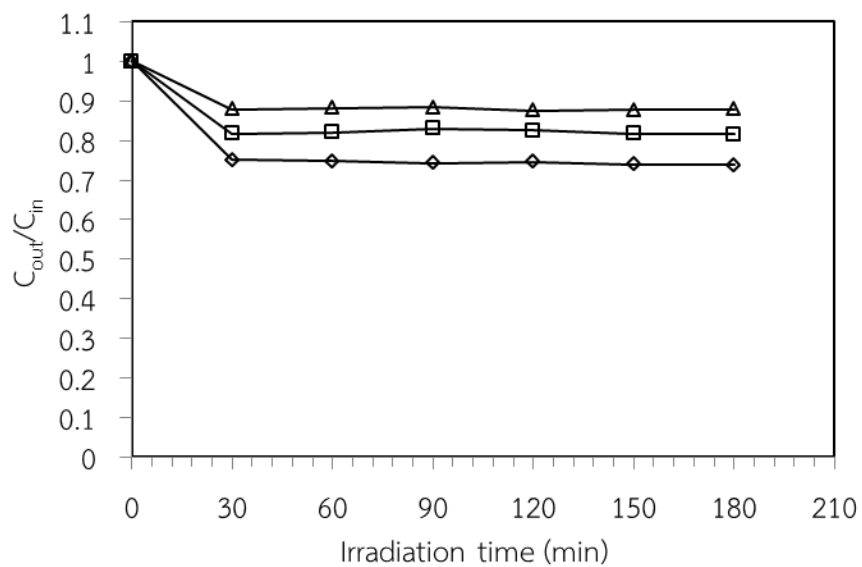


Figure 4.8 Concentration of diuron in the outlet stream from the reactor with consider to the initial concentration: (Δ) 750 μm , (\square) 500 μm and (\diamond) 250 μm . The residence time is 1 minute.

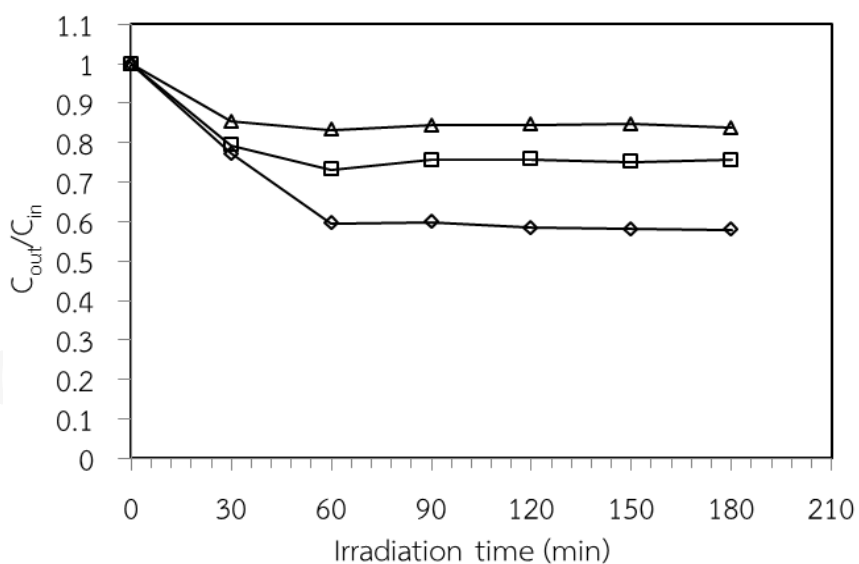


Figure 4.9 Concentration of diuron in the outlet stream from the reactor with consider to the initial concentration: (Δ) 750 μm , (\square) 500 μm and (\diamond) 250 μm . The residence time is 5 minutes.

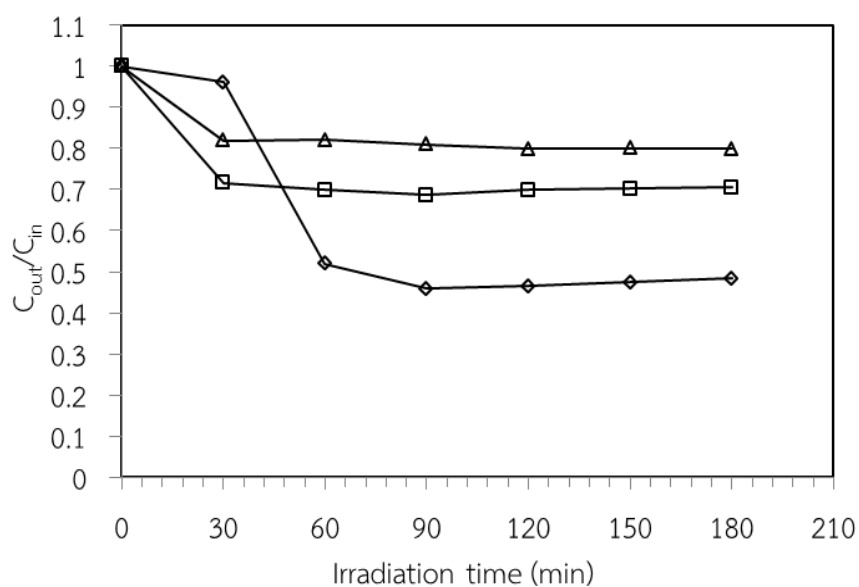


Figure 4.10 Concentration of diuron in the outlet stream from the reactor with consider to the initial concentration: (Δ) 750 μm , (\square) 500 μm and (\diamond) 250 μm . The residence time is 10 minutes.

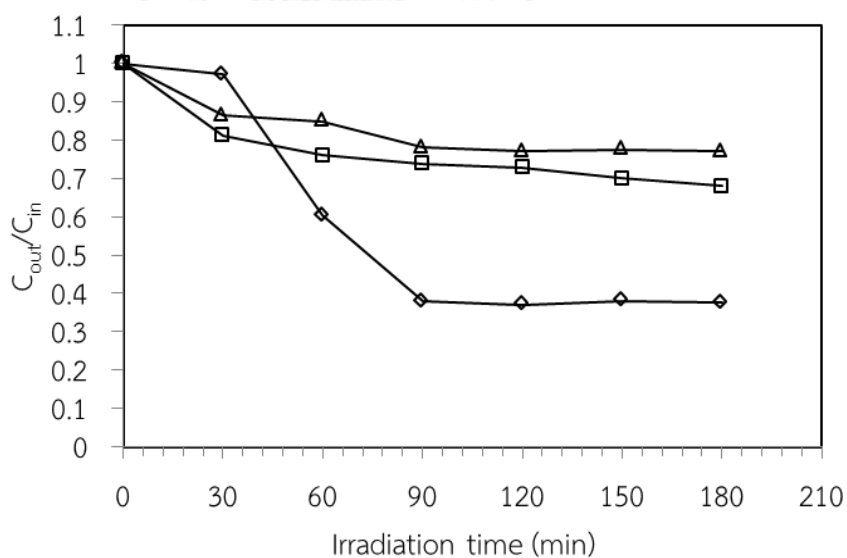


Figure 4.11 Concentration of diuron in the outlet stream from the reactor with consider to the initial concentration: (Δ) 750 μm , (\square) 500 μm and (\diamond) 250 μm . The residence time is 15 minutes.

According to the result in Figure 4.8-4.11, the time required for the system to reach steady state depends on the thickness of the micro-channel. The photocatalytic degradation is started after the light source, i.e. UV-A lamp, is turned on. It can be seen that 250 μm -thick channel requires more time to reach steady state than the channel of 500 and 750 μm thick, respectively. From the Figure 4.8, at the residence time of 1 minute, the system quickly reached steady state within 30 minutes because the flow rate was rather fast. Now consider the results in Figure 4.9-4.11, while the residence time was gradually increased, it resulted in the longer time to reach a steady state. Increasing the thickness leads to the decrease in the time to reach to steady state. This can also be pointed out that the decrease in the thickness of the microchannel also decreases the diffusion distance of diuron to the surface of the catalyst, which significantly enhances the degradation efficiency. It should be noted that the surface area of the catalyst is constant while the volume of the reactor is decreased as the thickness of the channel is decreased. The result is shown in Figure 4.12.

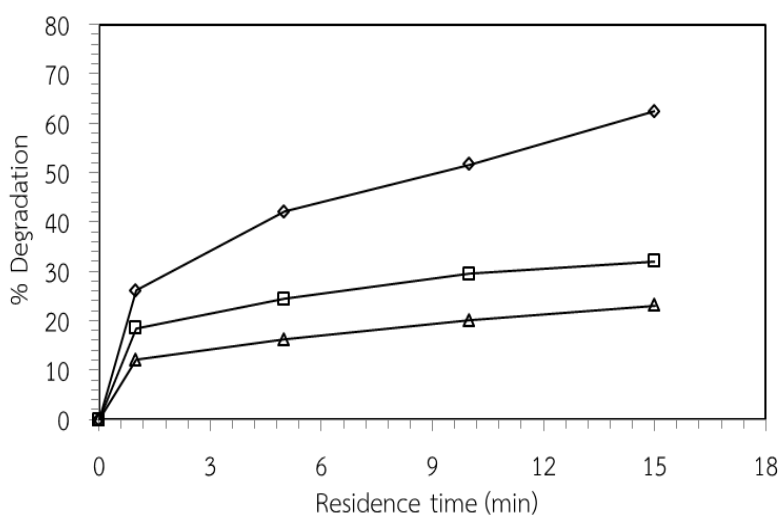


Figure 4.12 Efficiency of the degradation as a function of mean residence time: (Δ) 750 μm , (\square) 500 μm and (\diamond) 250 μm .

The limitation of the overall degradation rate by mass transfer could be excluded by evaluating appropriate Damköhler number. In this process, the value of 0.08645, 0.14498 and 0.48517 of Da_{II} are calculated at different thicknesses of 250, 500 and 750 micron, respectively. Therefore, mass transfer resistance can be neglected in the thickness of 250 and 500 micron. The important values in the Damköhler number are K and k_a that can be evaluated from the multiple linear regression model with matrix notation and analyzing the model using a script approach with MATLAB. The quantity y ($\ln C_0/C$, dependent variable) for several values of x_1 and x_2 (resident time and C , independent variables) was put in the MATLAB program to find the least squares estimators (Scott H. Brown, 2009).

In the change of the thickness of micro-channel, the Reynolds number (Re) should also be investigated. The Reynolds number (Re) is a dimensionless number used in fluid flow to predict the flow patterns in different fluid flow situations. There are in general three types of flow including laminar flow, transitional flow, and turbulent flow). The flow is

laminar flow when $Re < 2300$

transient flow when $2300 < Re < 4000$

turbulent flow when $4000 < Re$

The Reynolds number expresses the ratio of inertial (resistant to change or motion) forces to viscous (heavy and gluey) forces. It is defined below:

$$Re = \frac{\rho D v}{\mu} \quad (4.2)$$

Since this experimental is a situation for flow in a rectangular duct. The Reynolds number is generally defined as follow:

$$\text{Re} = \frac{\rho D_h v}{\mu} \quad (4.3)$$

where: D_h is the hydraulic equivalent diameter (m).

ρ is the fluid density (kg/m^3).

D is a diameter or other characteristic length of the system (m).

v is the mean velocity of the fluid (m/s).

μ is the viscosity of the fluid ($\text{kg}/(\text{m}\cdot\text{s})$).

For flow in shapes like squares, rectangular or annular ducts where the height and width are comparable, the feature dimension for internal flow situations is taken to be the hydraulic equivalent diameter, D_h , defined as follow [34]:

$$D_h = \frac{4A}{P} \quad (4.4)$$

where: A is the cross-sectional area (m^2).

P is the wetted perimeter (m).

In this work, the values of Reynolds number (Re) under various the thickness of micro-channel (250 μm , 500 μm and 750 μm) are estimated by using equation (4.3).

The result is shown in Figure 4.13. The results show the flow pattern in this system is laminar flow. For typical fluid dynamic conditions in microchannels, such as low flow rates and laminar flow, Sh numbers reach the asymptotic value of 3.66 (M. Fichtner, et al, 1998). The mass-transfer coefficient can be estimated from Sherwood numbers with $Sh = \beta d_h / D$, where d_h is the hydrodynamic diameter of a microchannel and D the molecular diffusion coefficient. The value of D for diuron is $8 \times 10^{-10} \text{ m}^2 \text{ s}^{-1}$ (Polcaro, 2004). Therefore, mass-transfer coefficients can be calculated with $\beta = 3.66D/d_h$.

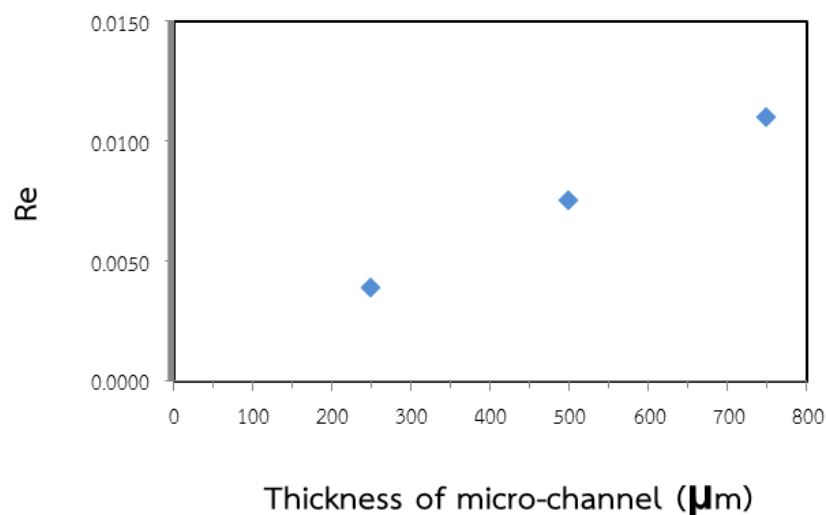
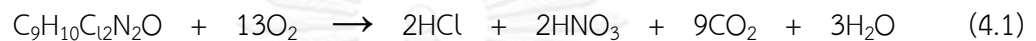


Figure 4.13 Reynolds number (Re) under various the thickness of micro-channel (250 μm , 500 μm and 750 μm).

4.2.3 Kinetics of diuron in microreactor

The photocatalytic degradation process is based on adsorption of photons leading to excitation of electron in the conductive band to the valence band after illuminated by light source at the surface of the photocatalyst. The promotion of an electron in the conductive band (e^-) resulting in formation of a

positive hole in the valence band (h^+). The h^+ and e^- are strong oxidizing and reducing agents, respectively. The positive holes can also oxidize the organic pollutants by reacting with water to generate hydroxyl radical ($\bullet\text{OH}$). Consequently, the $\bullet\text{OH}$ can react with organic pollutant resulting in intermediate products. The complete degradation products were CO_2 and water. The complete photocatalytic degradation of diuron can be shown as [3]:



In order to study the photocatalytic efficiency of the microreactor, it may be assumed that the mass transfer resistance can be neglected. The photocatalytic activity of diuron on TiO_2 coated films was investigated under UV-A irradiation. The initial concentration of diuron was 10 ppm. These results were shown in the effect of residence time and the results were discussed under various residence times. The photocatalytic activity of diuron on TiO_2 coated films was 63% in 15 minutes. The photocatalytic degradation of diuron with TiO_2 expressed apparent first order kinetics [3, 30, 31, 35]. This kinetic is based on Langmuir-Hiselmwood kinetic model described as:

$$r = -\frac{dC}{dt} = k_r \theta = k_r \frac{KC}{1+KC} \quad (4.4)$$

where, k_r is the reaction rate constant, K is the constant of adsorption equilibrium, t is the irradiation time, C is the concentration of the organic substrate (diuron) at any time, and C_0 is the initial concentration of the organic substrate (diuron). When C_0 is low, equation in (4.4) can be simplified to equation as follow:

$$r = -\frac{dC}{dt} = k_r KC = k_{app} C \quad (4.5)$$

where, k_{app} is the apparent rate constant of a pseudo first order model. For continuous operation, flow rates were converted to the residence time with $\tau = V/Q$ where V is the reactor volume and Q is the volumetric flow rate. It can be integrated equation (4.5) to equation (4.6) as:

$$\ln \frac{C_0}{C} = k_{app} \tau \quad (4.6)$$

where, C_0 is an initial concentration of diuron.

In this part, the apparent rate constant, k_{app} has been used to calculate degradation rate for the degradation of diuron on titanium dioxide coated films in microreactor. The pseudo first order kinetic model was chosen to estimate photocatalytic efficiency because the concentration of solution is rather diluted so the adsorption can be included in term of the apparent rate constant, k_{app} . The result is shown in Figure 4.14.

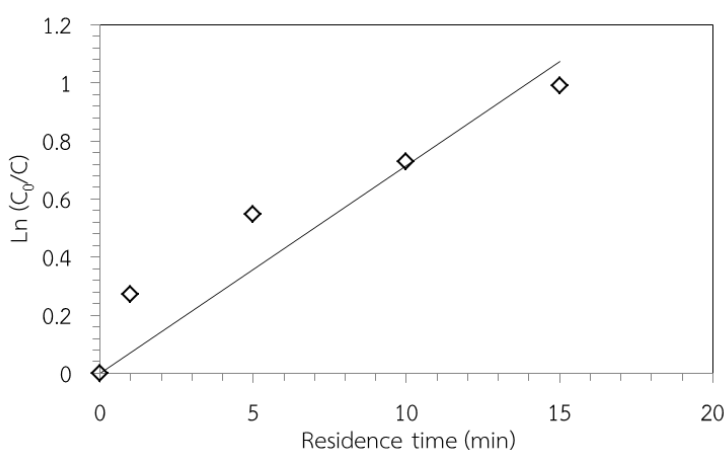


Figure 4.14 First-order linear transforms plot of the photocatalytic degradation of diuron on TiO_2 coated film.

4.2.4 Degradation kinetic of some intermediate standard

In this part, the degradation of three intermediate standards include 1-(3,4-dichlorophenyl)-3-methylurea, 3-(3,4-dichlorophenyl)-1-formyl-1-methylurea and 3,4-dichloroaniline was investigated. The kinetic studies followed pseudo first order kinetic like degradation of diuron. The initial concentration of each intermediate standard was 10 ppm. The results are shown in Figure 4.15. All parameters, the apparent rate constant (k_{app}) and R^2 value are shown in Table 4.1.

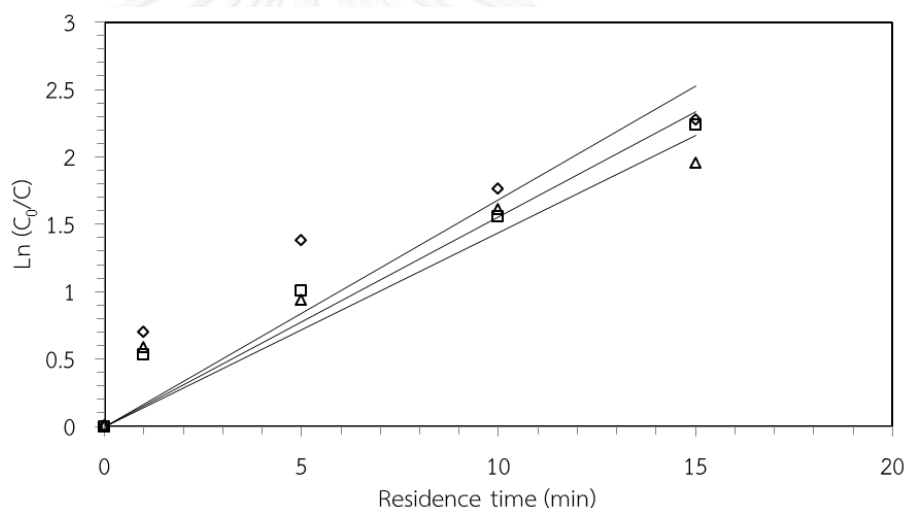


Figure 4.15 First-order linear transforms plot of the photocatalytic degradation of three intermediate standards on TiO_2 coated film: (\diamond)1-(3,4-dichlorophenyl)-3-methylurea, (\square) 3-(3,4-dichlorophenyl)-1-formyl-1-methylurea and (\triangle)3,4-dichloroaniline.

Table 4.1 The apparent rate constant (k_{app}) and R^2 value for the photocatalytic degradation of three intermediate standards using TiO_2 coated films

Intermediate standards	Pseudo-first order kinetic model	
	k_{app} (min^{-1})	R^2
1-(3,4-dichlorophenyl)-3-methylurea	0.1685	0.8027
3-(3,4-dichlorophenyl)-1-formyl-1-methylurea	0.1557	0.9325
3,4-dichloroaniline	0.1438	0.8748

These three intermediate standards can also be proposed the chemical structure from HPLC chromatogram. The other intermediate products was identified by LC-MS/MS.

4.3 Intermediate product of the photocatalytic degradation of diuron

In the photocatalytic process, the hydroxyl radical ($\bullet\text{OH}$) can be produced during the reaction. The hydroxyl radical is a powerful oxidizing agent. The intermediate products are occurred in the process, after the hydroxyl radical reacted with the organic compounds and finally converted to carbon dioxide and water. The intermediate products of degradation process do not occur instantaneously to form carbon dioxide, in fact the formation of long-lived intermediate species. In addition, the intermediates are often reported as more toxic or greater persistent than their parent compounds [1], [5]. So the detection and identification are required to determine which chemical structures are left at the end of the process and predict

the degradation pathways followed during the process. Moreover, this work also studied intermediate products that may not be involved with light. The intermediate products of the degradation process have been well known that there are formed from the reaction between hydroxyl radical and diuron. The diuron structure is shown in Figure 4.16.

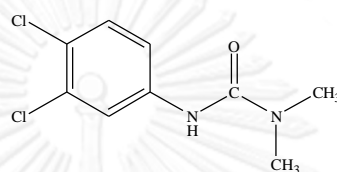


Figure 4.16 Chemical structure of diuron.

In a preliminary study the degradation of diuron from HPLC chromatogram, this result indicated that many intermediates were produced during the photocatalytic process. The peak height of many intermediates occurred during the photodegradation of diuron on titanium dioxide coated films in various residence time is shown in Figure 4.17 – Figure 4.20.

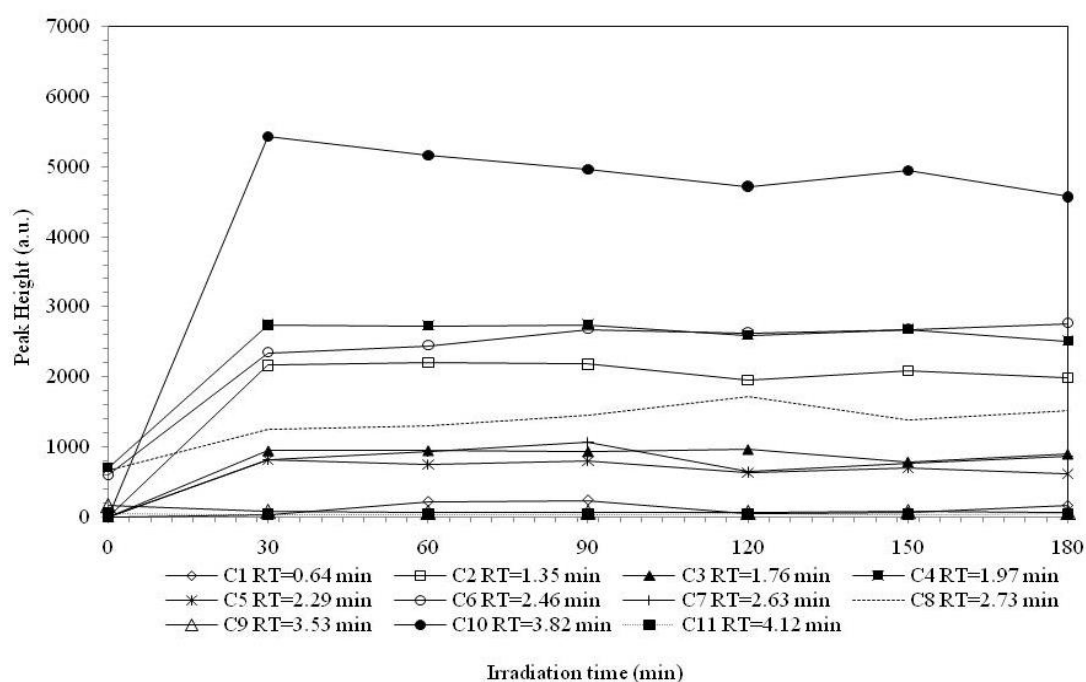


Figure 4.17 HPLC peak height of intermediates generated during photocatalytic degradation of diuron on TiO₂ coated film. The residence time is 1 minute.

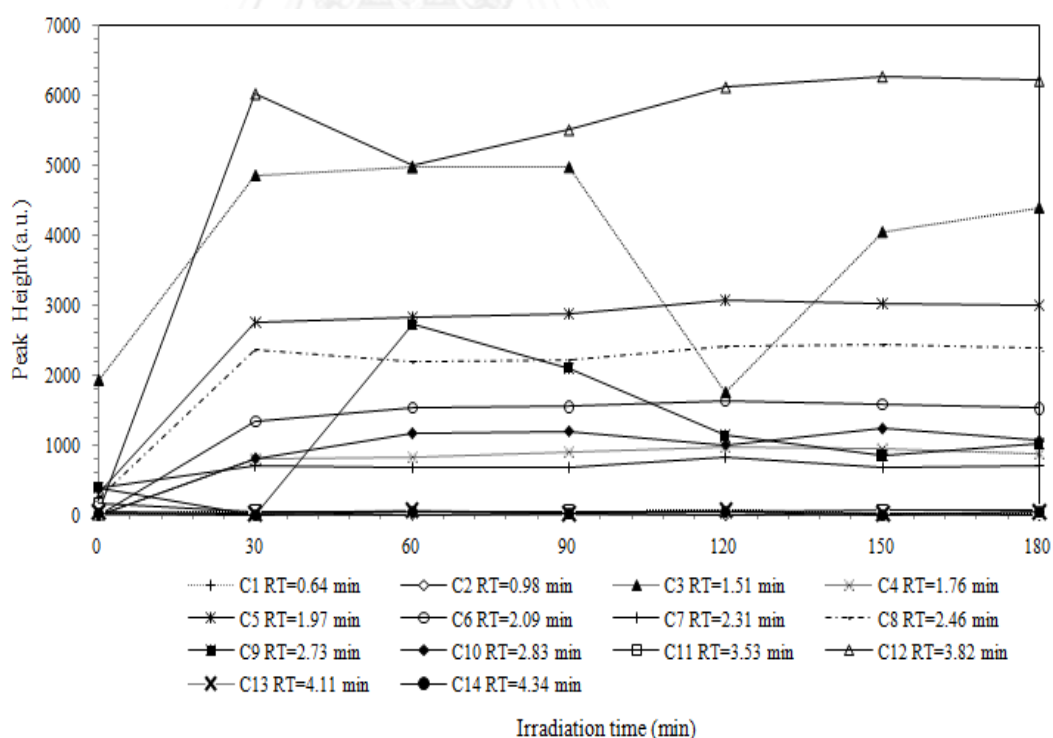


Figure 4.18 HPLC peak height of intermediates generated during photocatalytic degradation of diuron on TiO₂ coated film. The residence time is 5 minutes

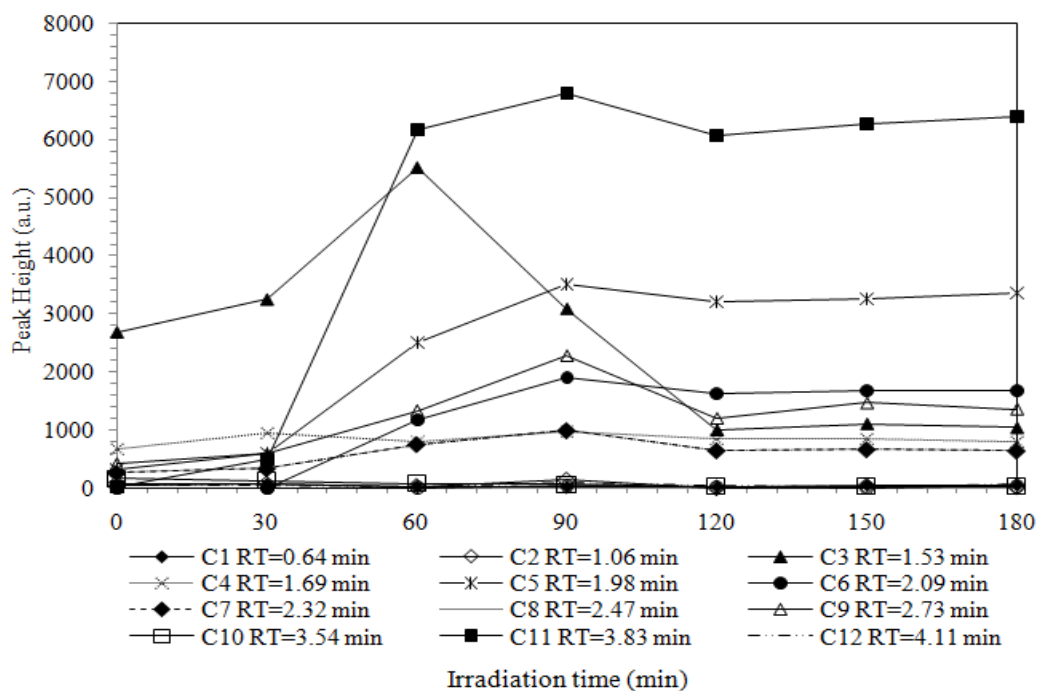


Figure 4.19 HPLC peak height of intermediates generated during photocatalytic degradation of diuron on TiO₂ coated film. The residence time is 10 minutes.

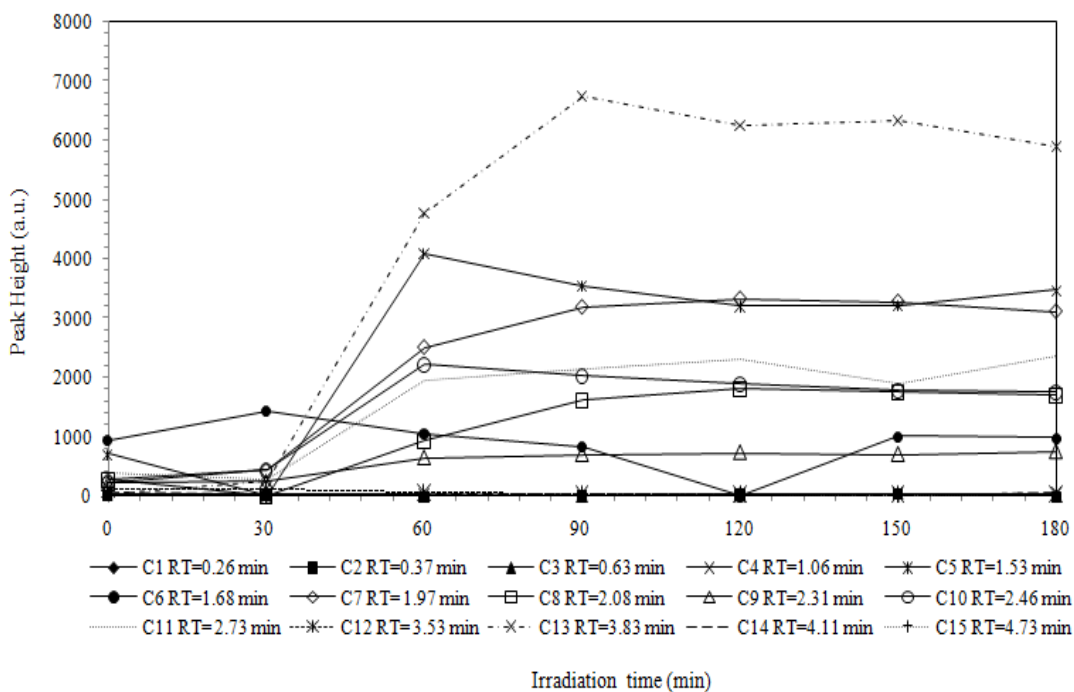
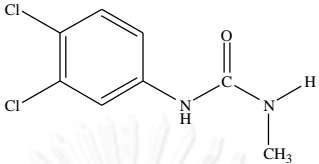
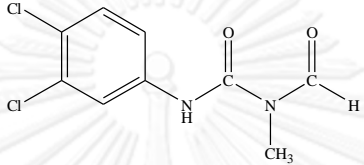
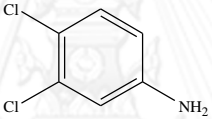


Figure 4.20 HPLC peak height of intermediates generated during photocatalytic degradation of diuron on TiO₂ coated film. The residence time is 15 minutes.

In Figure 4.17 and Figure 4.18, almost intermediate products are formed at the highest concentration within the first 30 min of the photodegradation reaction. At the residence time are 10 and 15 min in Figure 4.19 and Figure 4.20, almost intermediates are formed at the highest concentration within the first 90 min of reaction. From results, concentrations of some intermediates decrease with the increase in irradiation time and then some intermediates remain stable at low concentration after 3 hours of the reaction. On the other hand, the results of intermediate products indicate that the longer irradiation time would lead to the increase in concentration of the intermediates. Therefore, it shows that the degradation of diuron on titanium oxide in microreactor requires much longer time than 3 h to achieve complete mineralization. The actual concentration of almost intermediate products was not determined because of the lack of the standard samples.

In this thesis, the degradation of diuron and its intermediates were investigated. The informations of three standard samples, i.e., the chemical structure, molecular mass, the retention time from HPLC chromatogram are shown in Table 4.2. The photocatalytic degradation of three standard samples is examined in order to confirm its intermediate samples which corresponding to degraded diuron. The initial concentration of each standard samples in experiment was 10 ppm. The concentrations of diuron and its intermediates are shown in Figure 4.21.

Table 4.2 The informations of three standard samples.[5, 6, 31]

standard intermediate	chemical structure	molecular mass	retention time (min)
1-(3,4-dichlorophenyl)-3-methylurea		219	2.73
3-(3,4-dichlorophenyl)-1-formyl-1-methylurea		247	3.83
3,4-dichloroaniline		162	3.53

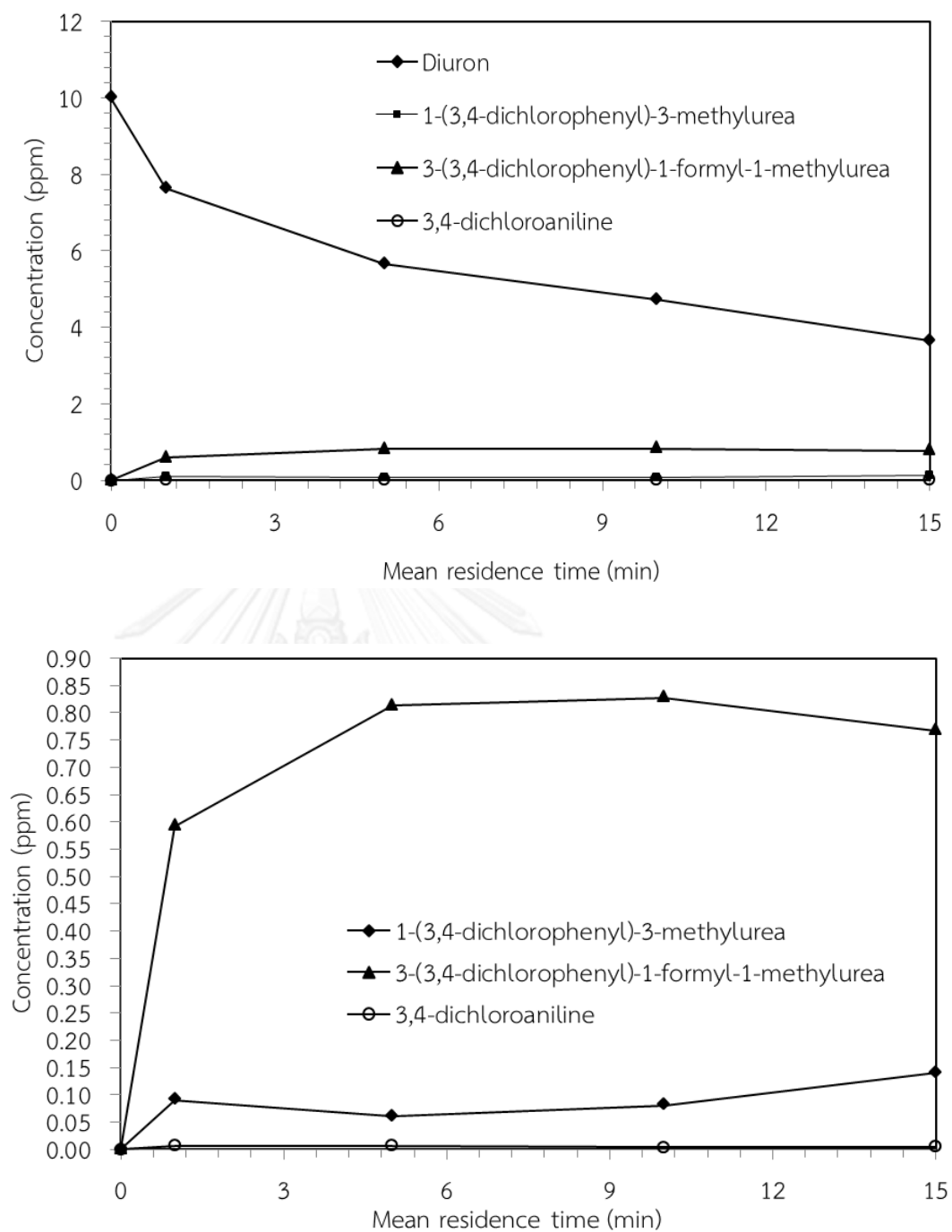


Figure 4.21 The concentrations of diuron and its intermediates under various mean residence times.

The intermediate products formed during the degradation process were analyzed by LC-MS/MS in order to identify structure of intermediate. The results confirm that the degradation of diuron generates several intermediate products corresponding to the results from HPLC analysis. The structures of intermediate were identified by the molecular ion and mass spectrometric fragmentation. Diuron peak was observed as reported in literature at 231m/z and 233 m/z in negative detection mode and positive mode, respectively. Due to the characteristic isotopic of the presence of chloride atoms in a molecule (Cl^{35} and Cl^{37}), it can be confirm that the presence of two chloride atoms in all structures determined. The propose structures of intermediate in this process as well as the main fragmentation are summarized in Table 4.3. Results from mass spectrum analysis indicate that degradation of diuron during the photocatalytic process leads to other products which can be smaller or larger molecules than diuron. The main intermediate products which were identified in this process are the same as detected by other authors [1, 3, 5, 33]. The limitation of the LC-MS/MS analysis could not detect some intermediate which has molecular weight lower than 70. In addition to the results in Figure 4.21, 3,4-dichloroaniline product was found in HPLC chromatogram but was not detected in the LC-MS/MS analysis. It should be that 3,4-dichloroaniline still possibly exist in the photocatalytic reaction but the concentration of its was very low corresponding to the HPLC analysis. By analytical the mass spectra, the intermediate products involving a reaction of hydroxyl radical ($\bullet OH$) is attacked to difference side of the diuron. The several of intermediates were found to be the product in which hydroxyl group attack at the aromatic ring and the alkyl group. The mechanism involving the reaction with the aromatic ring is shown as follows [36]:

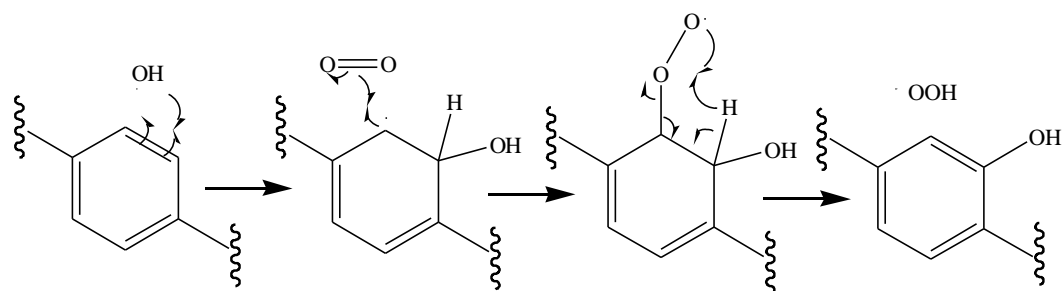


Figure 4.22 Hydroxylation reaction.

In this investigation, the other mechanism is oxidation of the alkyl side chain (removal of the methyl group). The oxidation of the methyl group leads to the corresponding alcohol. Alcohol readily oxidised to the aldehyde and acid, which then undergoes decarboxylation as shown in Figure 4.23 [36].

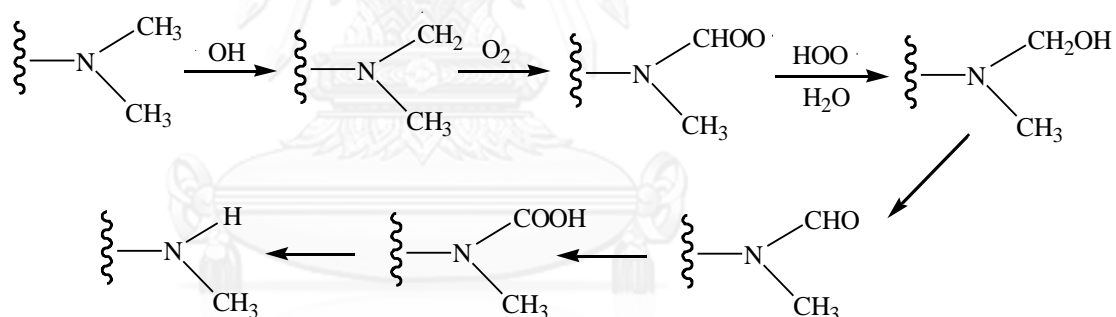


Figure 4.23 Decarboxylation reaction.

From the proposed structures, 11 intermediate products were identified. The result suggested that intermediate products are formed by dechlorination of the aromatic ring (compound 2), hydroxylation of the aromatic and the alkyl group (compound 4, 5, 7, 8, 9, 10, 11) and demethylation reaction (compound 1, 3, 6).

Table 4.3 Main fragments obtained from MS/MS spectra and proposed structures of intermediates generated from photodegradation of diuron.[1, 5, 11, 26, 27, 29-31, 35, 37]

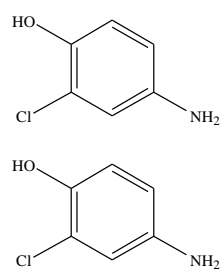
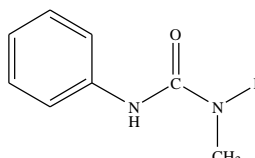
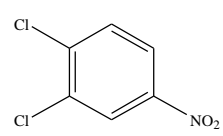
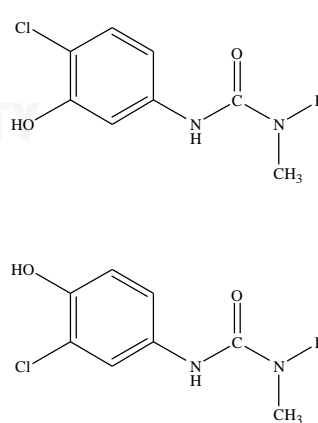
compound	MW (m/z)	MS/MS fragmentation	Proposed structure
1	144	127	 <p>Two chemical structures are shown. The first is 2-chloro-4-hydroxyaniline, a benzene ring with a hydroxyl group (HO) at the 4-position, a chlorine atom (Cl) at the 2-position, and an amino group (NH₂) at the 1-position. The second is 3-chloro-4-hydroxyaniline, a benzene ring with a hydroxyl group (HO) at the 4-position, a chlorine atom (Cl) at the 3-position, and an amino group (NH₂) at the 1-position.</p>
2	150	135, 107	 <p>Chemical structure of N-methylbenzamide: a benzene ring attached to a nitrogen atom (NH), which is bonded to a carbonyl group (C=O), which is further bonded to a methyl group (CH₃).</p>
3	192	147	 <p>Chemical structure of 2,4-dichloro-6-nitroaniline: a benzene ring with a chlorine atom (Cl) at the 2-position, another chlorine atom (Cl) at the 4-position, and a nitro group (NO₂) at the 6-position.</p>
4	201	184, 134	 <p>Two chemical structures are shown. The first is N-(2-chloro-4-hydroxyphenyl)acetamide, a benzene ring with a hydroxyl group (HO) at the 4-position, a chlorine atom (Cl) at the 2-position, and an acetamide group (NH-C(=O)-N(CH₃)-H) at the 1-position. The second is N-(3-chloro-4-hydroxyphenyl)acetamide, a benzene ring with a hydroxyl group (HO) at the 4-position, a chlorine atom (Cl) at the 3-position, and an acetamide group (NH-C(=O)-N(CH₃)-H) at the 1-position.</p>

Table 4.3 (continued).

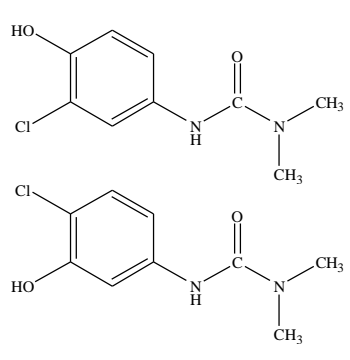
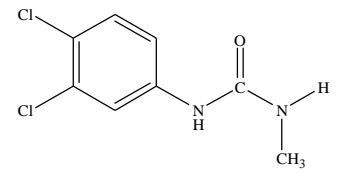
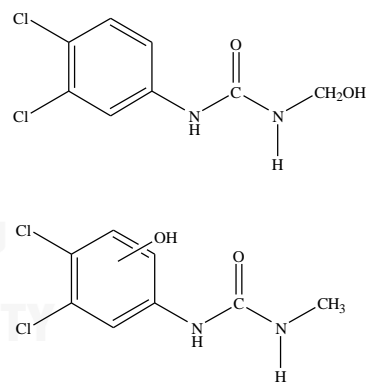
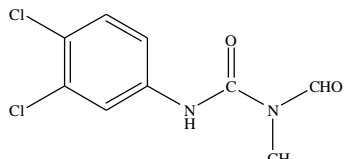
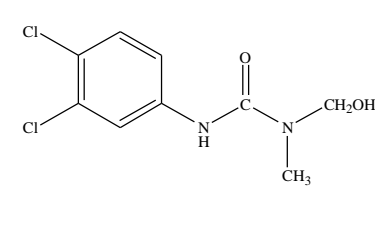
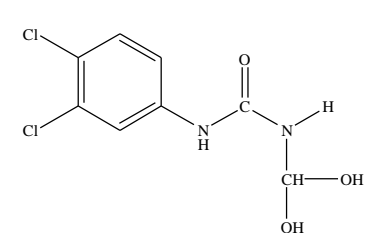
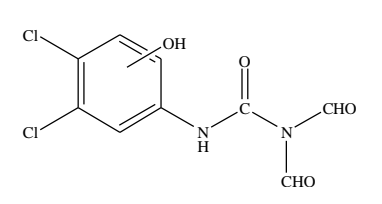
compound	MW (m/z)	MS/MS fragmentation	Proposed structure
5	214	196, 168	
6	218	203, 161	
7	234	219, 190, 176	
8	246	218	

Table 4.3 (continued).

compound	MW (m/z)	MS/MS fragmentation	Proposed structure
9	248	234, 202	
10	250	216, 161	
11	278	204, 148	

The identification of intermediate products confirmed the presence of two main pathways for diuron degradation: dehalogenation and hydroxylation on the aromatic ring. The possible degradation mechanism of diuron and the formation of the intermediate are described below in more detail. The hydroxyl group attack at the aromatic ring and the alkyl group. The pathway of photocatalytic degradation of diuron has been reported in several routes. However the initial degradation pathway of diuron is mainly hydroxylation. Mechanism of hydroxylation of the aromatic ring dechlorination is shown in Figure 4.24. [11]

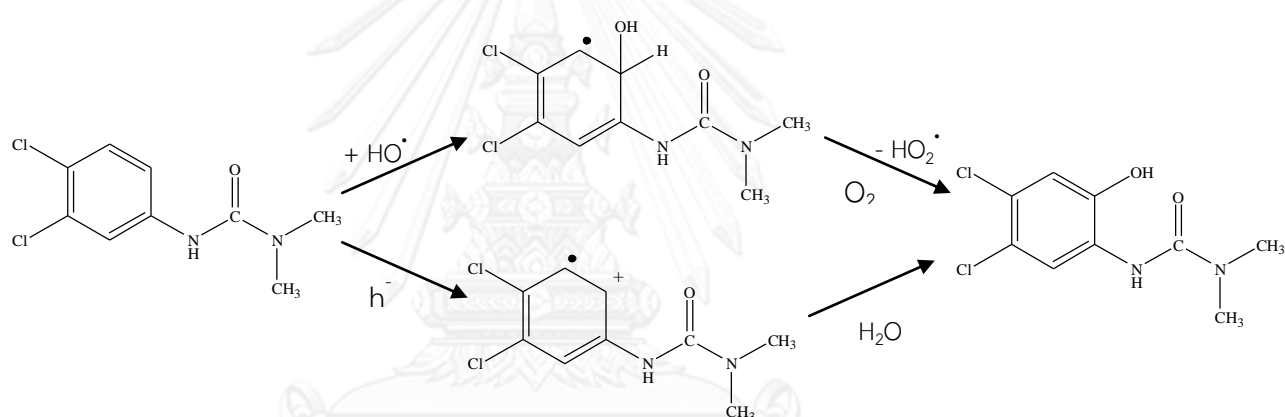


Figure 4.24 Hydroxylation of the aromatic ring during photocatalytic degradation of Diuron.

The main target for the degradation of diuron could be reduced the mechanism, which results to the dechlorination as show in Figure 4.25.[11]

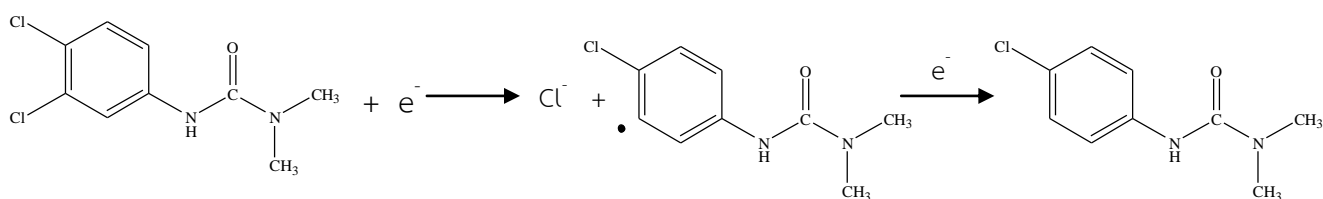


Figure 4.25 Dechlorination during photocatalytic degradation of Diuron.

Another mechanism involve oxidation of the ring is substitution of a Cl atom by the hydroxyl group on benzene ring. This formation of compound 5 was favoured with Degussa P-25. In this compound it has an isomer as shown in Figure 4.26. This mechanism of similar intermediates formation was reported by several researchers in the other degradation. [11]

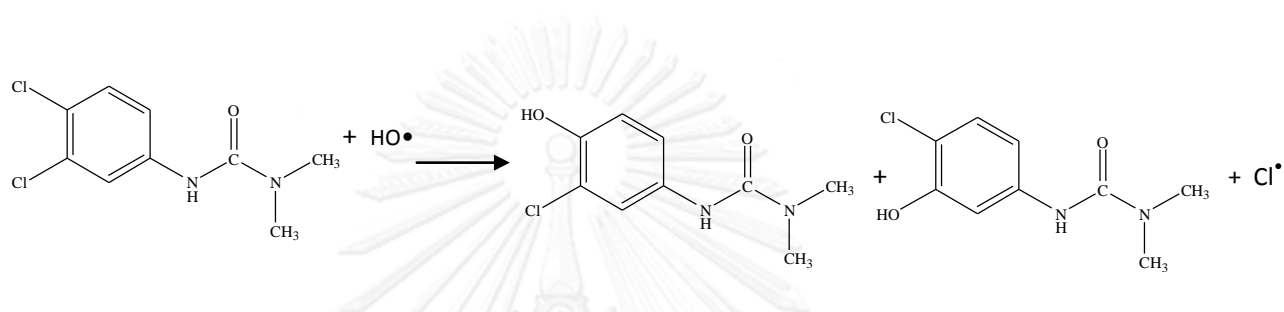


Figure 4.26 Chlorine substituted on the aromatic ring during photocatalytic degradation of Diuron.

The several intermediateds that were proposed in this work with the main one being the oxidation of the methyl group show in Figure 4.27.

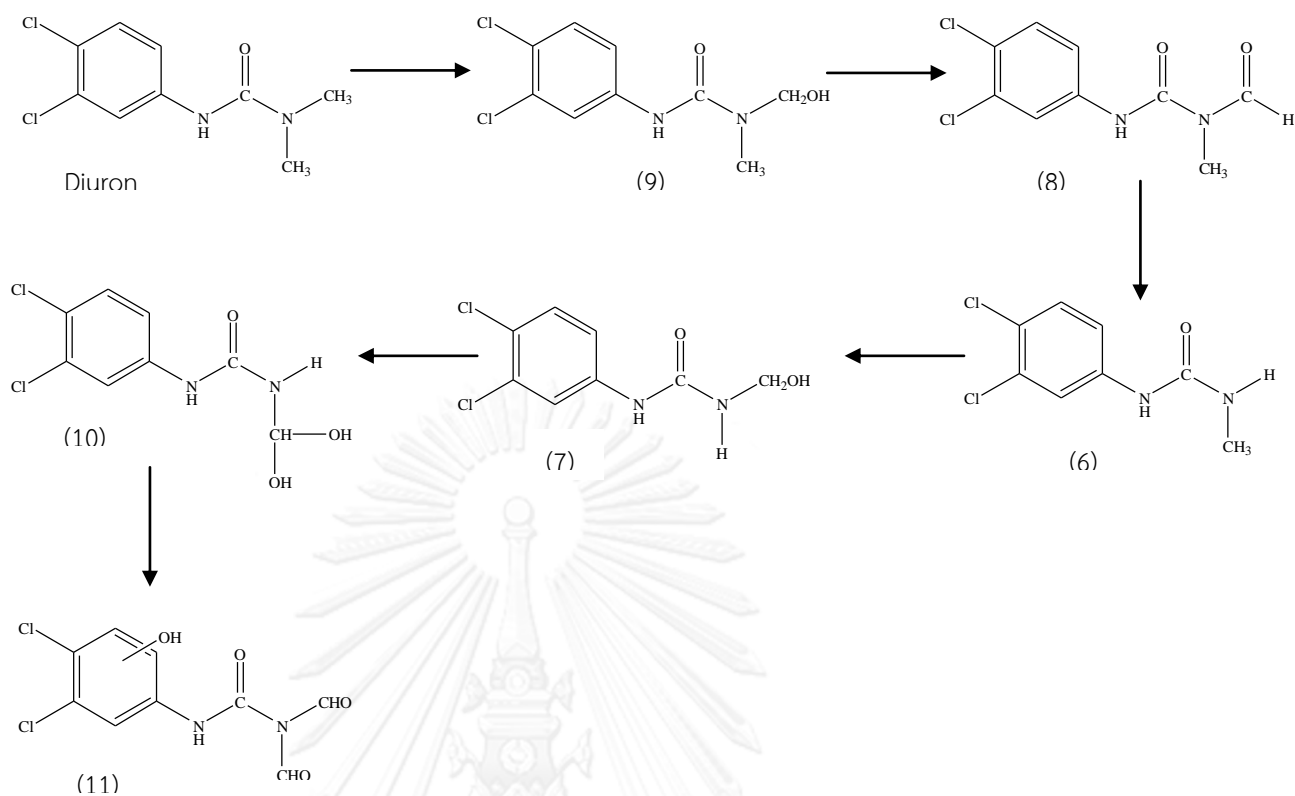


Figure 4.27 Oxidation of the alkyl side chain by $\bullet\text{OH}$.

From the literature, it was found that the intermediate formed from the degradation of diuron is considerably more toxic than diuron itself. Therefore, to avoid the intermediate that was more toxic than diuron itself, the intermediates formed from the process were investigated. To avoid the intermediates that could be toxic, it may be chosen the residence time that does not result in toxic intermediate compounds. Based on all intermediates in this work, a possible photocatalytic degradation pathway of diuron consisting of several steps was proposed in Figure 4.28.

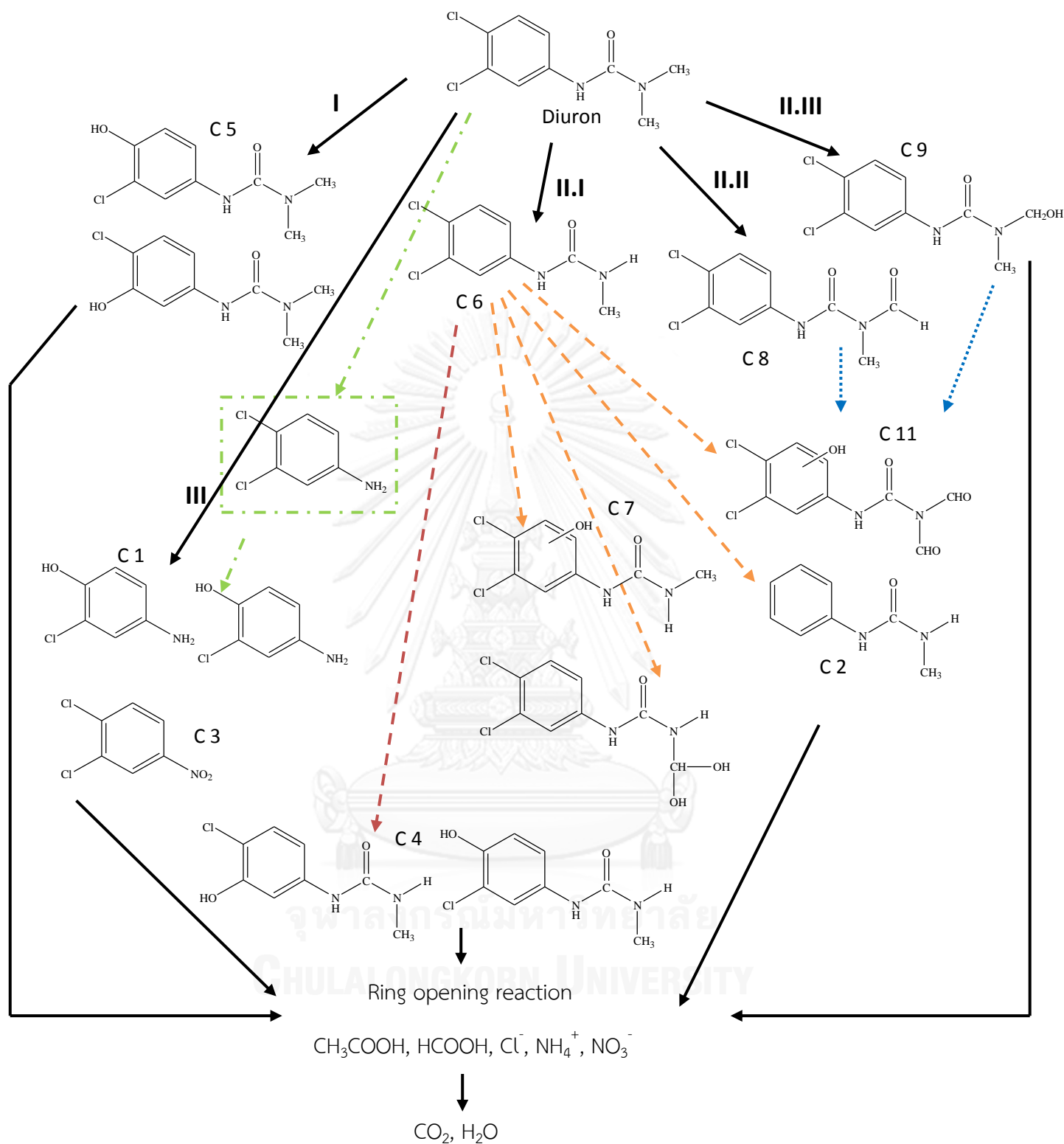


Figure 4.28 Proposed degradation mechanism of diuron. Numbers correspond to those in Table 4.3.

From propose pathway, there are three pair of isomer (C1, C4, C5) which are the intermediates of photocatalytic degradation. In route I, compound 5 or C5 was identified as the hydroxylation occurring on the aromatic ring. In route II, compound 6 was the results of the demethylation or the elimination of a methyl group. Compound 8 was the results of the oxidation by $\bullet\text{OH}$ with the elimination of a methyl group. Compound 9 was identified as the oxidation of the methyl group. In route III, compound 1 and 3 were identified as the compounds in which the alkyl was group eliminated. In addition, compound 1 was identified as the chlorine substitution on the aromatic ring of 3,4-dichloroaniline. From previously discussed, 3,4-dichloroaniline was not found in the LC-MS/MS analysis. It should be the result from the fact that the concentration of its very low corresponding to the HPLC analysis. Moreover, compound 10 was identified as the product of the hydroxylation occurring on the methyl group of compound 6. It was confirmed by the decrease of LC-MS/MS intensity of compound 6 and proposed from the chemical structure of product 6. Compound 2, 7 and 11 were identified as the hydroxylation forming on the methyl group of compound 6 the same as compound 10. Compound 11 was identified with the reason similarly to that of compound 2, 7 and 10. The last intermediate, compound 4 and its isomer, were identified as the hydroxylation occurring on the aromatic ring of compound 6. Furthermore, the identification of those products was used the information under various residence time. Then the order of the formed intermediate could be found as Figure 4.28. According to the literatures, 3,4-dichloroaniline is considerably more toxic than diuron itself and has higher water solubility so it can leach out from treated agricultural land. Therefore, to avoid 3,4-dichloroaniline formation, path way that may be less toxic is shown in Figure 4.29.

There are several reports about the opening of benzene ring (the oxidation of benzene ring). Nevertheless, due to limitation in LC-MS analysis, intermediates from the benzene ring opening were not detected.



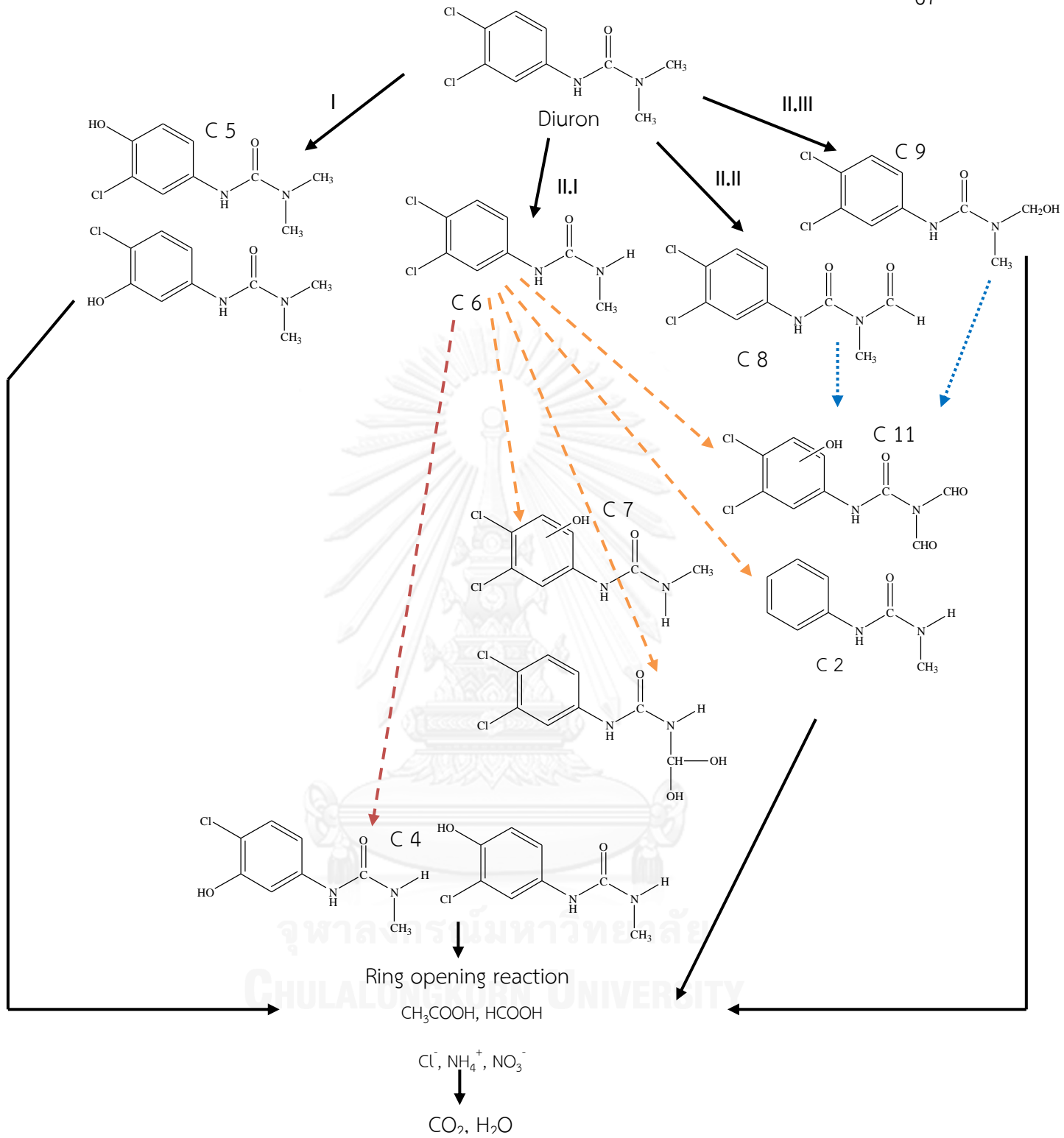


Figure 4.29 Proposed degradation mechanism of diuron that may less toxic.

4.4 Effect of light on intermediates formation

Intermediate products formed during the photocatalytic degradation of diuron were studied to obtain a better understanding of the pathway during photocatalysis. Recently, many researchers also reported the intermediates formed under exposure of light. From the literature survey, no one has ever reported the intermediates formed without exposure of light. Therefore, it is an interest of this research to identify the in-depth formation of intermediates during the photocatalytic degradation of diuron. The results in this part are compared with the information as explained in the previous section. The experiment was designed into six conditions. The results in each condition were shown below. It should be noted that in this section, the residence time was decreased from 15 minutes to 1-3 minutes.

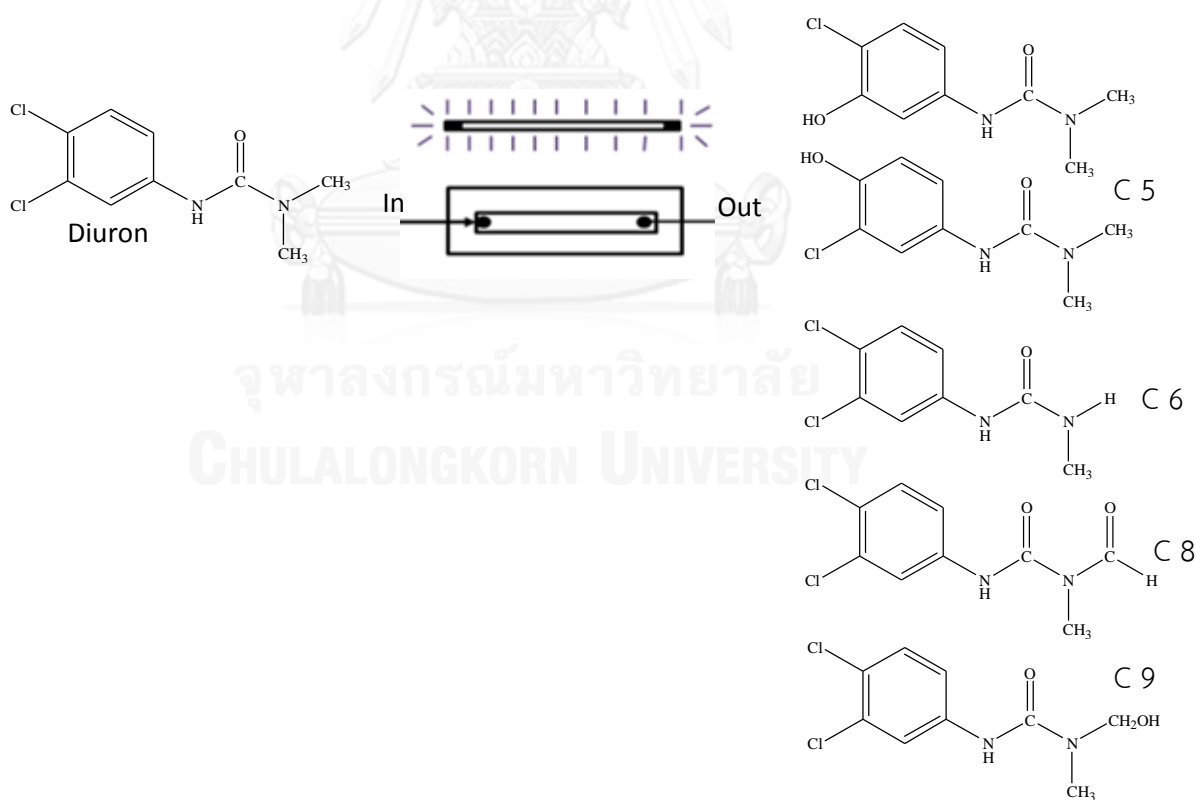


Figure 4.30 The intermediate compounds formed under exposure of light. The residence time is 1 minute.

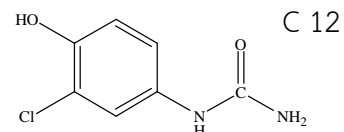
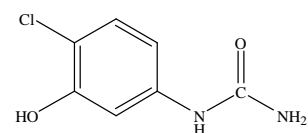
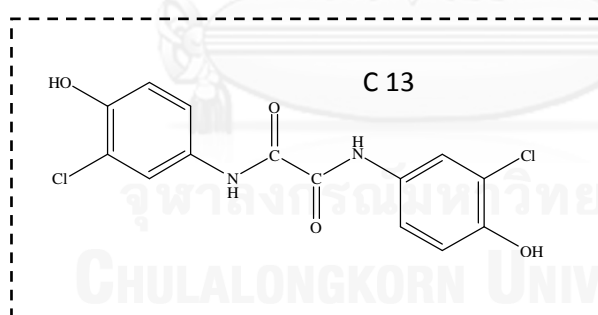
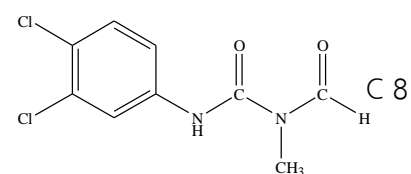
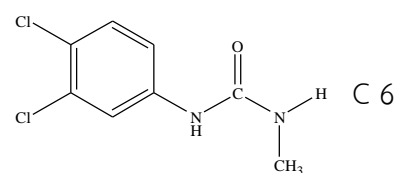
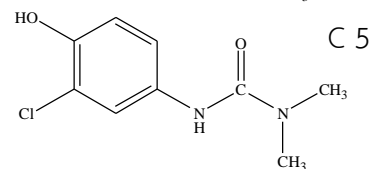
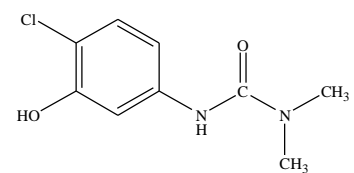
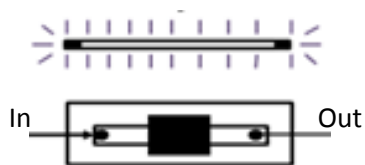
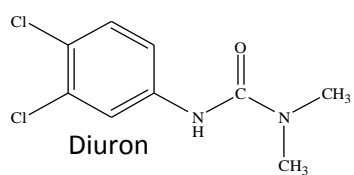


Figure 4.31 The intermediate compounds formed when the middle 1/3 section of the reactor was shaded. The residence time is 1 minute.

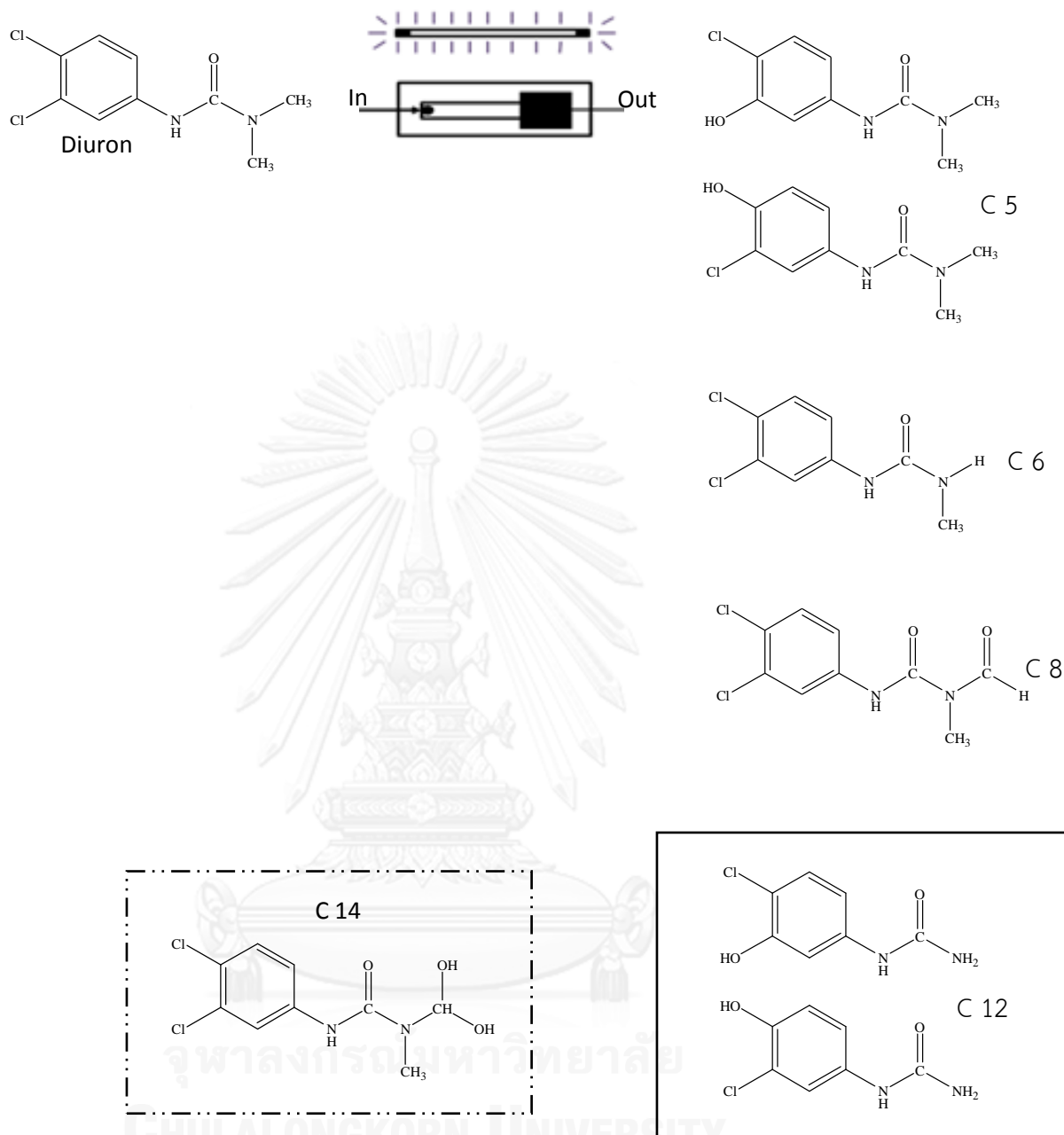


Figure 4.32 The intermediate compounds formed when the last 1/3 section of reaction was shaded. The residence time is 1 minute.

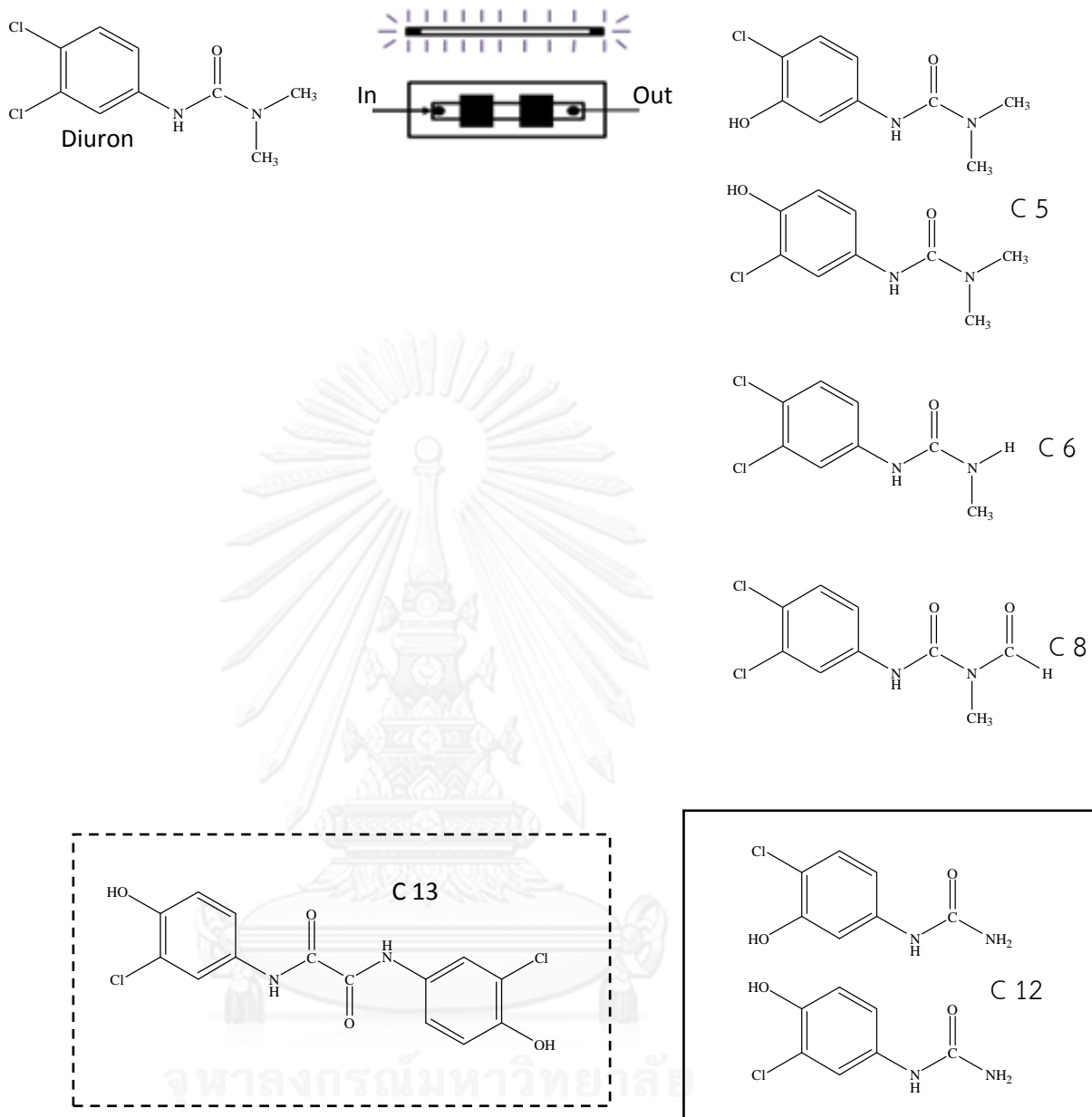


Figure 4.33 The intermediate compounds formed when the second and the fourth 1/5 section of the reactor was shaded. The residence time is 1 minute.

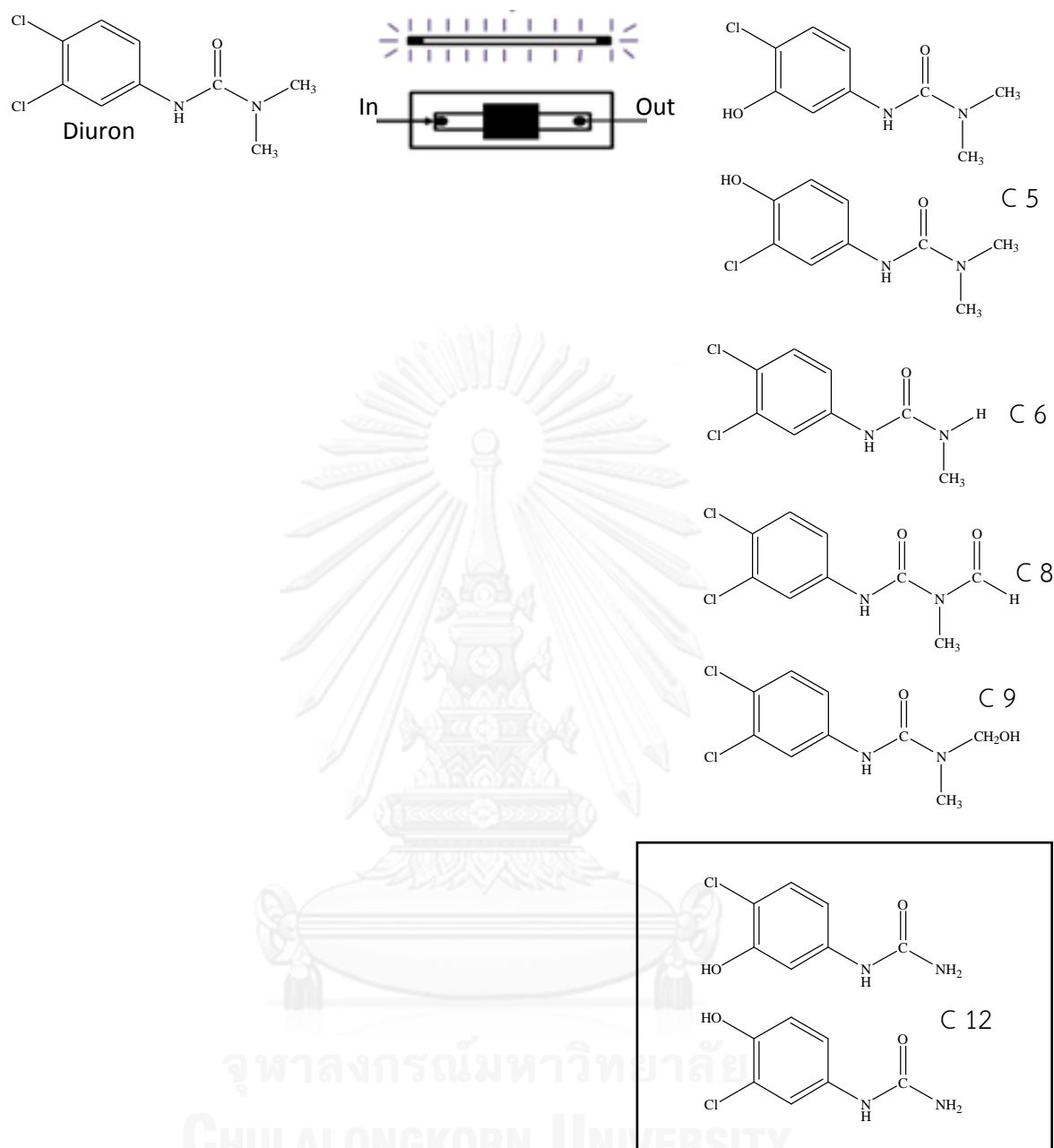


Figure 4.34 The intermediate compounds formed when the middle 1/3 section of the reactor was shaded. The residence time is 3 minute.

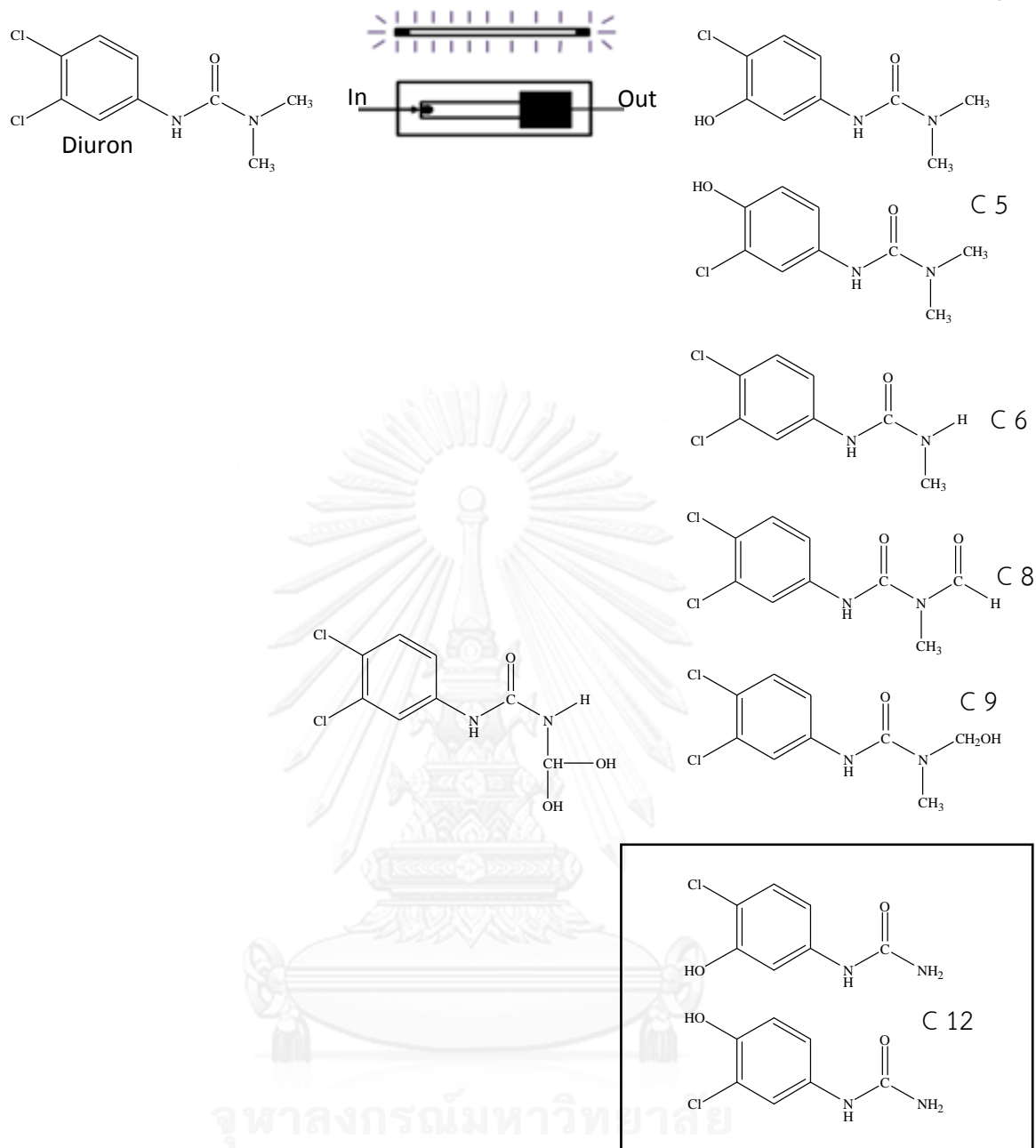


Figure 4.35 The intermediate compounds formed when the last 1/3 section of reaction was shaded. The residence time is 3 minute.

From the results, the intermediate compounds can occur without exposure of light. There are three intermediates (C12, C13 and C14) which are different from the compounds formed under exposure of light. Compound 12 was not found in the condition to exposure of light but was found in all conditions that part of the reactor was covered. From the structure of intermediate, it can be indicated that the products formed by the methyl groups had been eliminated. From LC/MS-MS chromatogram, it was confirmed that the decrease of LC-MS/MS intensity of compound 5 and proposed from the chemical structure of product 5. Compound 13 was found in the condition without exposure of light. Compound 13 was identified as conjugation of intermediates. It is suggested that the intermediate formed at the exposed position reach to without exposure, it may not have attacked from hydroxyl radical lead to the recombination of its intermediate. In addition, at residence time of 3 min, compound 13 was not found thus it may have more time to generate hydroxyl radical than combine the intermediate. It should be noted that some intermediate products which are formed from pattern I are different from pattern II because some intermediates formed in pattern II might have more time to generate hydroxyl radical than pattern I. Compound 14 was identified as hydroxylation occurring on the aromatic ring by continuous exposure for a long time. Considered Figure 4.31 and 4.34, compound 14 was not found in the larger area without exposure of light. It may be assumed is compound 14 was formed in a continuous exposure for a long time. When compound 14 stayed in the area without exposure of light in 3 minutes, it may not form. The last one, compound 10 was the results of hydroxylation at the methyl group of compound 6. It was confirmed by the decrease

of LC-MS/MS intensity of compound 6 and proposed from the chemical structure of product 6.

Based on the intermediates identified, the possible degradation pathway for diuron under exposure of light and without exposure of light is proposed in Figure 4.35.



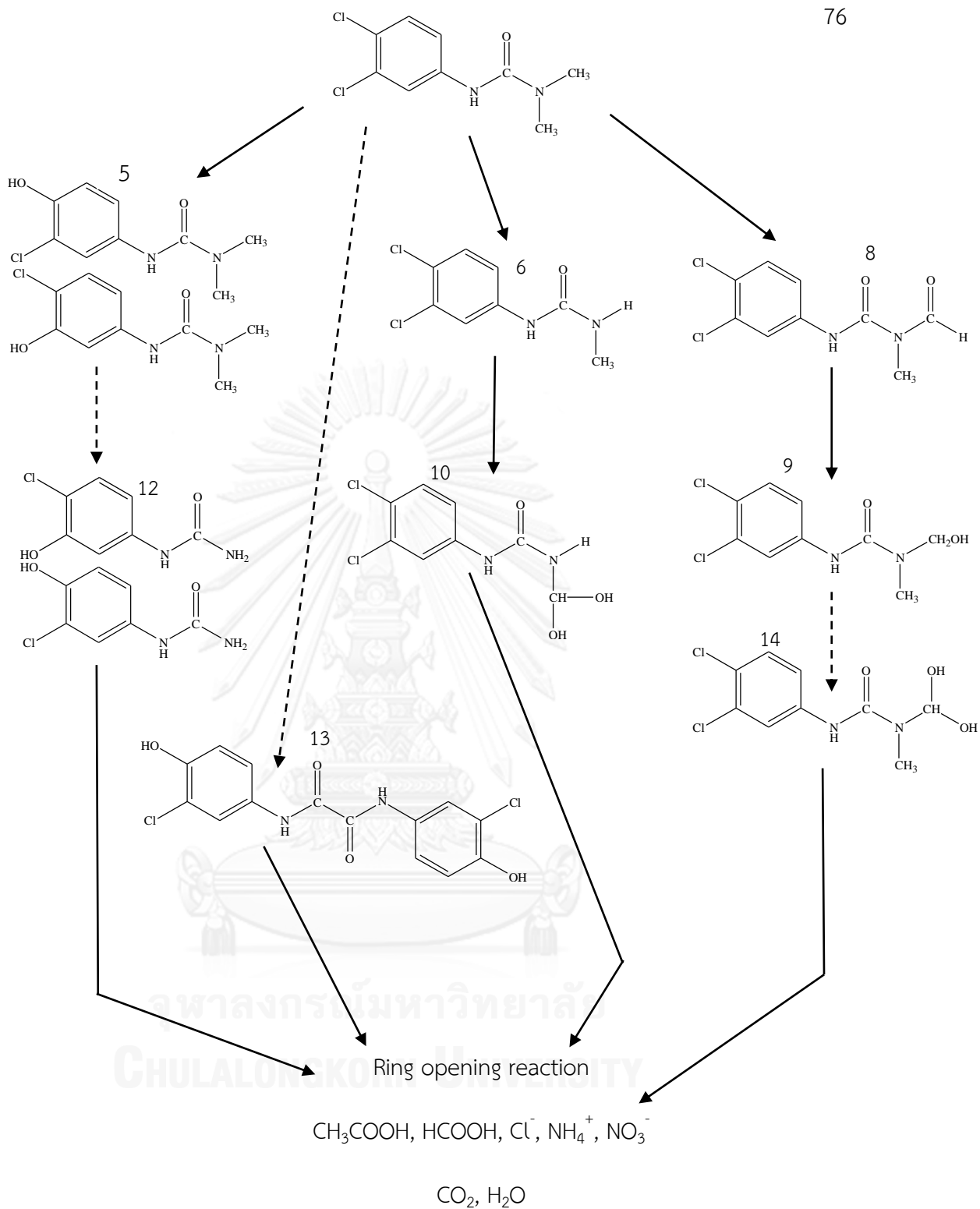


Figure 4.36 Proposed degradation mechanism of diuron. (Notes: solid arrows indicate under exposure of light process while dashed arrows indicate without exposure of light process.)

From the proposed intermediate data, the reaction without exposure of light can not be defined because this is not enough data to confirm. However, it was found that the intermediates that are formed without exposure of light formed from the intermediates previously formed by the degradation in irradiated area. The results suggest that intermediates from the degradation of diuron can be generated without exposure of light. There intermediates formed from formation of the hydroxyl radical are obviously not continuous that lead to conjugation or recombination of its intermediate on the dark area. Other intermediates can be generated from previous sample to another but the mechanism of the formation may differ from the intermediates that formed under exposure of light.

CHAPTER V

CONCLUSIONS AND RECOMMENDATIONS

5.1 Summary of Results

The summary of the results of the present research is the following:

1. Microreactor can be used to enhance the degradation of diuron on titanium dioxide. The benefits of the reaction in this system include negligible mass transfer resistance and high light penetration throughout the reactor.
2. The increase in residence time results in increased degradation. The efficiency of degradation can also be increased by decreasing the diffusion distance within the micro-channel.
3. Several intermediates are formed during the degradation by dechlorination, hydroxylation and demethylation of diuron. The degradation pathway is proposed.
4. Some intermediates can be formed without the exposure of the light.

5.2 Conclusions

The photocatalytic degradation of diuron on titanium dioxide can be operated in a microreactor. The effect of mass transfer resistance can be neglected. The degradation efficiency can be increased by decreasing the diffusion distance within the micro-channel and increasing of residence time. Several intermediates are formed during the degradation of diuron. The intermediates are formed by attacking of hydroxyl radical to several sites of diuron structure during the degradation process. Moreover, the intermediates are generated from hydroxylation of aromatic ring,

hydroxylation of methyl group and demethylation. In addition, the intermediates which are formed under exposure of the light and those formed without light were identified and proposed the pathway.

5.3 Recommendations

Recommendations for the future work, based on the results of this work, are followings.

1. Further identification of intermediate of diuron under exposure and without exposure of the light in longer residence time.
2. Control temperature of the reaction.
3. Monitor the concentration of the hydroxyl radical ($\text{OH}\cdot$).
4. Quantify concentration of the generated intermediates.

REFERENCES

- [1] Oturan, M.A., et al., *Kinetics of oxidative degradation/mineralization pathways of the phenylurea herbicides diuron, monuron and fenuron in water during application of the electro-Fenton process*. Applied Catalysis B: Environmental, 97(1-2): p. 82-89.
- [2] Sayeh, R., et al., *Elimination of Pollutants Phenylurea Herbicides by Advanced Oxidation Processes in Aqueous Solution*. Vol. 2. 2007.
- [3] Katsumata, H., et al., *Photocatalytic degradation of diuron in aqueous solution by platinized TiO₂*. Journal of Hazardous Materials, 2009. 171: p. 1081-1087.
- [4] Vijayabalan, A., et al., *Photocatalytic activity of surface fluorinated TiO₂-P25 in the degradation of Reactive Orange 4*. Journal of Hazardous Materials, 2009. 172(2-3): p. 914-921.
- [5] Marion Carrier, C.G., Miche`le Besson, Claire Bordes and and H. Chermette, *Photocatalytic Degradation of Diuron: Experimental Analyses and Simulation of HO° Radical Attacks by Density Functional Theory Calculations*. J. Phys. Chem., 2009. 113: p. 6365–6374.
- [6] Bamba, D., et al., *Photocatalytic degradation of the diuron pesticide*. Environmental Chemistry Letters, 2008. 6(3): p. 163-167.
- [7] Salvestrini, S., P. Di Cerbo, and S. Capasso, *Kinetics of the chemical degradation of diuron*. Chemosphere, 2002. 48(1): p. 69-73.

- [8] Ehrfeld, W., V. Hessel, and H. Lowe, *Microreactors*. Germany: Wiley-VCH. 2000.
- [9] Matsushita, Y., et al., *N-Alkylation of amines by photocatalytic reaction in a microreaction system*. *Catalysis Today*, 2008. 132(1-4): p. 153-158.
- [10] Patil, K.R., et al., *Preparation of TiO₂ thin films by modified spin-coating method using an aqueous precursor*. *Materials Letters*, 2003. 57(12): p. 1775-1780.
- [11] Addamo, M., et al., *Photocatalytic thin films of TiO₂ formed by a sol-gel process using titanium tetraisopropoxide as the precursor*. *Thin Solid Films*, 2008. 516(12): p. 3802-3807.
- [12] Chung-Yi Wu, Y.-L.L., Yu-Shiu Lo, Chen-Jui Lin, Chien-Hou Wu, *Thickness-dependent photocatalytic performance of nanocrystalline TiO₂ thin films prepared by sol-gel spin coating*. *Applied Surface Science*, 2013. 280: p. 737- 744.
- [13] Canle López, M., et al., *Mechanisms of Direct and TiO₂-Photocatalysed UV Degradation of Phenylurea Herbicides*. *ChemPhysChem*, 2005. 6(10): p. 2064-2074.
- [14] Mestankova, H., et al., *Evolution of algal toxicity during (photo)oxidative degradation of diuron*. *Aquatic Toxicology*, 2011.101(2): p. 466-473.
- [15] Romero, A., et al., *Diuron abatement using activated persulphate: Effect of pH, Fe(II) and oxidant dosage*. *Chemical Engineering Journal*, 2010. 162(1): p. 257-265.

- [16] Acero, J.L., et al., *Kinetics of reactions between chlorine or bromine and the herbicides diuron and isoproturon*. Journal of Chemical Technology & Biotechnology, 2007. 82(2): p. 214-222.
- [17] Gargee Mohanty, J.M., Shubha Dipta Jena and S.K. Dutta, *Genotoxicity Testing in Pesticide Safety Evaluation*. 2011: p. 403-426.
- [18] Zhao, J. and X. Yang, *Photocatalytic oxidation for indoor air purification: a literature review*. Building and Environment, 2003. 38(5): p. 645-654.
- [19] Fujishima, A., X. Zhang, and D.A. Tryk, *TiO₂ photocatalysis and related surface phenomena*. Surface Science Reports, 2008. 63(12): p. 515-582.
- [20] Carp, O., C.L. Huisman, and A. Reller, *Photoinduced reactivity of titanium dioxide*. Progress in Solid State Chemistry, 2004. 32(1-2): p. 33-177.
- [21] Ramirez, A.M., et al., *Titanium dioxide coated cementitious materials for air purifying purposes: Preparation, characterization and toluene removal potential*. Building and Environment, 2010. 45(4): p. 832-838.
- [22] Houas, A., et al., *Photocatalytic degradation pathway of methylene blue in water*. Applied Catalysis B: Environmental, 2001. 31(2): p. 145-157.
- [23] Bentez, F.J., et al., *Nanofiltration processes applied to the removal of phenyl-ureas in natural waters*. Journal of Hazardous Materials, 2009. 165(1-3): p. 714-723.

- [24] Acero, J.L., et al., *Removal of phenyl-urea herbicides in natural waters by UF membranes: Permeate flux, analysis of resistances and rejection coefficients*. Separation and Purification Technology, 2009. 65(3): p. 322-330.
- [25] Benitez, F.J., et al., *Removal of phenyl-urea herbicides in ultrapure water by ultrafiltration and nanofiltration processes*. Water Research, 2009. 43(2): p. 267-276.
- [26] Anna, S., S. Nadine, and B. Thomas, *Sorption of Phenyl Urea Herbicides to Black Carbon*. Environ. Sci. Technol, 2009. 43: p. 8147-8152.
- [27] Wang, P. and A.A. Keller, *Sorption and desorption of atrazine and diuron onto water dispersible soil primary size fractions*. Water Research, 2009. 43(5): p. 1448-1456.
- [28] Benitez, F.J., et al., *Photochemical oxidation processes for the elimination of phenyl-urea herbicides in waters*. Journal of Hazardous Materials, 2006. 138(2): p. 278-287.
- [29] Farre, M.a.J., et al., *Evaluation of the intermediates generated during the degradation of Diuron and Linuron herbicides by the photo-Fenton reaction*. Journal of Photochemistry and Photobiology A: Chemistry, 2007. 189(2-3): p. 364-373.
- [30] Gorges, R., S. Meyer, and G. Kreisel, *Photocatalysis in microreactors*. Journal of Photochemistry and Photobiology A: Chemistry, 2004. 167(2-3): p. 95-99.

- [31] Gorges, R., S. Meyer, and G. Kreisel, *Photocatalysis in microreactors*. Journal of Photochemistry and Photobiology A: Chemistry, 2004. 167(2-3): p. 95-99.
- [32] Tosun, I., D. Uner, and C. Ozgen, *Critical Reynolds number for Newtonian flow in rectangular ducts*. Industrial & Engineering Chemistry Research, 1988. 27(10): p. 1955-1957.
- [33] Malato, S., et al., *Photocatalytic Treatment of Diuron by Solar Photocatalysis: Evaluation of Main Intermediates and Toxicity*. Environmental Science & Technology, 2003. 37(11): p. 2516-2524.
- [34] S. Chusaksri, J.L., T. Saleepochn, P. Sutthivaiyakit, *Photocatalytic degradation of 3,4-dichlorophenylurea in aqueous gold nanoparticles-modified titanium dioxide suspension under simulated solar light*. Hazardous Materials, 2011. 190(1-3): p. 930-937.
- [35] Wannipa Pradittakan, E.S., Alisa S. Vangnai and V. Pavarajarn. *Comparative Study on Mechanism of Photocatalytic Degradation of Diuron on Titanium Dioxide and Zinc Oxide*. Master, Chemical Engineering, Chulalongkorn University, 2011.
- [36] Saowalux Sittichoktum and V. Pavarajarn. *Photocatalytic Degradation of Linuron on Titania and Zinc Oxide*. Master, Chemical Engineering, Chulalongkorn University, 2012.
- [37] Fenoll, J., et al., *Photocatalytic transformation of sixteen substituted phenylurea herbicides in aqueous semiconductor suspensions:*

Intermediates and degradation pathways. Journal of Hazardous
Materials, 2013. 244-245(0): p. 370-379.





APPENDIX

จุฬาลงกรณ์มหาวิทยาลัย
CHULALONGKORN UNIVERSITY

APPENDIX A
DIURON CARIBRATION CURVE

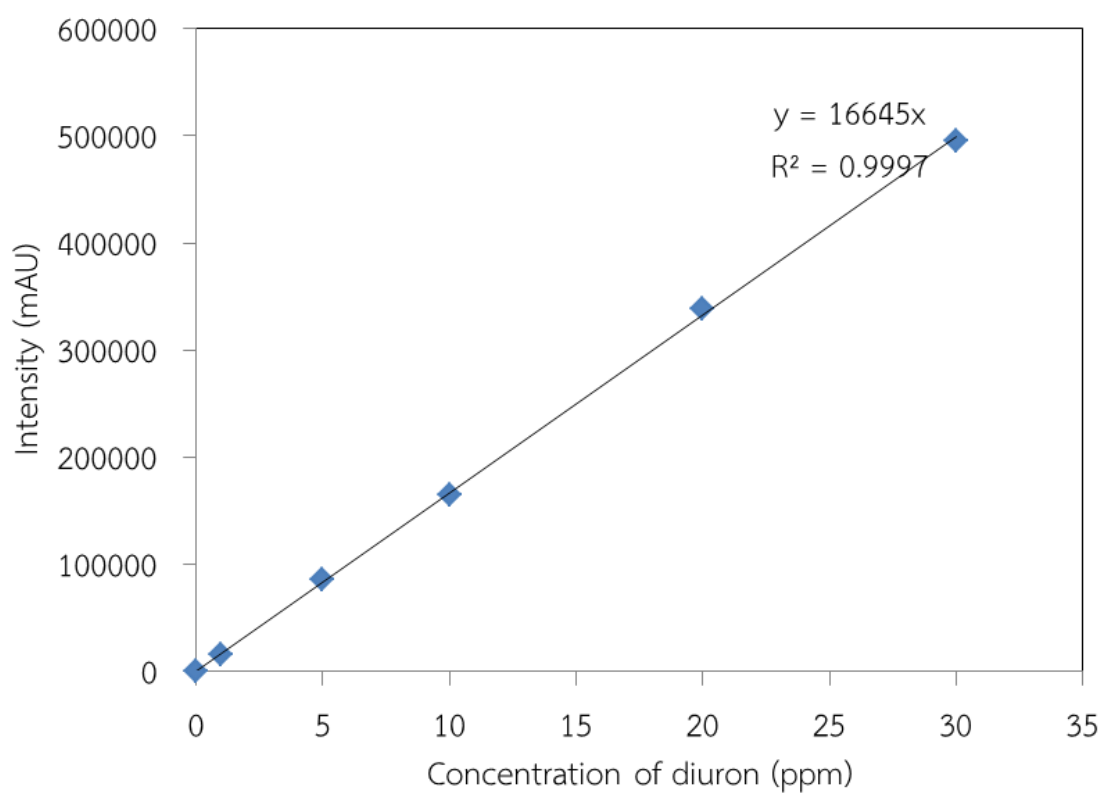


Figure A.1 The calibration curve of diuron.

APPENDIX B

CALCULATION OF TITANIUM DIOXIDE IN SOLUTION

The amounts of titanium dioxide in the solution were analyzed by inductively coupled plasma optical emission spectroscopy (ICP-OES). A concentration of 0.0941 mg/L of titanium dioxide in a sample was calculated into a mass of titanium dioxide in a solution by Eq. below. Based on flow rate 5.8 ml/h reaction. All the solutions were 25 ml.

$$\begin{aligned}
 \text{Mass of TiO}_2 &= \text{concentration of Ti from ICP} \times \text{all the solutions in the} \\
 \text{reaction} & \\
 &= 0.0941 \text{ mg/L} \times 25 \text{ ml} \\
 &= 0.002353 \text{ mg}
 \end{aligned}$$

The percentage of the amounts of the titanium dioxide in the solution respect to the initial mass TiO₂ coated:

$$\begin{aligned}
 \% \text{ TiO}_2 &= (0.002353 \text{ mg} / 2 \text{ mg}) \times 100 \\
 &\leq 0.1 \%
 \end{aligned}$$

The results confirm that these solution classes contained low amounts of titanium or titanium dioxide does not remove well and remain on the surface.

APPENDIX C

CALCULATION OF REYNOLDS NUMBER

For the evaluation of the Reynolds number (Re) of a rectangular duct, substituting an equivalent diameter for the rectangular duct. The Reynolds number (Re) is defined as follows:

$$\text{Re} = \frac{\rho D_h v}{\mu} \quad (\text{C.1})$$

The equivalent diameter D_h , which is set equal to four times the “Hydraulic Radius,” R_h is defined as follows:

$$D_h = 4R_h = 4A/P \quad (\text{C.2})$$

Where: D_h is the hydraulic equivalent diameter (m).

ρ is the fluid density (kg/m^3).

v is the mean velocity of the fluid (m/s).

μ is the viscosity of the fluid ($\text{kg}/(\text{m}\cdot\text{s})$).

A is cross-section area (m^2).

P is wetted perimeter (m).

Example: Calculation of the Reynolds number (Re) by using 250 μm thick.

$$\rho = 1000 \text{ kg/m}^3$$

$$\mu = 0.1 \text{ kg}/(\text{m}\cdot\text{s})$$

$$v = Q/A = (5.8 \text{ ml/h}) / ((250 \times 10^{-6} \text{ m})(0.8 \times 10^{-2} \text{ m})) = 0.008 \text{ m/s}$$

$$\begin{aligned} D_h &= 4A/P = 4(250 \times 10^{-6} \text{ m})(0.8 \times 10^{-2} \text{ m}) / 2((250 \times 10^{-6} \text{ m}) + (0.8 \times 10^{-2} \text{ m})) \\ &= 4(0.000002) / (0.0165) \\ &= 0.000484848 \end{aligned}$$

$$\begin{aligned} Re &= \rho D_h v / \mu \\ &= (1000)(0.000484848)(0.008) / (0.1) \\ &= 0.003878788 \end{aligned}$$

APPENDIX D

LC-MS/MS MASS SPECTRUM

All samples were sent for analysis at Scientific and Technological Research Equipment Centre. The mass spectrometer was equipped with phenyl column (Vertisep UPS column, 2.1x100mm) and an ESI ion source operating in negative ion and positive ion mode in the range 70-1,000 m/z. The mobile phase was 60% (v/v) acetonitrile mixed with 40% (v/v) deionized water and total flow rate was 0.2 ml/min.

D.1 Mass spectrum of diuron solution

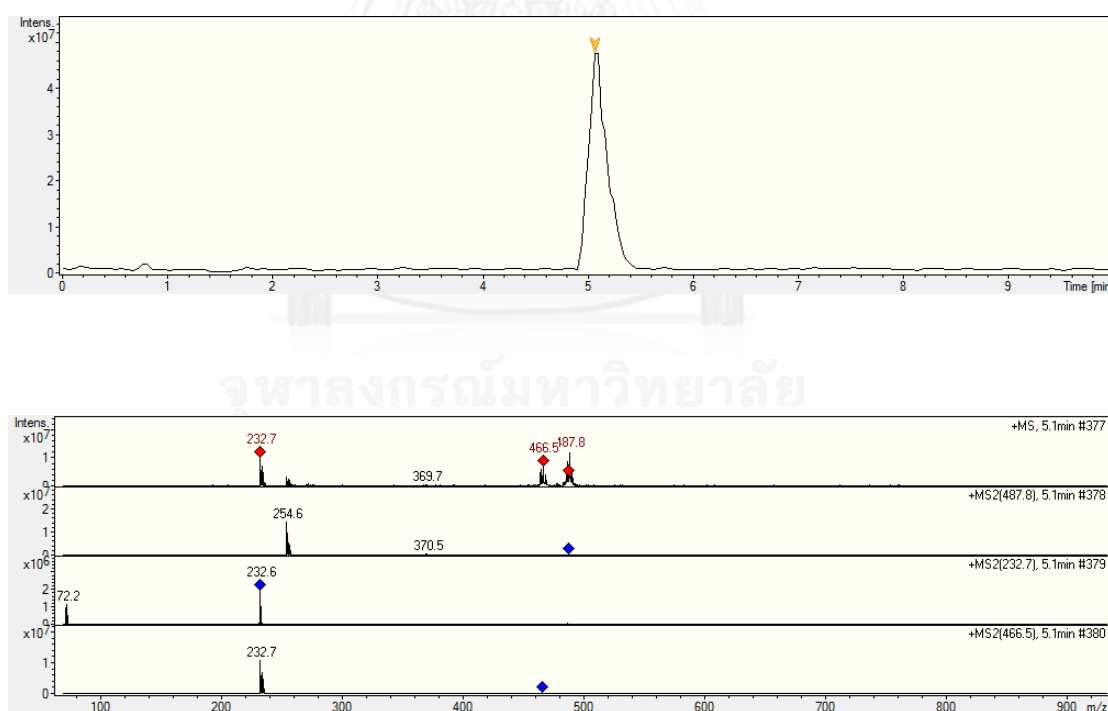


Figure D.1 (a) Chromatogram of diuron solution in positive ion mode.

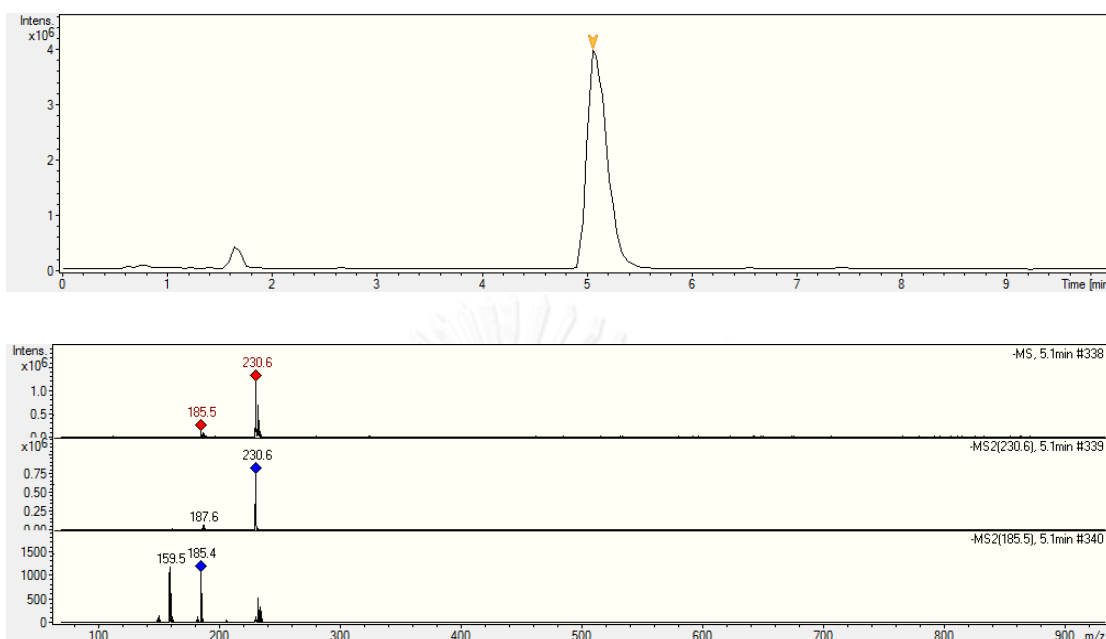


Figure D.1 (b) Chromatogram of diuron solution in negative ion mode.

D.2 MS/MS spectrum of diuron solution from photodegradation process.

D2.1 At residence time 1 min.

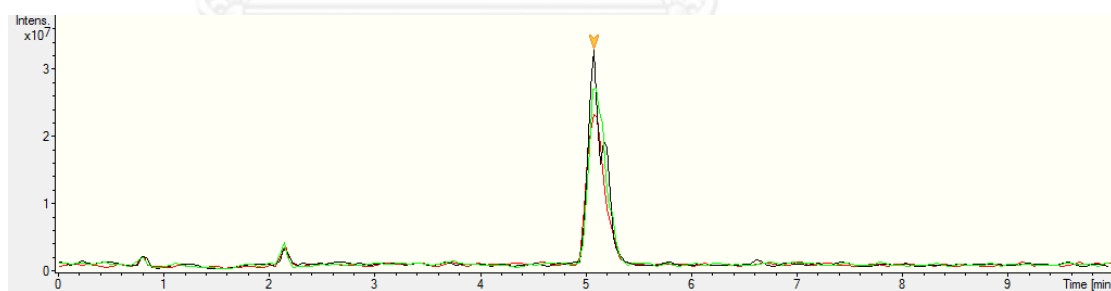
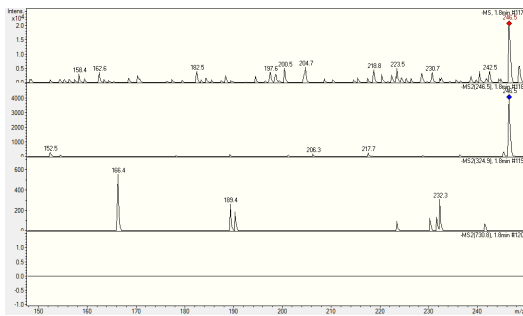
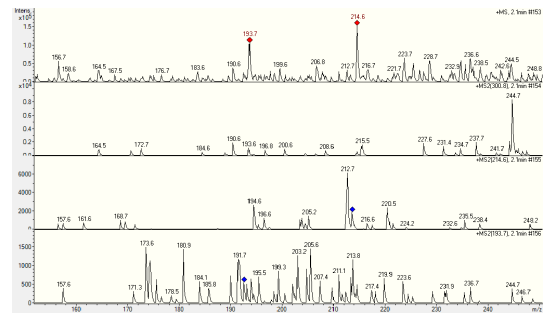


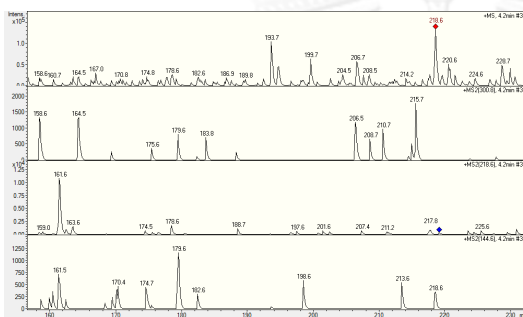
Figure D.2 Chromatogram of diuron solution during photodegradation process at residence time 1 minute (120, 150 and 180 min during reaction process) are shown in (a). MS/MS spectrums at various retention times are display in (b)-(e).



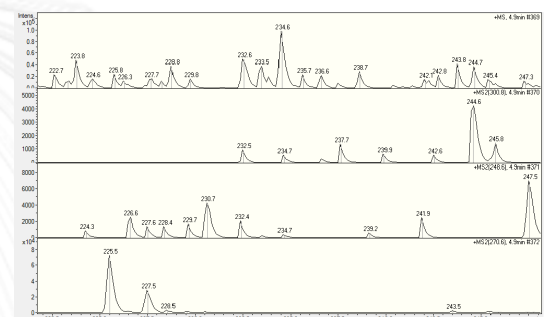
(b) Retention time 1.8 min



(c) Retention time 2.1 min



(d) Retention time 1.8 min



(e) Retention time 2.1 min

Figure D.2 (continued)

D2.2 At residence time 5 min.

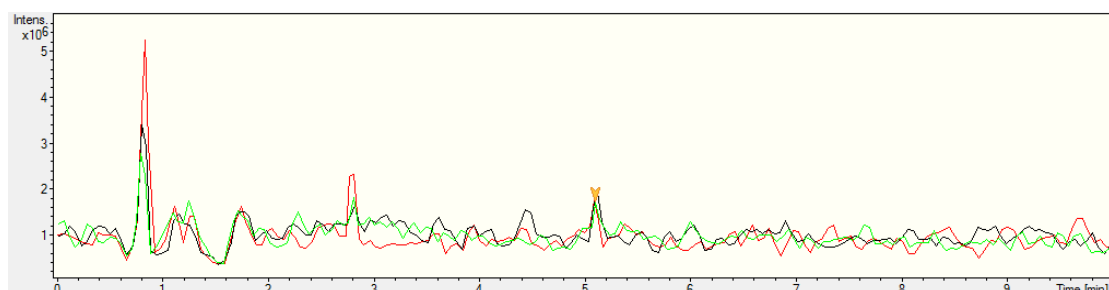
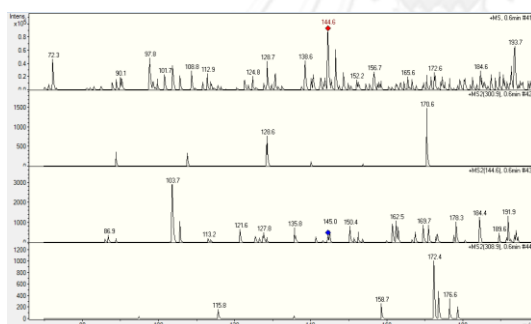
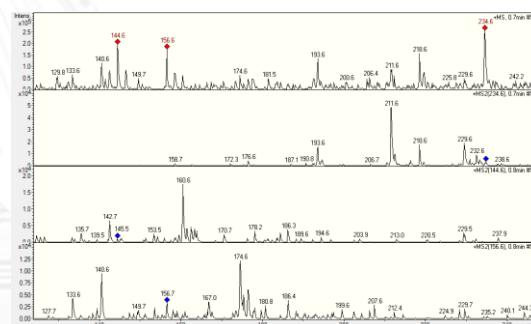


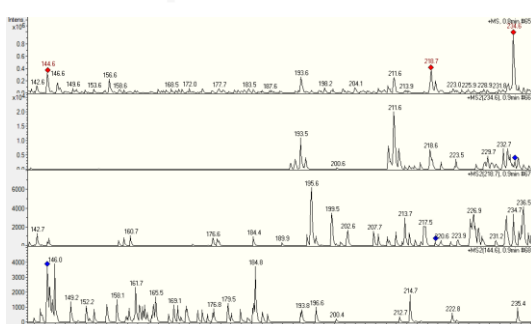
Figure D.3 Chromatogram of diuron solution during photodegradation process at residence time 5 minutes (120, 150 and 180 min during reaction process) are shown in (a). MS/MS spectrums at various retention times are display in (b)-(j).



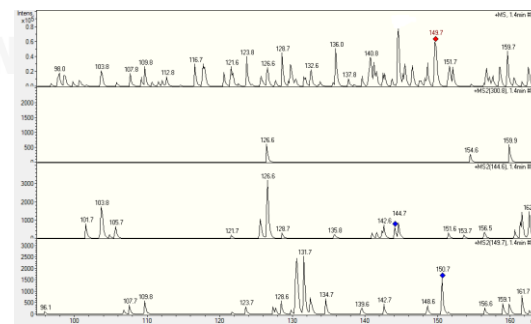
(b) Retention time 0.6 min



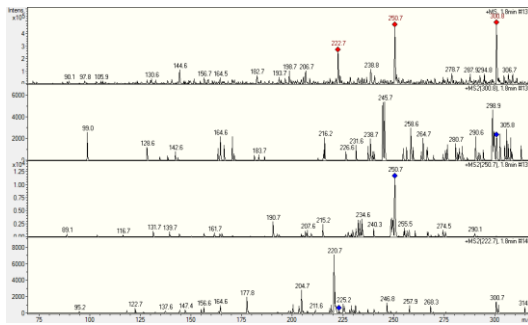
(c) Retention time 0.7 min



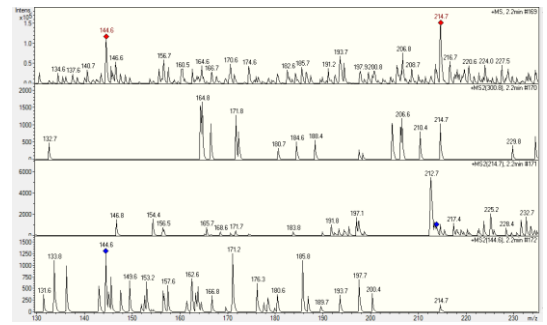
(d) Retention time 0.9 min



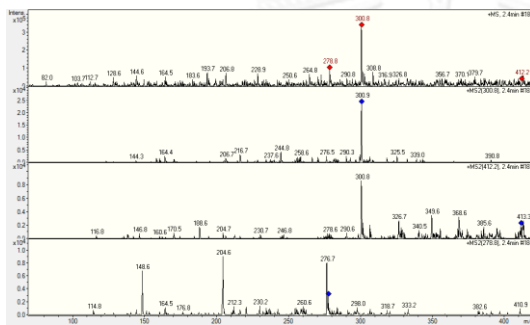
(e) Retention time 1.4 min



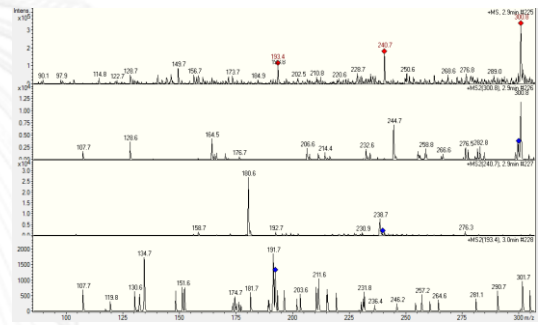
(f) Retention time 1.8 min



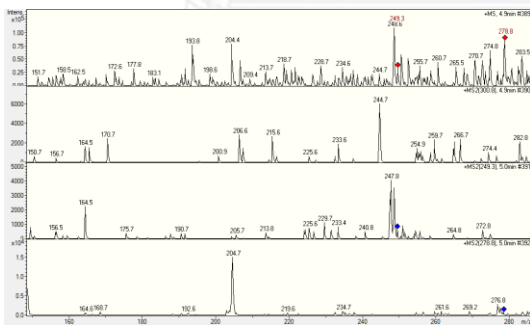
(g) Retention time 2.2 min



(h) Retention time 2.4 min



(i) Retention time 2.9 min



(j) Retention time 4.9 min

Figure D.3 (continued)

D2.3 At residence time 10 min.

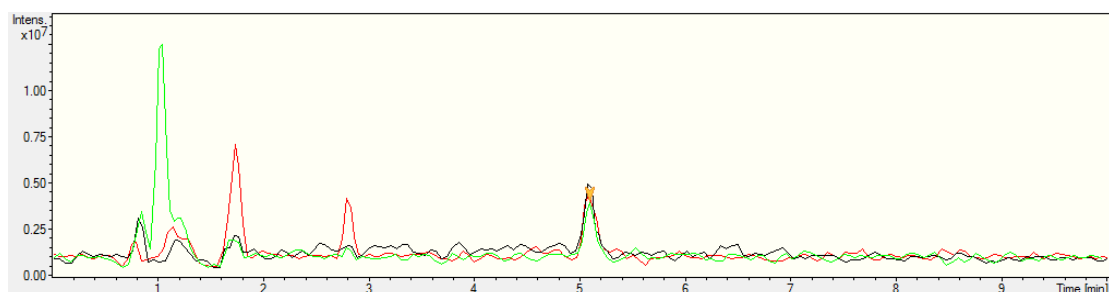
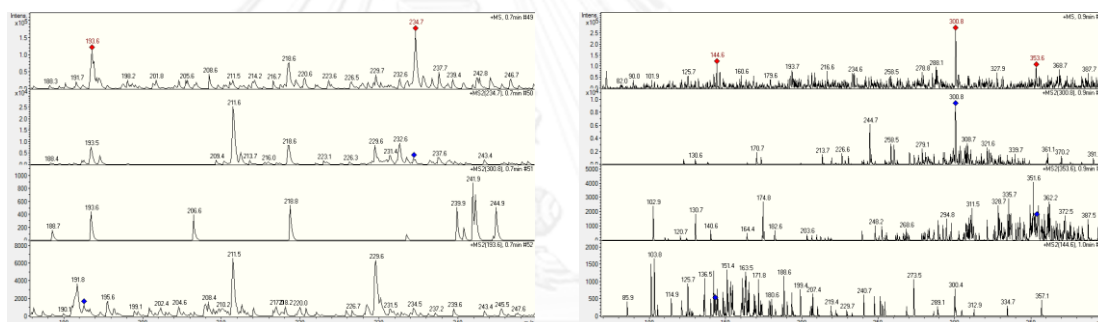
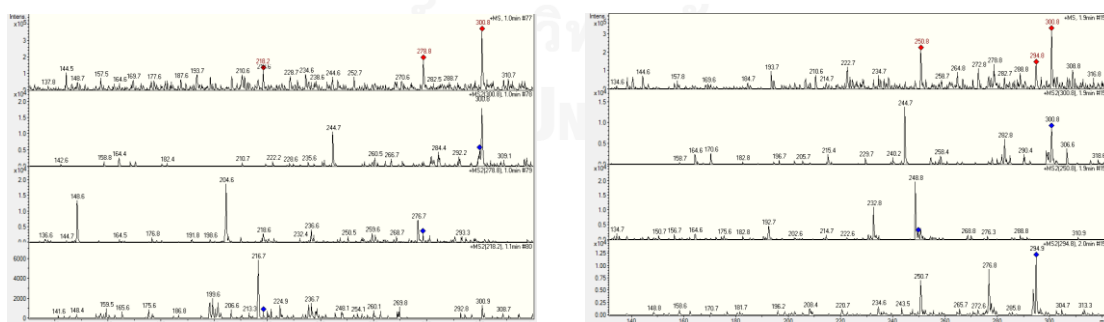


Figure D.4 Chromatogram of diuron solution during photodegradation process at residence time 10 minutes (120, 150 and 180 min during reaction process) are shown in (a). MS/MS spectrums at various retention times are display in (b)-(j).



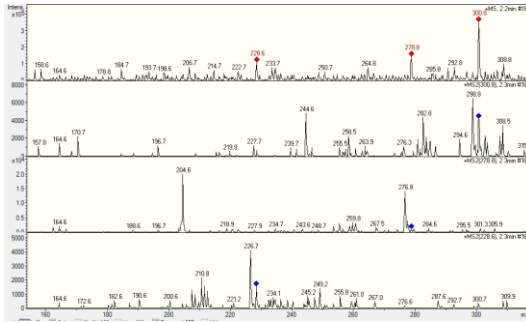
(b) Retention time 0.7 min

(c) Retention time 0.9 min

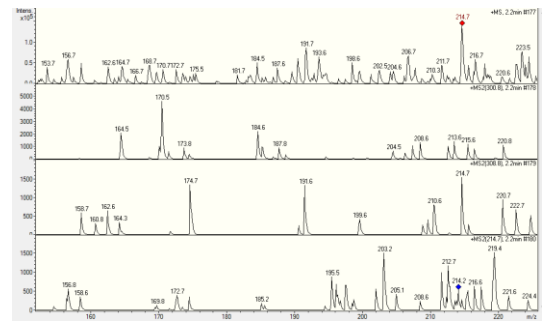


d) Retention time 1.0 min

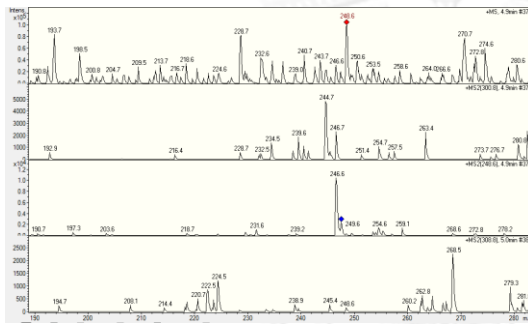
(e) Retention time 1.9 min



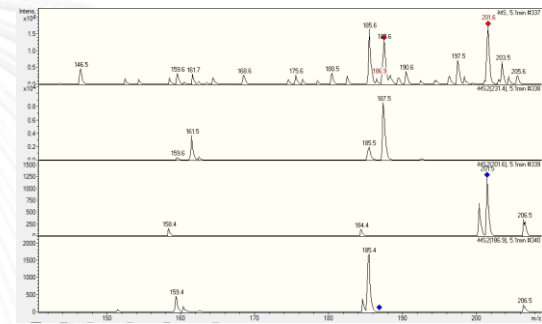
(f) Retention time 2.2 min



(g) Retention time 2.2 min



(h) Retention time 4.9 min



(i) Retention time 5.1 min

Figure D.4 (continued)

D2.3 At residence time 15 min.

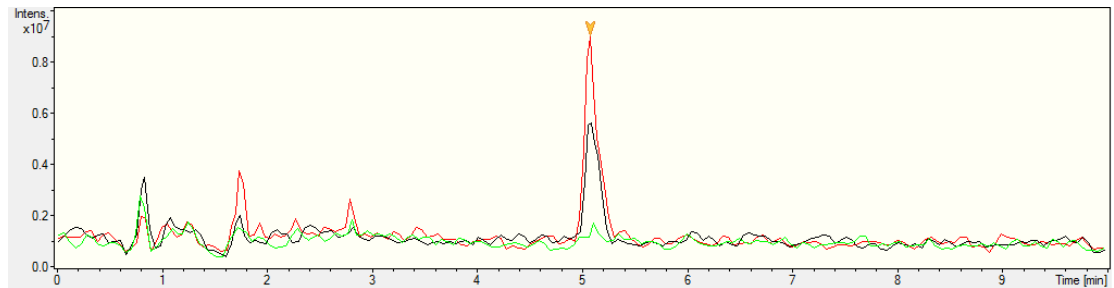
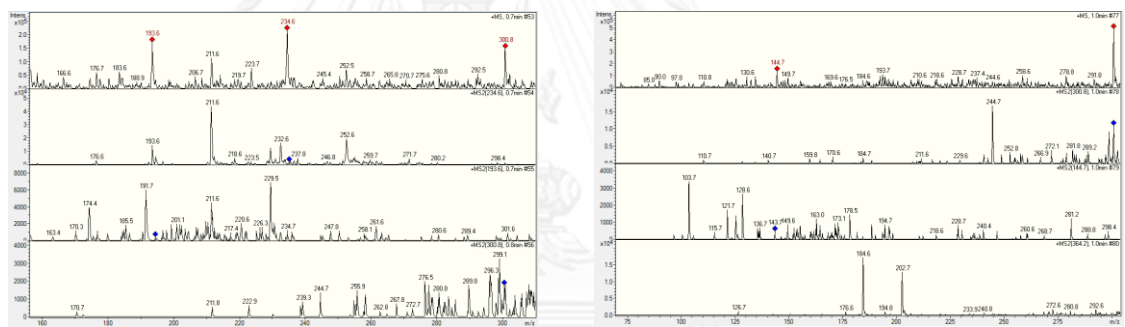
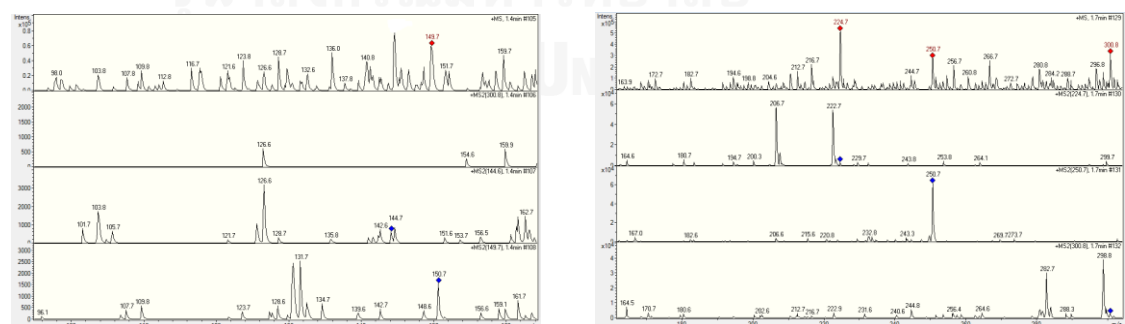


Figure D.5 Chromatogram of diuron solution during photodegradation process at residence time 15 minutes (120, 150 and 180 min during reaction process) are shown in (a). MS/MS spectrums at various retention times are display in (b)-(h).



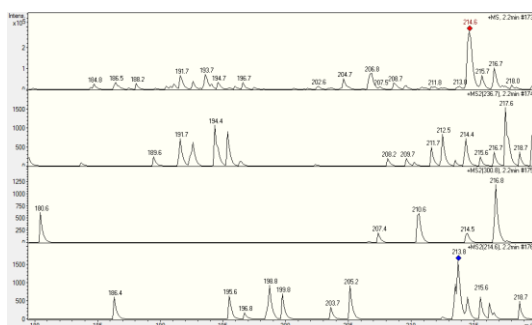
(b) Retention time 0.7 min

(c) Retention time 1.0 min

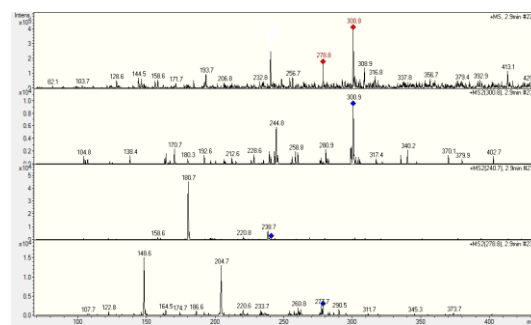


(d) Retention time 1.4 min

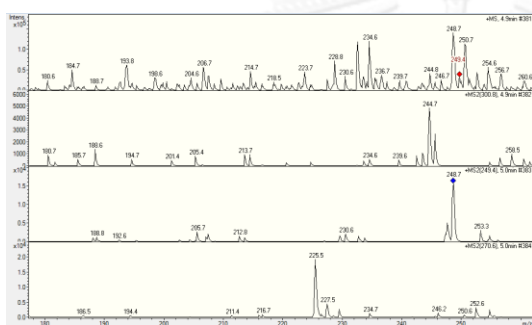
(e) Retention time 1.7 min



(f) Retention time 2.2 min



(g) Retention time 2.9 min



(h) Retention time 4.9 min

Figure D.5 (continued)

D.3 MS/MS spectrum of diuron solution under exposure and without exposure of light.

D3.1 At residence time 1 min

D3.1.1 At residence time 1 min: light-dark-light

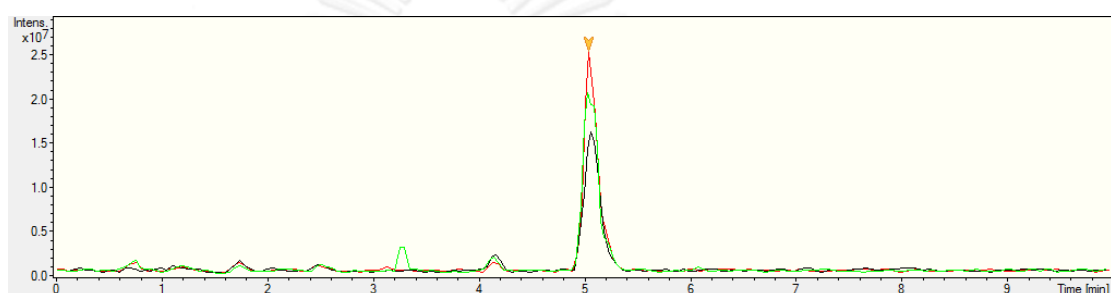
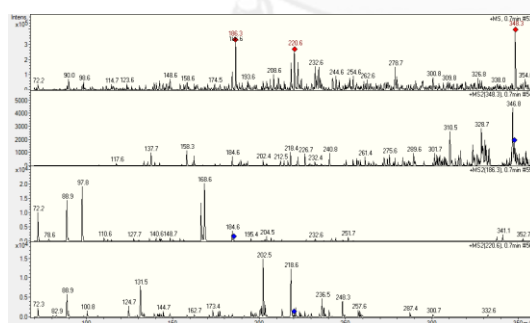
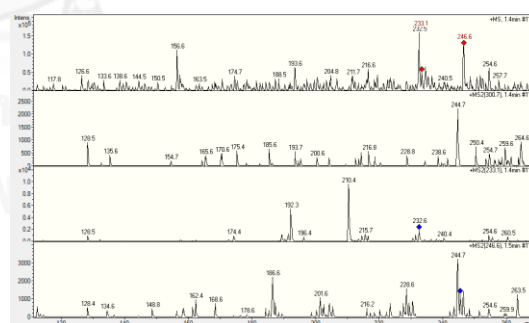


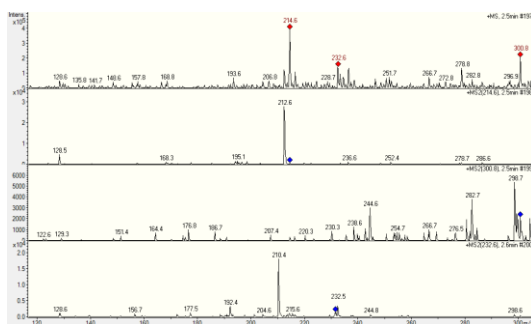
Figure D.6 Chromatogram of diuron solution under exposure and without exposure of light at residence time 1 minutes: light-dark-light (120, 150 and 180 min during reaction process) are shown in (a). MS/MS spectrums at various retention times are display in (b)-(f).



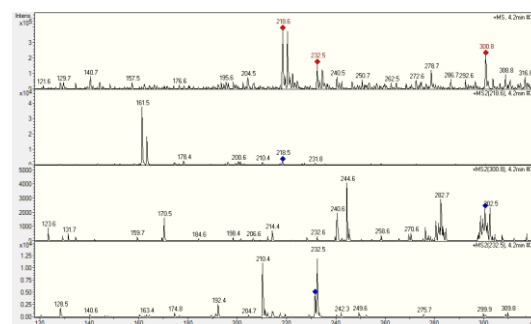
(b) Retention time 0.7 min



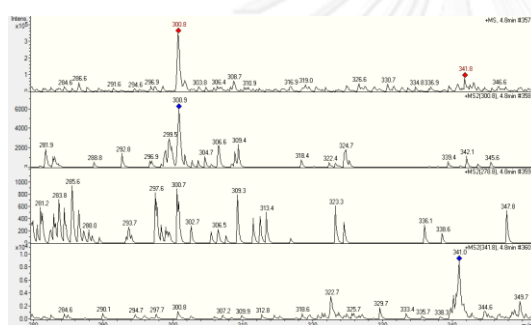
(c) Retention time 1.4 min



(d) Retention time 2.5 min



(e) Retention time 4.2 min



(f) Retention time 4.8 min

Figure D.6 (continued)

D3.1.2 At residence time 1 min: light-light-dark

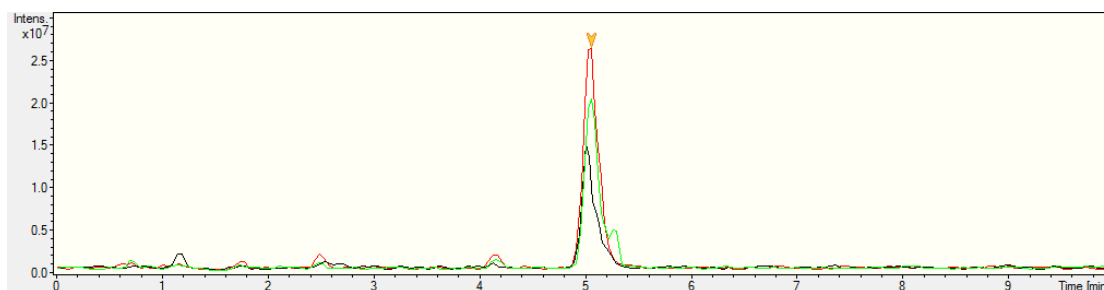
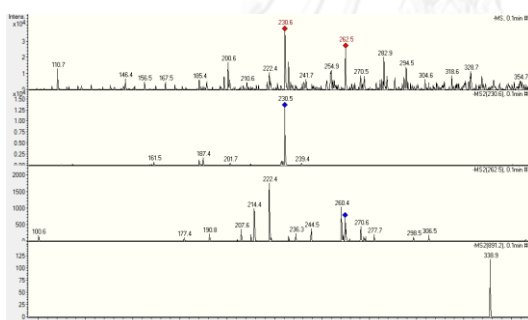
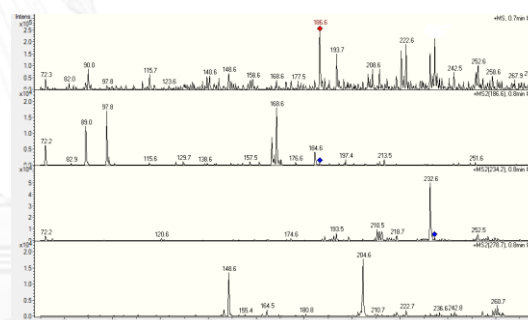


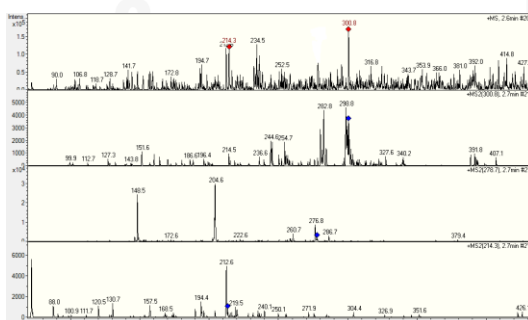
Figure D.7 Chromatogram of diuron solution under exposure and without exposure of light at residence time 1 minutes: light-light-dark (120, 150 and 180 min during reaction process) are shown in (a). MS/MS spectrums at various retention times are display in (b)-(f).



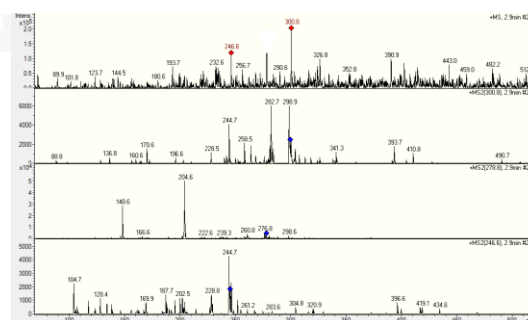
(b) Retention time 0.1 min



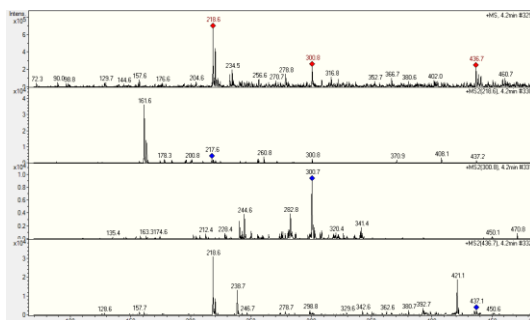
(c) Retention time 0.7 min



(d) Retention time 2.6 min



(e) Retention time 2.9 min



(f) Retention time 4.2 min

Figure D.7 (continued)

D3.1.3 At residence time 1 min: light-dark-light-dark- light

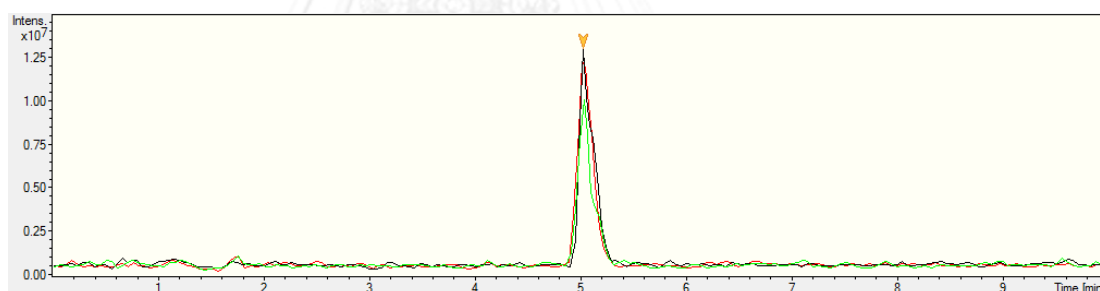
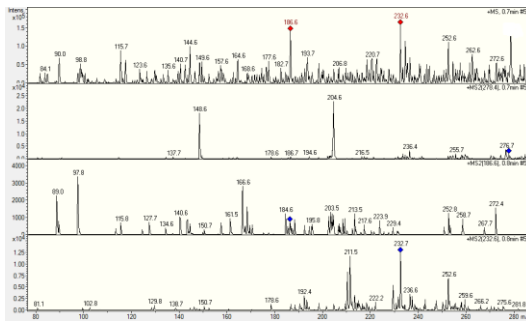
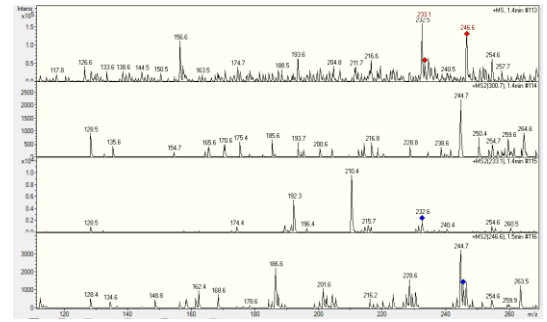


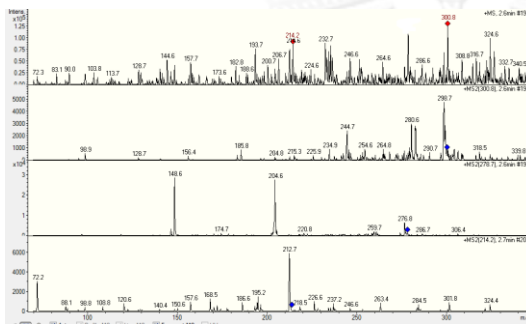
Figure D.8 Chromatogram of diuron solution under exposure and without exposure of light at residence time 1 minutes: light-dark-light-dark- light (120, 150 and 180 min during reaction process) are shown in (a). MS/MS spectrums at various retention times are display in (b)-(f).



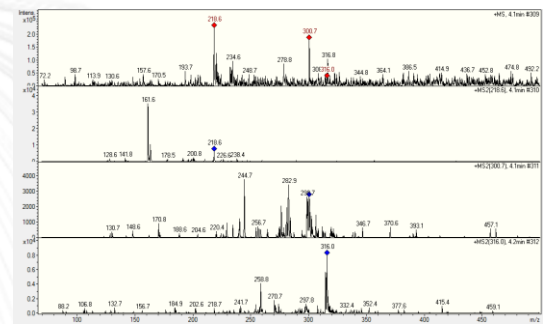
(b) Retention time 0.7 min



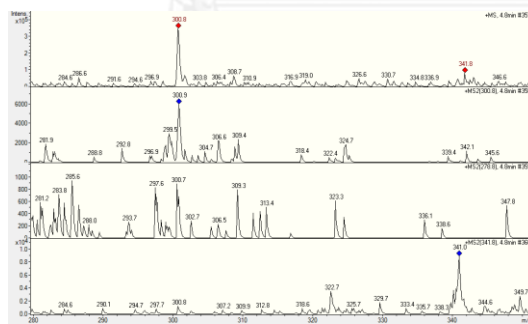
(c) Retention time 1.4 min



(d) Retention time 2.6 min



(e) Retention time 4.1 min



(f) Retention time 4.8 min

Figure D.8 (continued)

D3.2 At residence time 3 min

D3.2.1 At residence time 3 min: light-dark-light

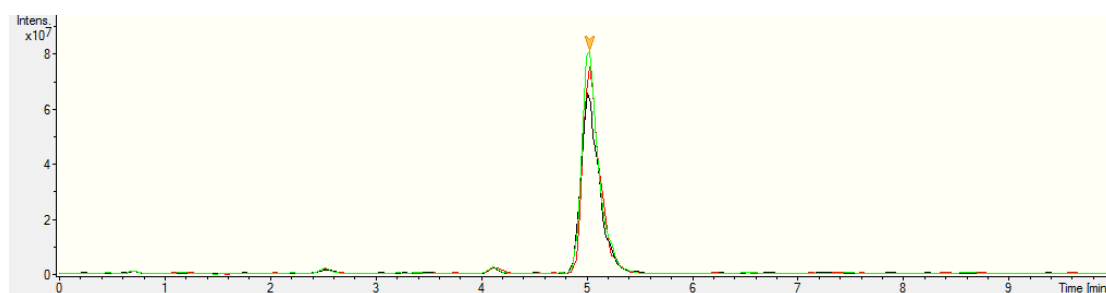
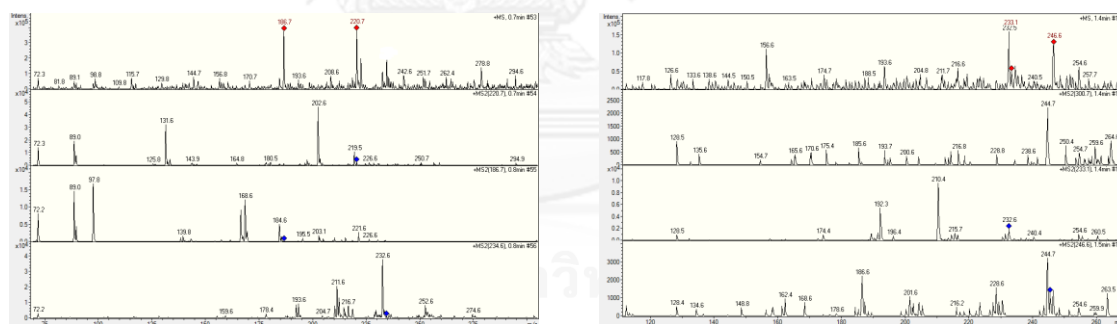
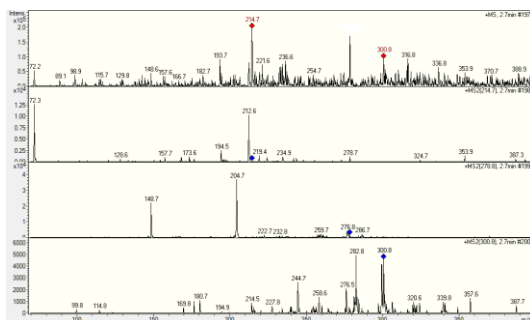


Figure D.9 Chromatogram of diuron solution under exposure and without exposure of light at residence time 3 minutes: light-dark-light (120, 150 and 180 min during reaction process) are shown in (a). MS/MS spectrums at various retention times are display in (b)-(f).

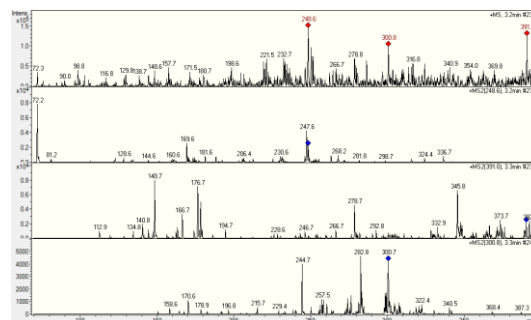


(b) Retention time 0.7 min

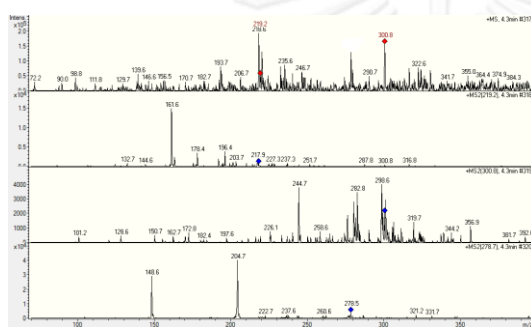
(c) Retention time 1.4 min



(d) Retention time 2.7 min



(e) Retention time 3.2 min



(f) Retention time 4.3 min

Figure D.9 (continued)

D3.2.2 At residence time 3 min: light-light-dark

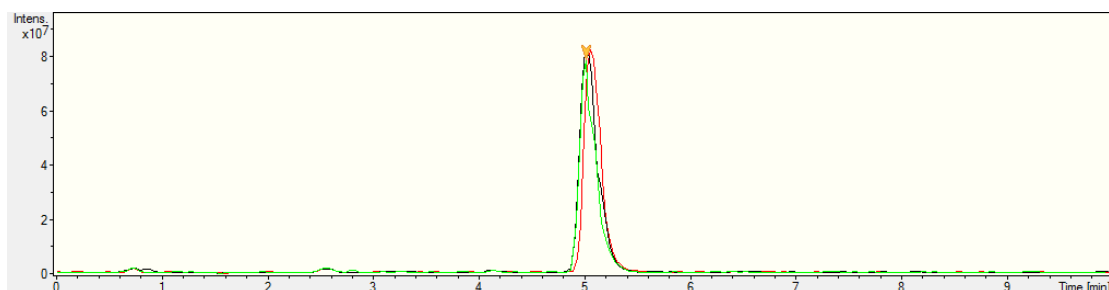
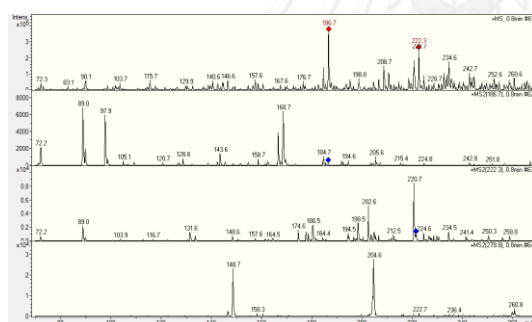
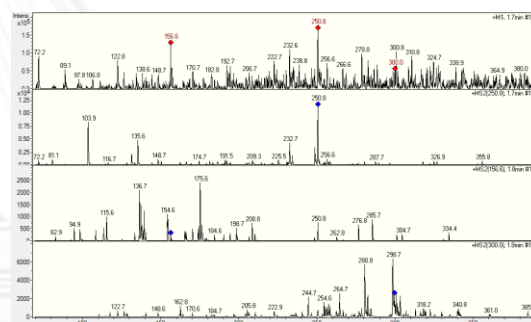


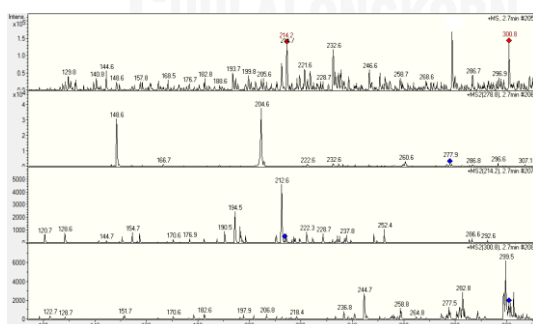
Figure D.10 Chromatogram of diuron solution under exposure and without exposure of light at residence time 3 minutes: light-light-dark (120, 150 and 180 min during reaction process) are shown in (a). MS/MS spectrums at various retention times are display in (b)-(g).



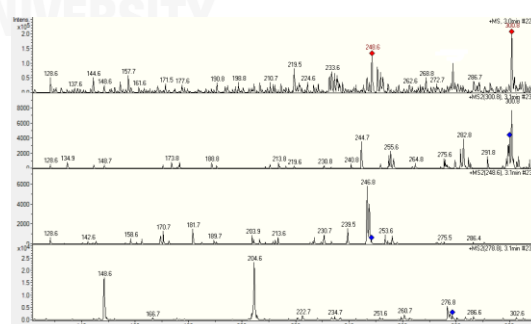
(b) Retention time 0.8 min



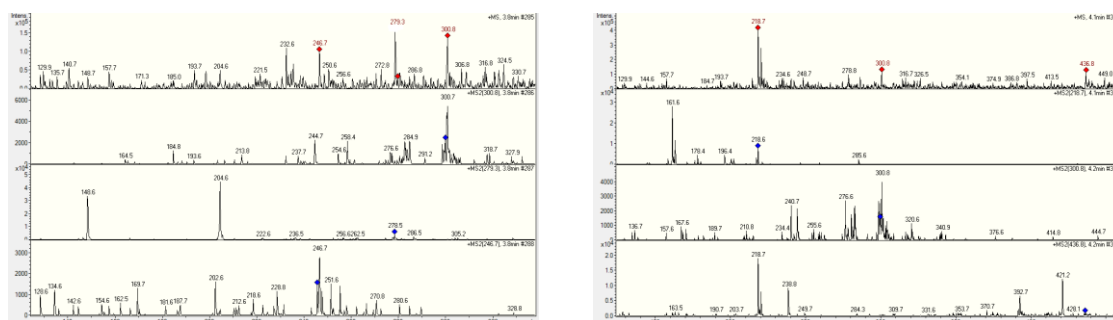
(c) Retention time 1.7 min



(d) Retention time 2.7 min



(e) Retention time 3.0 min



(f) Retention time 3.8 min

(g) Retention time 4.1 min

Figure D.10 (continued)

APPENDIX E

LIST OF PUBLICATION

1. Rungthip Noisumran, Worachate Khongthon and Varong Pavarajarn.
“Photocatalytic Degradation of Diuron on Titanium Dioxide in Microreactor”.
The 9th World Congress of Chemical Engineering *Incorporating* 15th Asian
Pacific Confederation of Chemical Engineering Congress, Coex, Seoul, Korea,
August 18-23, 2013.

VITA

Miss Rungthip Noisumran was born on November 30, 1988 in Phetchaburi Province, Thailand. She received the Bachelor Degree of Chemical Engineering from Faculty of Engineer, Thammasat University in 2011. She continued her Master's study at Chulalongkorn University in June, 2012.

